NTNU – Trondheim
Norwegian University of
Science and Technology

Characterization of alkyd emulsions

Characterization of phase inversion and
emulsification properties pre- and
post-inversion.

Martine Lefsaker

Chemical Engineering and Biotechnology
Submission date: June 2013
Supervisor: Wilhelm Robert Glomm, IKP
Co-supervisor: Tina Helland, Jotun AS
Stian Engebretsen, Jotun AS

Norwegian University of Science and Technology
Department of Chemical Engineering

Abstract

This report presents the results of work performed in cooperation with the Binding lab (Jotun AS) and the Colloid and Polymer Chemistry group at Department of Chemical Engineering, Norwegian University of Science and Technology (NTNU).

The research performed is on the emulsification process of alkyds by catastrophic phase inversion (CPI). Focus has been on the development of emulsion properties such as viscosity, conductivity and optical density, during the emulsification process. The definition of properties at inversion point, from a water-in-oil (w/o) to an oil-in-water (o/w) continuous emulsion, and the influence changes in these properties have on emulsion quality.

The techniques used to investigate the properties are the conductivity, the e-critical cell, the Near infrared spectroscopy (NIR) and a cone and plate rheometre. One emulsification has also been evaluated using Nuclear magnetic resonance (NMR). A brief introduction to alkyds and alkyd emulsions is provided along with general theory on surfactants and emulsification procedures.

Trends that illustrate the importance of the development of, and changes in, these properties on the emulsification process and emulsion quality has been investigated. Emulsifications with alternative emulsification systems and process conditions were performed in order to investigate possible deviations from the trends further illustrating the importance of the property development.

The reference system proves to be a robust system with a clear trend in the development of the properties. The emulsion quality for the reference system, determined by the droplet size distribution, was not significantly affected by small deviations and failures in the process conditions. The reference system shows clear trends in the property development, and especially the viscosity proves to be an important property. Surfactants, and surfactant amounts and combinations, seems to be important for the viscosity development, along with the alkyd properties.

The trend showed that the emulsification process could be divided in to four periods. First an introduction period, then a period where significant changes in the properties occur prior to a period covering the inversion point and finally a period where the inverted emulsion is stabilized.

Sammendrag

Denne rapporten presenterer resultatene av arbeid utført i samarbeid med Bindemiddellaboratoriet ved Jotun AS, og Kolloid og POlymerkjemi gruppen ved Institutt for Kjemisk Prosessteknologi, Norges teknisk-naturvitenskaplige universitet (NTNU).

En emulgeringsprosess av alkyd i vann, ved bruk av catastrophic phase inversion (CPI), er undersøkt med hensyn på emulsjonsegenskaper. Det ble lagt vekt på utvikling av egenskaper, på definisjonen av egenskaper ved inversjonspunktet for vann-i-alkyd (w / o) til alkyd-i-vann (o / w) emulsjoner, og på innflytelsen forandringene har på det endelige emulgeringsresultatet.

Egenskapene som er undersøkt er ledningsevne, e-kritisk verdi, optisk tetthet (NIR) og viskositeten til emulsjonen. En av emulgeringene er også vurdert ved hjelp av NMR. En kort innføring i alkyder og alkyd emulsjoner er gitt, sammen med generell teori om surfaktanter og emulgeringsteknikker.

Det er fokusert på hvordan egenskapene utvikler seg i løpet av prosessen, og på trender som kan illustrere viktigheten av endringer i egenskapene og innflytelsen disse har på endelig emulsjonskvalitet. Emulgeringer med alternative surfaktanter, surfaktantblandinger og alkyder ble testet. Alternative prosessvilkår ble også testet for å undersøke mulige avvik fra trendene. Dette kan ytterligere illustrere viktigheten av utviklingen til egenskapene. En oversikt over de utførte emulgeringene er gitt i Appendix A.

En evaluering av testresultatene er presentert med diskusjon for alle vellykkede emulgeringer, og emulgeringer som gir ytterligere interessant informasjon om emulgeringsprosessen. Referansesystemet som referanseemulsjonen er basert på, viste seg å være et robust system. Den endelige emulsjonskvaliteten, som bestemmes på bakgrunn av dråpestørrelsesfordelingen, ble ikke betydelig påvirket av variasjoner og feil i prosessvilkårene. Referansesystemet viste klare trender i utviklingen av egenskapene. Særlig viskositeten viste seg å være en viktig egenskap. Mengden surfaktant, surfaktanttyper og kombinasjoner av disse synes å være viktig for viskositetsutviklingen, sammen med alkydegenskaper.

Resultatene viste at emulgeringsprosessen kan deles inn i fire perioder. Først en introduksjonsperiode, Periode 1, inntil tilsats av 200 mL vann. Første endring i emulsjonsegenskaper ble observert i Periode 2, mellom 200 mL og 350 mL. Periode 3, 350 mL – 550 mL, dekket inversjonspunktet i emulgeringsprosessen. Dette oppsto etter en tilsetning av ca 500 mL vann. De største dynamiske endringene skjedde i løpet av en tilsats på ca 400 mL vann, fra 200 mL til det stabiliserte seg etter ca. 600 mL. Stabiliseringsperioden ble identifisert som Periode 4.

Preface

This master's thesis in was performed in cooperation with Jotun AS, Binder lab, Exterior R & D, Jotun Decorative (Jotun AS), and Department of Chemical engineering, Colloid and Polymer Chemistry group at Norwegian University of Science and Technology (NTNU). The emulsification method was developed and taught at the Binder lab (Jotun AS) and the experiments were performed at the Ugelstad laboratory (NTNU), except for the external NMR tests performed by Antek AS.

I would like to thank my supervisors, Wilhelm Robert Glomm (NTNU), Tina Helland and Stian Engebretsen (Jotun AS), for support during the project and valuable discussions and evaluations of the results and report at the end of the process. Geir Humborstad Sørland (Anvendt Teknologi AS) deserves thanks for help with the theory and evaluation of the result from the NMR research of the emulsification. I would also like to thank the technical staff, by Caterina Lesaint, Bicheng Gao and May Grete Sætran at the Ugelstad laboratory for training on the different analytical instruments and help with the practical aspect of the thesis. Thanks also to Dr. Kristofer Paso, for training on the rheometer.

A last thanks to supervisor Wilhelm Robert Glomm and Sophie Glas for proofreading, and my father Jan Åge Lefsaker for feedback on the readability and comprehensibility of graphs and general concepts.

The picture on the cover is taken from an earlier study (Lefsaker, 2012) and shows a fluorescent dyed alkyd emulsion through a microscope.

I declare that this is an independent work according to the exam regulations of the Norwegian University of Science and Technology (NTNU).

Trondheim, June 17., 2013

Martine Lefsaker

Supervisor:

Wilhelm Glomm, NTNU

Co-supervisors:

Tina Helland & Stian Engebretsen, Jotun AS

Contents

1 Introduction

Waterborne surface coatings constitute an important research and development field within the paint industry. They have little or no organic solvents and are thereby considered more environmentally friendly both in production and in use. The use of renewable, non-petroleum based, raw materials reduce the dependency on petroleum prices and encourage greener technology and more environmentally friendly products (Gooch, 2002). An example of renewable greener materials for coating binders are vegetable oil alkyds.

Alkyds are synthetic resins derived from ester-based polymers that are modified with oil or fatty acids. It is a binder with good wood penetration, which is important in exterior paints. Due to its good protective properties alkyd emulsions are expected to be one of the good alternatives for the base of the next generation waterborne paints. Research in this field is therefore both relevant and important (Gooch, 2002).

Traditionally alkyds have a high viscosity and need solvents in order to be useful in paint. The solvents contribute to high volatile organic compound (VOC) levels, which has restricted the use of alkyds. There is a need to find a way to use the alkyds without using the solvents conventional emulsion-polymerization is not directly applicable to alkyd resins (Gooch, 2002).

There has been developed other methods to emulsify alkyds, including two distinct commercial alkyd emulsions. These are based on internal and external emulsifier technology (Tuck, 2000). Internal emulsifiers have polar groups, mainly hydrophilic and carboxylic groups, introduced into the alkyd during alkyd synthesis, in order to ionically or sterically stabilize the emulsion. These carboxylic acid groups on the alkyd usually needs to be neutralized using amines in order to be compatible with the paint. The range of resins using this technology includes alkyds with oil lengths from 20-60% and all types of chemical modifications such as urethane, epoxy and acrylic addition (Tuck, 2000).

The external emulsifiers are added to the molten resin prior to emulsification. The need for neutralisation is dependent on the emulsifier and the amount of acid groups on the alkyd. It is possible to make the external emulsifier emulsion with a reduced level of VOC compared to the internal emulsifier technology. It is proved that an emulsion produced by external emulsifying technology possess the quality of penetrating wood cells almost as good as solvent-based alkyds (Tuck, 2000). The process is a batch process where water is gradually added to the alkyd mixture containing emulsifier. When a sufficient amount of water is added, the emulsion reaches a phase inversion point, meaning that the emulsion goes from being alkyd continuous to water continuous (Tuck, 2000).

One of the most important properties of an alkyd emulsion is colloidal and mechanical stability. The most important parameter affecting the stability is the size

of the emulsion droplets. The droplet size has to be small enough (<300 nm) to withstand destabilization by creaming, flocculation, sedimentation and coalescence (Holmberg, et al., 2003). The factors influencing the alkyd droplet size include emulsification procedure, energy input and shear rate along with emulsifier amount and type, and alkyd parameters such as acid and hydroxyl number and oil length (Tuck, 2000).

Few things are certain about the details of the phase inversion processes of alkyd emulsion (Jahanzad, et al., 2009). The catastrophic phase inversion point is the critical phase ratio where the emulsion inverts from a water-in-oil emulsion (w/o) to an oil-in-water (o/w) emulsion. Research has been performed on catastrophic phase inversion during oil emulsification (Jahanzad, et al., 2009) and polymer emulsification (Sajjadi, et al., 2000). However, these emulsions have droplet sizes in micro range as opposed to the nano range, which is needed to have a sufficiently stable alkyd emulsion (Tuck, 2000).

Despite efforts made, there are still uncertainties about the underlying processes by which finer emulsions are produced. Development of emulsion properties, and their effect on the emulsification process and the emulsion quality are uncertain. There are several ways of testing the properties during a catastrophic phase inversion. The test possibilities available in the Ugelstad laboratory were investigated in an earlier study (Lefsaker, 2012). Several methods were found to provide useful information about the properties of the emulsion at different stages of the process. The processes and property developments responsible for producing finer emulsions are further enlightened in this research through a study of the properties, and the changes in properties during a catastrophic phase inversion emulsification of alkyd in water using an anchor impeller and a jetstream mixer.

The research project was conducted in cooperation with Binding lab, Exterior lab, Jotun AS the Colloid and Polymer Chemistry group at Department of Chemical Engineering, NTNU. Jotun uses alkyd emulsions as binder in several of their exterior products, and it is in their interest to gain more knowledge about the phase inversion and the properties affecting it, in order to expand the use of alkyd emulsions.

In this project, different variations of a reference emulsification system have been tested in order to gain knowledge of the inversion point and the emulsion properties pre and post inversion. The conductivity was measured continuously during the emulsification process, and samples were taken at different intervals. The samples where tested in order to find continuous phase, droplet size distribution, e-critical values for current conduction, optical density (NIR) and viscosity. One of the emulsions was tested with NMR by Antek AS on behalf of Jotun AS. An overview of all the performed emulsifications with some key results are presented in Appendix A.

The droplet size and droplet size distribution are important for the stability of the emulsion. The knowledge of the rheological properties is important for effective processing to be achieved. The high viscosity of the alkyd resin and emulsion

presents difficulties during dispersion manufacturing (Watson, et al., 2002) and affect the final droplet size. The conductivity and e-critical value offer information on the continuous phase of the emulsion, and on how close to water continuous phase the emulsification is.

2 Theory

An emulsion is a thermodynamically unstable mixture of two immiscible liquids, in this case alkyds and water. In the case of alkyd emulsions they can be classified as a water-in-oil (w/o) or an oil-in-water (o/w) emulsion and need to be stabilized by the use of surfactants. The theory is retrieved from an earlier study; Alkyd emulsification: A screening of different analytical methods to gain knowledge of the inversion point during alkyd emulsification (Lefsaker, 2012). The theory in chapter 2.1 is from (Guren, 2008) and (Bjerve, 1995) provided by Jotun, and (Mørk, 1991) and (Opedal, 2011), if not specified otherwise.

2.1 The Chemistry

2.1.1 Alkyds

An alkyd is an ester-based polymer that is modified with an oil or fatty acid. The polyester is derived from a polycondensation reaction between a polyhydric alcohol and a polybasic organic acid as seen in equation 2-1.

$$\boldsymbol{Alcohol}\,(-\boldsymbol{COH}\,) + \boldsymbol{Acid}\,(-\boldsymbol{COOH}) \rightarrow \boldsymbol{Ester}\,(-\boldsymbol{COOC}\,-) + \boldsymbol{Water}\,(\,\boldsymbol{H_2O}) \qquad 2\text{-}1$$

An example of a typical condensation polymerization is shown in Figure 1.

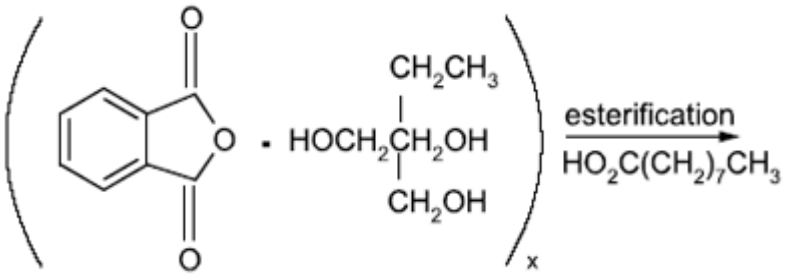

Figure 1: Phthalic Anhydride and Trimethylol propane form a typical esterification process (Can, 2010)

In addition the alkyd contains an oil or a fatty acid. These are all of vegetable nature and contain a chain of about 18 carbon atoms. The type and extent of oil or fatty acid addition has a significant effect on the properties as well as the oil length and acid number. Increased oil length gives decreased viscosity and the size of the chain is important for properties as drying time, hardness, flexibility and durability of the film. A typical alkyd molecule is shown in Figure 2.

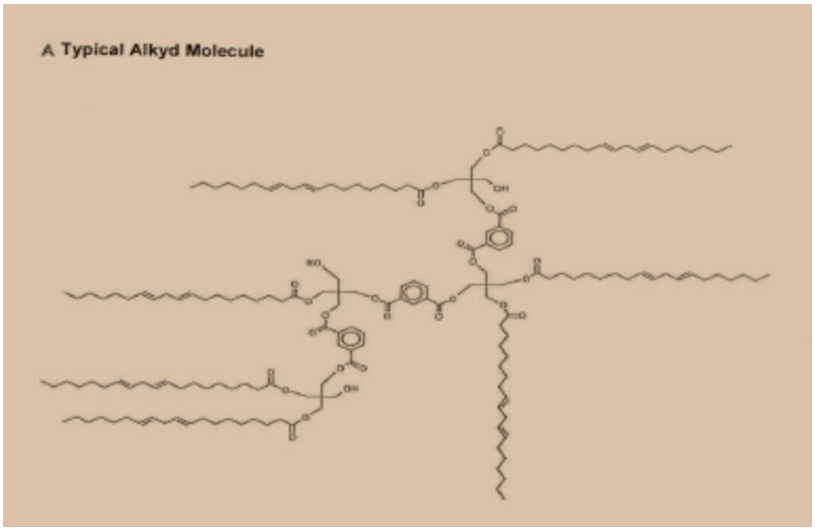

Figure 2: An example of an alkyd molecule consisting of 7 parts fatty acids, 3 parts of Isophatalic acid (dibasic acid) and 4 parts Pentaerythritol (tetravalent alcohol) (Guren, 2008).

A pure alkyd is often very viscous (~200 Pa *s, 20^{o}C) and difficult to handle (Watson, et al., 2002). To be useful in paint production it needs to obtain a lower viscosity. To obtain this viscosity it needs to be thinned with a solvent. Commonly used solvents include white spirit, high flash and dearomatized white spirit and xylene. It can also be made water borne by emulsification.

2.1.2 Surfactants

Surfactants are amphiphilic substances containing both hydrophilic and lipophilic groups. They have a tendency to adsorb onto a surface or interface and hence affect interfacial properties. In an emulsion the surfactants usually are classified as emulsifying agents. A surfactant is, due to the amphiphilic properties, unwanted in both the oil and water phases, the hydrophilic part will orient itself towards the water while the hydrophobic part will form the border layer to the oil phase.

Micelles are thermodynamically stable aggregates of surfactants. At a certain surfactant concentration, known as the critical micelle concentration (CMC), saturation of surfaces occurs and micelles will start to form in the solution. The CMC can be affected by any counter ions or electrolytes present, by pH and by temperature conditions.

The formation of micelles is a thermodynamically favourable spontaneous process, having a negative ΔG, and affects properties such as viscosity, solubility and osmotic pressure of the solution. They can have different structures dependent on the composition of the solution, fraction of surfactants and temperature. The surfactants will orient in micelles or reversed micelles in an emulsion depending on whether the emulsion is water continuous or alkyd continuous. Other structures are formed in situations and solutions where these are more thermodynamically favourable. Figure 3 shows possible micelle aggregate structures dependant on emulsion type.

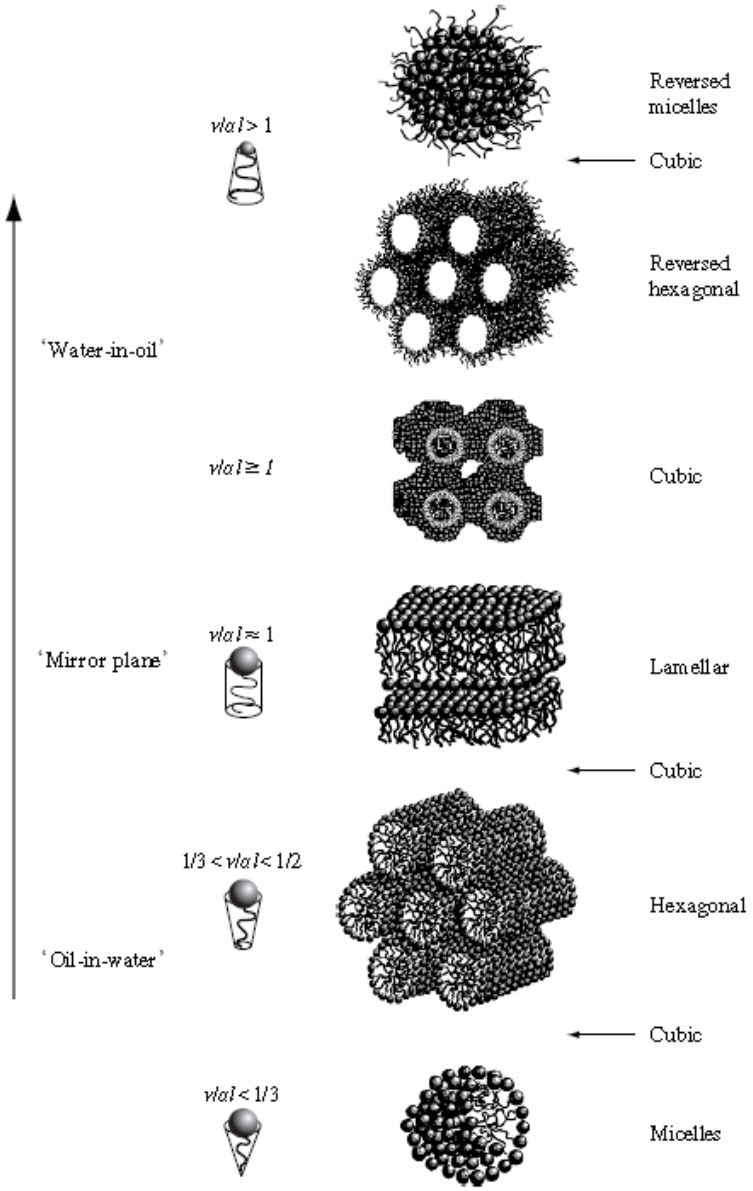

Figure 3.27 Critical packing parameters (CPPs) of surfactant molecules and preferred aggregate structures for geometrical packing reasons

Figure 3: Micelle structures dependent on critical packing parameter and continuous phase (Holmberg, et al., 2003).

Surfactants can be classified as natural and synthetic, and the synthetic surfactants can be either traditional or polymeric. There are four different groups of traditional surfactants classified by their hydrophilic properties and low molecular weight, anionic, cationic, amphoteric or non-ionic. The anionic surfactants are the largest group of surfactants. They are generally not compatible with cations and are sensitive to hard water and salts, as in electrolytes.

The polymeric, non-ionic, surfactants have high molecular weight and complex structures. They adsorb permanently and more strongly than the traditional surfactants. These properties apply even at higher temperatures and more concentrated electrolyte solutions (Holmberg, et al., 2003).

A schematic drawing of a proposed non-ionic surfactant addition to polymers can be seen in Figure 4 (Wang, et al., 1996). The non-ionic surfactant can be used as thickener and an initial thickening effect can be attributed to the increase in the polymer effective volume due to surfactant addition as seen in picture a, Figure 4 (Wang, et al., 1996). Further addition of surfactant can result in a polymer complex being surrounded by surfactants as seen in picture b, Figure 4. This will decrease the effective volume and the polymer micelle interaction and the viscosity will go down. As even more surfactants are added the intermolecular attraction between the hydrophobic groups of the excess surfactant will results in clusters and a rising viscosity (Wang, et al., 1996).

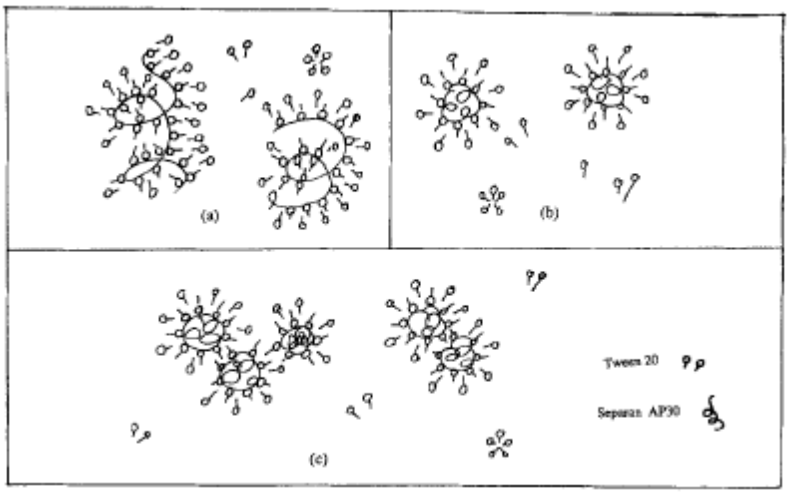

Figure 4: A possible sequence of events for surfactant addition to a polymer chain (Wang, et al., 1996)

Similar observations have been seen using non-ionic surfactant and an aquatic solvent (Kientz, et al., 1994). It is suggested that the attraction between the ethylene oxide segments of the surfactants is through hydrogen bonds with water molecules as seen in Figure 5. In this way, the interactions will be water dependent and the amount of bonds will increase with increased amount of water.

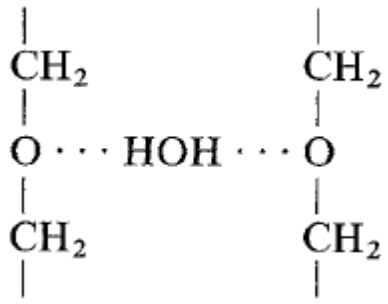

Figure 5: A suggested hydrogen bonding between the ethylene oxide segments of non-ionic surfactants via water (Kientz, et al., 1994).

2.1.2.1 Hydrophilic lipophilic balance (HLB)

As stated the surfactant contains both hydrophilic and lipophilic groups. The relationship between these, called the hydrophilic lipophilic balance (HLB), controls the emulsifying properties of the surfactant. It is a concept proposed by Griffin in 1949 in order to have a quantitative, but empirical, scale to describe the dispersal efficiency behaviour. The HLB is a numerical, but non-theoretical concept based on an experimental method. Each emulsifier is assigned a HLB number based on the observed stability of the emulsion. The HLB number summarises a vast amount of experimental work and expresses it through a single numerical scale indicating the HLB in the emulsion (Gooch, 2002).

The procedure is based on a specified test oil and water to be emulsified. The two primary reference emulsifiers are Oleic acid and Potassium oleate, Oleic acid given HLB number 1.0 and Potassium oleate HLB number of 20.0. The numbers indicate that the Oleic acid is the lipophilic component and the Potassium oleate is the hydrophilic component. All subsequent values for HLB can be derived from these standard references. Emulsifiers can also be utilized as mixed components having Wx as weight of emulsifier x and HLBx as HLB number of component x. The new HLB number can be found using equation 2-2 (Gooch, 2002).

$$\frac{W_a+HLB_a+W_b+HLB_b}{W_a+W_b} = HLB_{ab} \qquad 2\text{-}2$$

Some HLB numbers for different applications are indicated in Table 1. It can be seen that emulsifiers for w/o emulsions should be hydrophobic, low HLB numbers, and for o/w it should be significantly higher in terms with Bancroft's rule. The essence of Bancroft's rule is that water-soluble emulsifiers tend to facilitate o/w emulsions and oil-soluble w/o emulsions (Holmberg, et al., 2003) (Bancroft, 1913).

Table 1: HLB numbers in range for different applications (Elementis Specialties, 2011)

HLB value	Surfactant properties
0 – 3	anti-foaming agent
4 – 6	W/O (water in oil) emulsifier
7 – 9	wetting agent
8 – 18	O/W (oil in water) emulsifier
13 – 15	detergents
> 15	solubiliser or hydrotrope

The HLB requirement of a specific oil is determined as the HLB number of the ratio of reference emulsifiers giving the most stabile emulsion (McCutcheon, 1977). An understanding of the HLB values and solubility is important with respect to chemical relationships, between resins and monomers, and conditions when selecting

surfactants. Arbitrary surfactant selection for emulsification of monomers will most likely produce unacceptable results. In general, two surfactants are used when stabilizing an emulsion, one with low HLB and one with high HLB, from internal and external side of the interphases (Aserin, 2008).

2.1.2.2 Neutralization

The emulsion needs to be neutralized in order for it to be more compatible for use in paints. Neutralization of the alkyd means to neutralize the carboxylic acid groups present on the alkyd chain, by transferring a proton. Neutralization of the carboxyl groups also contributes to a higher charge density and a reduction of the interfacial tension, minimizing the need for expensive surfactants (Tuck, 2000). It makes the emulsification process easier to perform by creating ionic groups on the alkyd, making it more dipole and reducing the interfacial tension towards the water. The more neutral the smaller the droplets and the droplet size distribution (Zhaoting, et al., 2001). The neutralization mechanism, making the soluble salt, is illustrated in Figure 6.

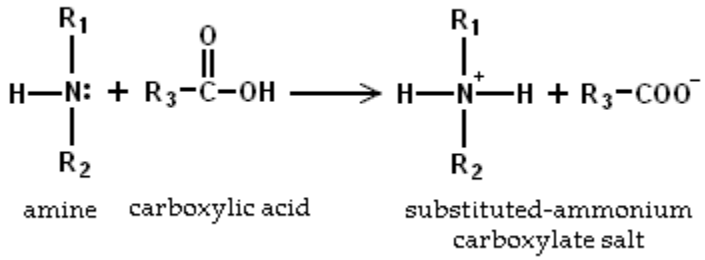

Figure 6: Amine neutralization of a carboxylic acid

The positive ammonium group can stabilize the charge, for example on the oxygen on the non-ionic surfactant, reducing its ability to connect to water.

Without neutralization, the non-ionic surfactant is more active towards the water and the viscosity will rise.

2.1.3 Emulsions

An emulsion is per definition a mixture of two immiscible liquids where the dispersed phase is solubilized as small droplets (0,1 – 10 µm) in a continuous phase (Chen, 2006). They can be characterized in two general ways; oil-in-water (o/w) and water-in-oil (w/o) emulsions. Other more complex double emulsions, water-in-oil-in-water (w/o/w) or oil-in-water-in-oil (o/w/o), may also occur, but of these the knowledge is more limited (Garti, et al., 2001). Double or even more multiple emulsions, are emulsions of emulsions consisting of one dispersed liquid that are further dispersed in another liquid and so on. The liquid layers can be repetitive as for the w/o/w/o or consisting of different liquids (Aserin, 2008). A schematic over the different emulsion types is shown in Figure 7.

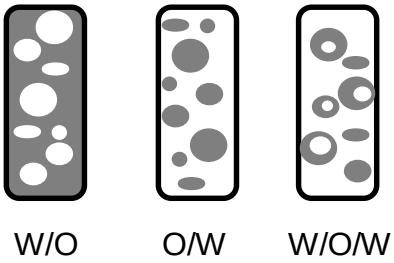

Figure 7: Emulsion types (Opedal, 2011). Left: Water-in-oil, Centre: Oil-in-water, Right: Water-in-oil-in-water

Emulsions are rated thermodynamically unstable but several emulsion systems exhibit a lifetimes of several days and months. These emulsions are kinetically stabilized and the stability can be studied considering three different scenarios, flocculation, sedimentation /creaming and coalescence (Chen, 2006). Figure 8 shows an illustration of the different scenarios. An emulsion is considered kinetically stabile when the number of droplets, droplet size distribution and arrangement of droplets do not undergo any significant change over the storage time scale (Sanchez, et al., 2001).

The droplets need to be small enough to withstand these destabilizing scenarios for a reasonable amount of time. The droplet size depends on surfactant-to-oil ratio, and route of emulsion preparation. For nano-emulsions (20-500 nm), Brownian motion prevents sedimentation or creaming increasing the stability of the emulsion (Patrick, et al., 2004).

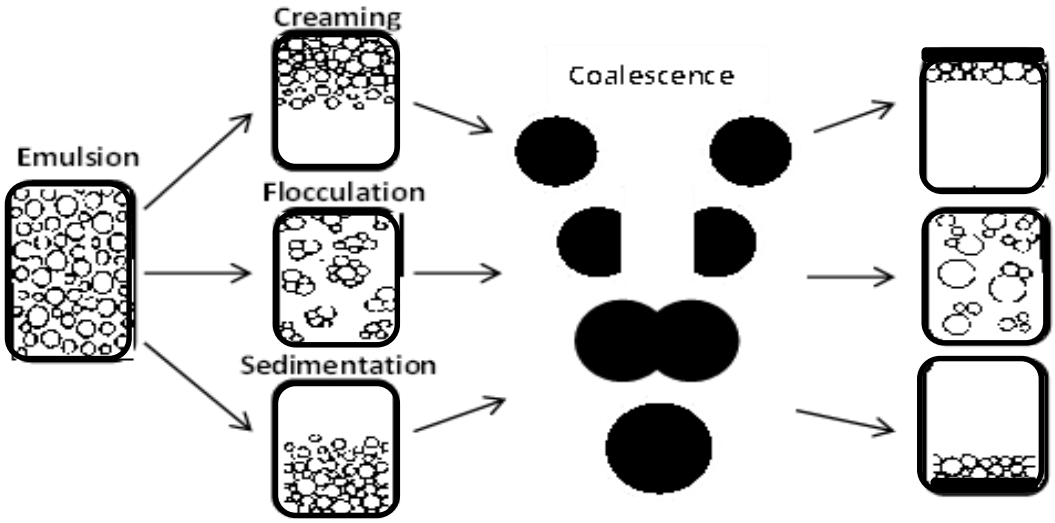

Figure 8: Illustration of possible stability and breakdown scenarios for an emulsion (Holmberg, et al., 2003)

Double emulsions consist in practice of large and poly-disperse droplets that are thermodynamically unstable and have a strong tendency for coalescence, flocculation and creaming (Aserin, 2008).

2.2 The emulsification process

Since emulsions are thermodynamically unstable they will not be forming spontaneously. Energy must be provided in order to make emulsions. The energy must be sufficient to break up one of the phases into small droplets, which can be dispersed and stabilized in the other phase.

2.2.1 Emulsification procedures

Emulsions can be made by rotating devices making shear forces in the solution. The shear stress induces different effects on the dispersed droplets. First they start to rotate, and by that inducing a momentum within the large droplets. The momentum makes the liquid start to circulate within the boundaries of the droplet. Circulation velocity of the liquid within the droplet will at a certain level make the droplet elongate. As the droplet elongates the momentum will make the droplet eventually breakup, as can be seen in Figure 9 (Opedal, 2011). Break-up occurs if the stress due to the circulating flow is greater than the stress from interfacial tension stabilizing it (Nienow, 2004). This mechanism of stretching of droplet interface and eventual breakup is explained further in (Sanchez, et al., 2001).

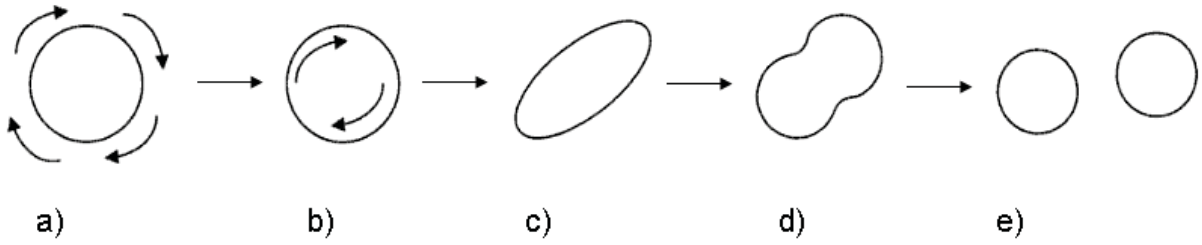

Figure 9: Droplet breakup induced by shear flow (Opedal, 2011). a) Droplet rotation, b) Circulation of liquid within droplet boundaries, c) Elongation of droplet, d) Increased elongation, e) Droplet disruption.

The viscosity of the alkyd resin should preferably provide the shear necessary for this type of droplet size reduction.

Emulsification conditions are critical because they have a great influence on the intermediate and final emulsion properties. Especially the conditions before the inversion point are critical. This is especially linked to the viscosity of the oil and the possibility of multiple emulsion formation (Galindo-Alvarez, et al., 2011) The conditions determine the water droplet size in the W/O emulsion, and are therefore proposed to determine the final resin droplet size as well (Sanchez, et al., 2001).

To create an emulsion an impeller driven by a powerful motor, capable of providing good mixing and axial flow within a high viscosity system, is required. Temperature control of the reaction is also required to control the quality of the emulsion product. The droplet size will be lower because the coalescence rate is lower at lower temperatures. The mixing and flow is critical for a successful emulsification. There is no need for high-speed stirring; in fact, low speed stirring minimizes the risk of air bubbles and foaming, and decreases the energy consumption (Sanchez, et al., 2001).

2.2.2 Direct emulsification

During direct emulsification the phase in which the surfactants is most soluble is placed in the vessel first. The second phase is gradually added and dispersed during direct emulsification (Jahanzad, et al., 2009). The process corresponds to Bancroft's rule; saying that the phase were the surfactant is most soluble becomes the continuous phase (Bancroft, 1913). When creating an alkyd emulsion this means to start with the water phase and gradually add, and disperse, the alkyd.

2.2.3 Catastrophic Phase Invention (CPI)

The emulsification procedure applying the catastrophic phase inversion (CPI) involves the addition of water to a mixture of alkyd and surfactants. Emulsion inversion is a process in which the curvature of the liquid-liquid interface changes towards the initially continuous phase (Galindo-Alvarez, et al., 2011). When fist starting to add water, an abnormal emulsion is created. An abnormal emulsion is an emulsion in which the surfactant has more affinity toward the dispersed phase. Abnormal emulsions do not obey Bancroft's rule and are extremely unstable (Bancroft, 1913).

As more water is added the viscosity of the emulsion increases, and at a critical phase ratio the emulsion inverts the water-in-oil (w/o) emulsion to an oil-in-water (o/w) emulsion. Catastrophic inversion occurs because of the complete coalescence of an unstable emulsion morphology. The inversion point is when the dispersed phase, initially water, becomes the continuous phase (Jahanzad, et al., 2009). Figure 10 shows an overview of the possible schematics of the catastrophic phase inversion.

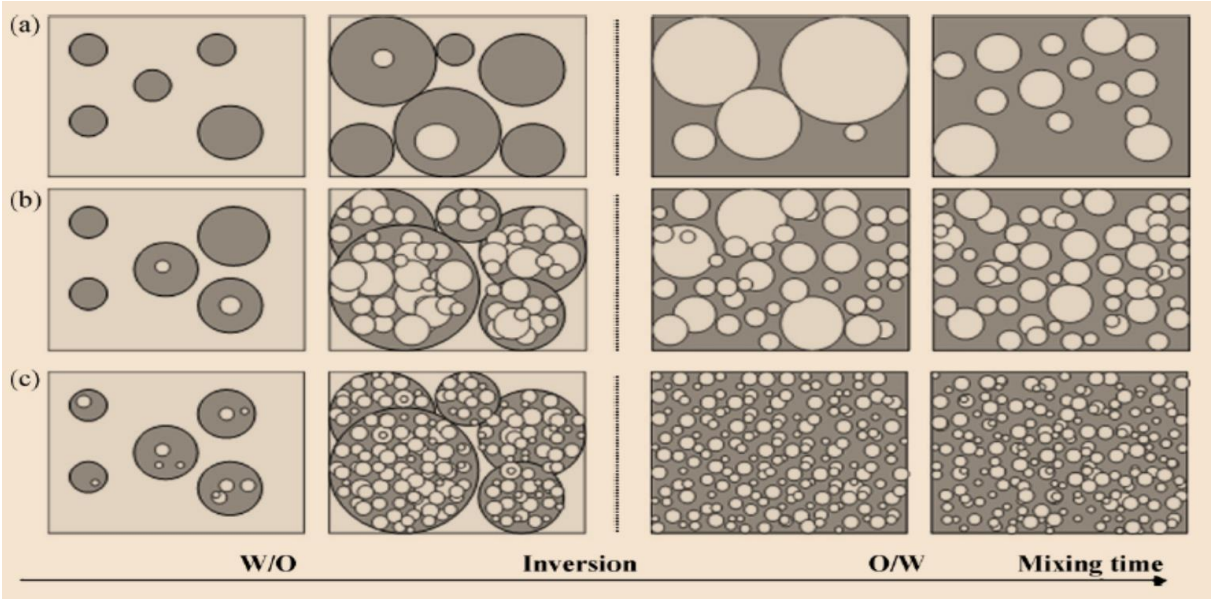

Figure 10: A schematic presentation over the time evolution of droplet size and morphology with mixing time before and after inversion. a: low [s] b: high [s] and high HLB c: high [s] low HLB (Jahanzad, et al., 2009)

The CPI is a preferred emulsification procedure over direct emulsification when making alkyd emulsion with external emulsifier. This is due to the results yielding smaller resin droplets and narrower droplet size distribution (DSD) at lower surfactant concentration. It also possesses good reproducibility and emulsion control (Jahanzad, et al., 2009).

2.2.4 Agitation

Agitation or other types of energy addition are necessary in order to form an emulsion. There exist many different techniques, but in this study, two different agitators are tested.

The anchor impeller, seen in Figure 11 a), is an agitator suitable for mixing of high viscosity liquids (5 – 100 Pa s) (Autoclave, 2013). As can be seen in Figure 11 a), it has a simple fluid pattern suitable for stirring viscous, pseudo plastic and thixotropic fluids (Pedrosa, et al., 2000). The impeller blades make it an effective stirrer even at low speeds (200 – 400 rpm).However the flow is radial, and will not secure mixing in non-radial directions. It is also crucial that the anchor follow the curvature of the bottom of the vessel in order to capture the discharge flow of the system. Stirring can be improved by increasing the height of the blades and putting in a blade support. However, considerations needs to be made concerning the energy consumption (Pedrosa, et al., 2000).

a)  b) 

Figure 11:a) Anchor impeller with stirring pattern (Autoclave, 2013). b) Jet stream mixer with stirring pattern (Ystral gmbh, 2013)

The alternative stirrer is a Jetstream mixer, as seen in Figure 11 b). Due to the low contact surface with the liquid, the speed needs to be higher (4500 rpm). The high-speed stirring will generate a jet stream directed towards the bottom of the vessel insuring a more effective mixing (Ystral gmbh, 2013). This stirrer provide a flow pattern more suitable for a homogenized mixing, not only stirring of the liquid. In comparison to the anchor impellor, it will homogenize the emulsion without any dead zones. On the other side, it is observed to be more sensitive to higher viscosity due to heat generation and high flow resistance.

3 Testing

3.1 Droplet size and droplet size distribution measurements

The testing of particle size and size distribution is important due to its impact on emulsions stability and viscosity, and hence on the final properties of the emulsion. It is only usable after the emulsion has started to invert, hence started to be soluble in water.

It was performed using the Malvern Zetasizer Nano ZS. The Zetasizer is used to study particle size and zeta potential of dispersions, emulsions, gas hydrates and similar chemical components using Dynamic Light Scattering.

3.1.1 Dynamic Light Scattering (DLS)

Dynamic light scattering (DLS), also called Photon Correlation Spectroscopy, is method for measuring particle size and particle size distribution of dilute suspensions from 2nm - 1µm. The DLS measures the Brownian motion and relates this to the size of the particles. The particles are illuminated by laser and the intensity fluctuations in the detected scattered light is analysed and related to Brownian motion (Malvern Instruments, 2004), as can be seen in Figure 12.

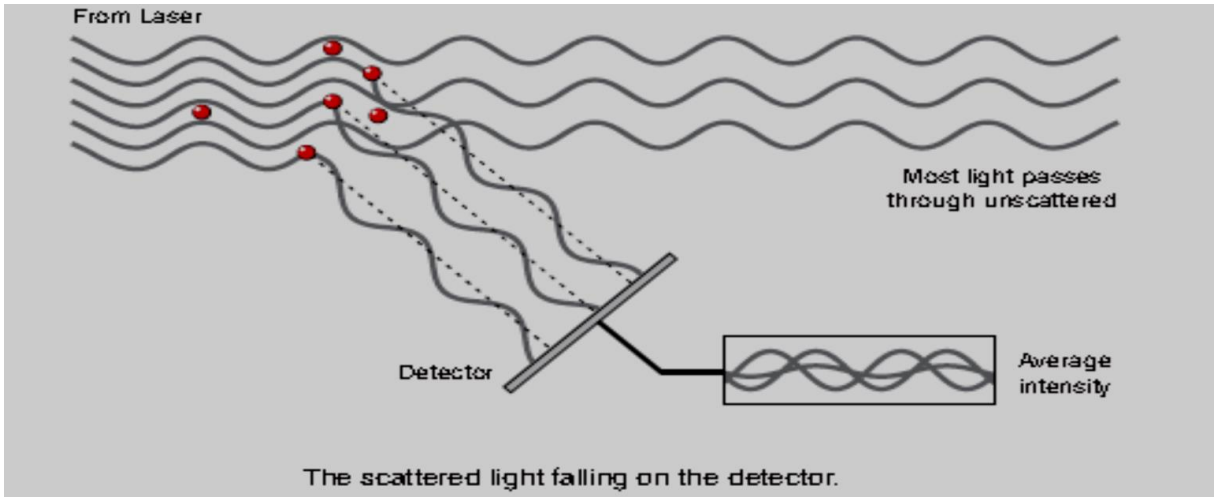

Figure 12: DLS principle. The scattered light is detected, and the average intensity and intensity fluctuating is recorded (Malvern Instruments, 2004).

If a small particle is illuminated it will scatter the light in all directions. The speckle pattern registered from the scattered light is affected by the Brownian motion and the intensity of bright spots detected can be seen to fluctuate. An important feature of Brownian motion related to the DLS theory is that small particles move quickly while large particles move more slowly. This means that the fluctuation will fluctuate quickly or slowly relative to particle size. The relationship between the size of the particle and the speed due to Brownian motion is defined in the Stokes-Einstein equation 3-1 (Sharma, et al., 2007).

$$\boldsymbol{D = \frac{RT}{N_A}\ \frac{1}{6\pi\eta r_u}} \qquad \text{3-1}$$

The D represents the diffusivity, or the Brownian speed of motion (NanoSight, 2012), R is the universal gas constant, T is the temperature, N_A is the Avogadro constant, ɳ is the viscosity and finally r_u is the hydrodynamic radius.

The Zetasizer measures this fluctuation, analyses it using a digital correlator, the correlation function can be seen in Figure 13, and relates it to the Brownian motion and further to the particle size by the Stokes-Einstein equation 3-1.

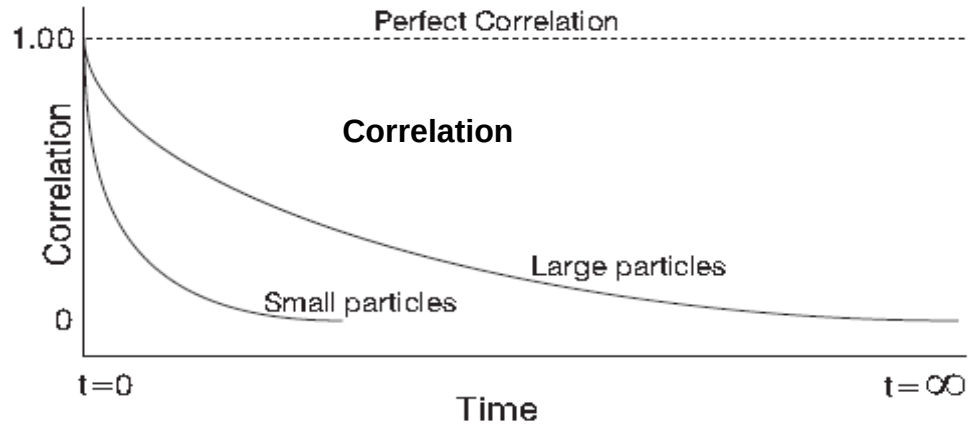

Figure 13: The correlation function (Malvern Instruments, 2004)

The correlation analysis also gives information about the polydispersity index (PDI). Non-Invasive Back Scatter technology (NIBS) is used, in order to achieve a higher sensitivity simultaneously with the size and concentration range. (Malvern Instruments, 2004)**.**

The emulsion should be diluted in order to avoid multiple spreading of the light, risking saturation of the light receptor. The standard operating procedure (SOP), describing the applied model, was provided by Jotun.

3.2 Conductivity

The conductivity of the emulsion during the emulsification process is important to track in order to follow the emulsion development through the whole process. It detect the changes in conductivity from oil continuous, through the inversion, to water continuous. Tracking the temperature is important considering its large impact on viscosity, hence influencing droplet size and quality of the final emulsion.

For mapping of conductivity and temperature of the emulsification the conductivity meter WTW Cond 315i, with a TetraCon^R 325 conductivity cell (cell constant 0.475 cm-1 ±1.5 %), was used. The WTW TetraCon325 conductivity measuring cell has a temperature sensor integrated in it (WTW, 2004). The conductivity is measured in µS/cm.

The electronic conductivity (κ) is defined as a solutions ability to transfer an electric current. It is the reciprocal of electrical resistivity (ρ), related to Ohm's law, as seen in equation 3-2, 3-3 and 3-4 (Young, et al., 2007). The conductivity cell measures the electrical resistance (R_E) between two similar electrodes. An alternating potential difference (V) is applied to one of the electrodes in order to attract the ions in the solution. The more ions in the solution, the more electric current (I) the solution can transfer. The conductivity meter measures the conductivity cell induced current (I) and uses Ohm's law, equation 3-4, to calculate the conductance (G). The conductivity (κ) can be calculated using the conductance (G) and the cell constant (C_{cell}), related to areas (S) and length between probes (L) for the cell, as shown in equation 3-5 (Xylem Inc, 2011).

$$\boldsymbol{R_E = \frac{V}{I}} \qquad 3\text{-}2$$

$$\boldsymbol{\rho = \frac{R * S}{L}} \qquad 3\text{-}3$$

$$\mathbf{G = \frac{1}{\rho}} \qquad 3\text{-}4$$

$$\boldsymbol{\kappa = G * C_{cell}} \qquad 3\text{-}5$$

The alkyd mixture does in itself not conduct any electric current, but at a certain water concentration the emulsion will invert from a w/o emulsion to an o/w emulsion and start to conduct a current (Weissenborn, et al., 2000).

3.3 E-critical cell

To control the conductivity measurements, and investigate the stability of the emulsion at different stages, it was necessary to apply an additional conductivity measurement. The e-critical cell gives useful information on the mobility and conductibility of water in the range prior to inversion.

Critical electric field emulsion stability cell is a method for testing of the stability of water within a water in oil emulsion. The method works by applying an electrical field, potential difference (V), to the emulsion. The critical electric field, E (V/cm), is defined as the electric field necessary to induce the formation of a water bridge that can carry the full current for the given distance, L (cm). The field is increased while the current (I) that passes through the emulsion is measured and logged against the volt applied (V) as seen in Figure 14.

The value of the will give information about the emulsion stability and relative information of how fare from the phase inversion point the emulsion is. The area and distance used for the cell is provided by a 10 mm diameter whole in a 0,5 mm thick Teflon sheet between two brass plates as seen in Figure 15 (Aske, et al., 2002).

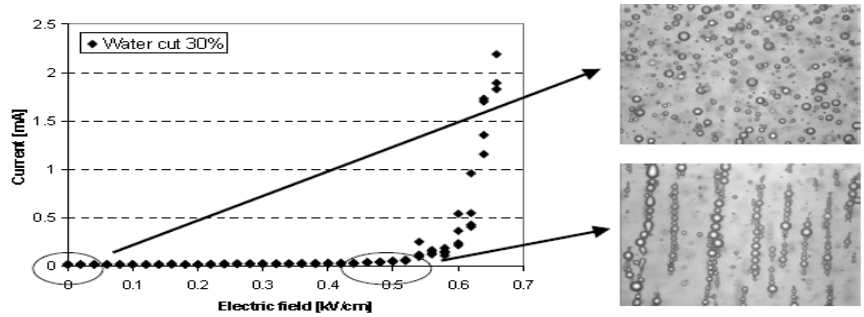

Figure 14: Emulsion droplets in an increasing electric field. Formations of water droplet lines make the transfer of currents possible (Aske, et al., 2002).

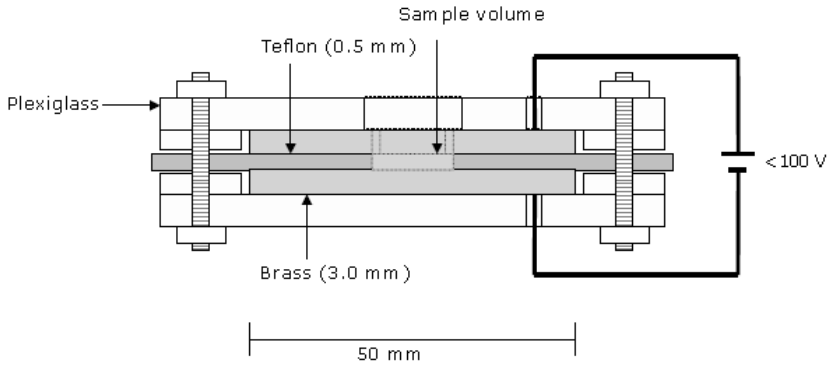

Figure 15: Critical electric field cell for emulsion stability measurements (Aske, et al., 2002).

3.4 Near Infrared Spectrophotometer (NIR)

The particle size evolution of water droplets in the oil phase is believed to give information of the pre-inversion and inversion part of the emulsification.

Fourier-Transform (Near) Infrared Spectrophotometer(NIR), Multi-Purpose Analyzer (Bruker Optics) is used for studies on particle growth and concentration. It has a spectral range from 12,800 - 4,000 cm^{-1} which allows for spectral characterisation in the near-infrared regime (Ugelstadlab, 2009).

In addition to provide absorption spectres, containing both overtone and combination bands which are not within the scope of this project, the near infrared spectra will provide information about particle size via baseline elevation (Kerker, 1969). The baseline elevation is due to light scattering by aggregates or particles in the solution. Lord Rayleigh has deducted an expression for the scattering cross section of a particle (σ_{sc}), presented in equation 3-6 (Kerker, 1969). This equation is presumed to be valid for particles with a small radius (r_p) relative to the wavelength ($r/\lambda \leq 0.05$).

$$\boldsymbol{\sigma_{sc}} = \frac{\mathbf{128\pi^5 {r_p}^6}}{\mathbf{3\lambda^4}} \left(\frac{\mathbf{n^2-1}}{\mathbf{n^2+2}}\right)^{\mathbf{2}} \qquad 3\text{-}6$$

Here λ represents the wave length and n is the ratio of the discrete phase to the continuous phase index of refraction. There are two assumptions to take in to consideration; the particle is so small that the electromagnetic field it experiences is uniform over the particle and that the particles are slightly lossy and dielectric. Fewer, but larger spheres are much more efficient scatters than the same mass of smaller spheres.

The light extinction, within the Rayleigh limit, can be considered a sum of the cross sectional contributions from the absorbance $\sigma_{abs}$and scattering σ_{sc} as seen in equation 3-7 (Mullins, 1990).

$$\boldsymbol{\sigma_{tot} = \sigma_{sc} + \sigma_{abs}} \qquad 3\text{-}7$$

The light extinction (I/I_0) depends on the number of particles (N) and the total cross section σ_{tot} according to equation 3-8 (Mullins, 1990).

$$\boldsymbol{\frac{I}{I_0} = \exp(-N\sigma_{tot})} \qquad 3\text{-}8$$

The optical density (OD), which is the scale used to measure the NIR spectra, can be related to the light extinction and the number of particles and particle cross sectional area by equation 3-9 (Mullins, 1990).

$$\boldsymbol{OD = \log\left(\frac{I_0}{I}\right) = 0,434N\sigma_{tot}} \qquad 3\text{-}9$$

The effect of multiple scattering is not accounted for in this equation. Figure 16 demonstrates the base line elevation for silica particles formed by a sol-gel process (Aske, et al., 2002).

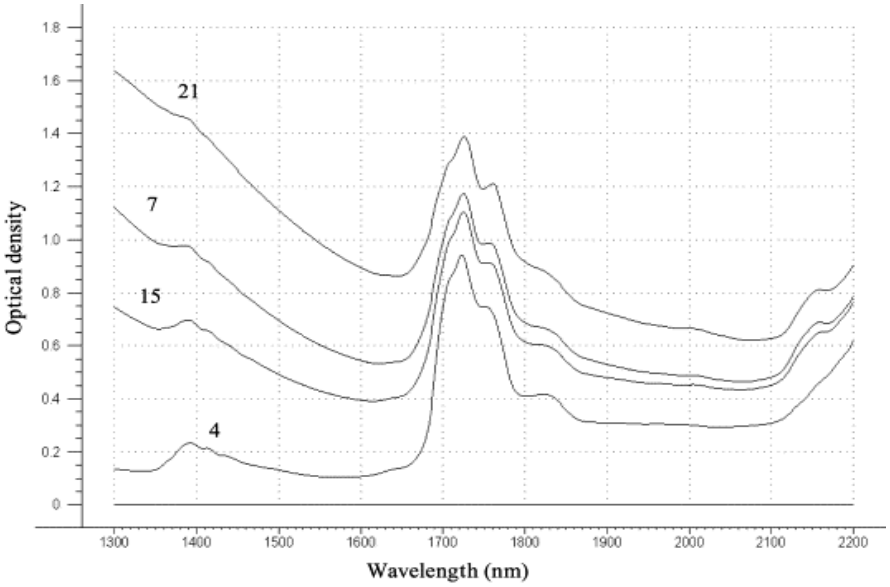

Figure 16: NIR spectra of the crude oils and condensates. The base line shift is clearly seen by the difference in optical density for sample 4, 15, 7 and 21 (Aske, et al., 2002).

3.5 Viscosity

The viscosity of an emulsion is an important property. It tells something about inter particle attraction within the emulsion. It can be considered a measure of frictional forces between the molecules in a liquid (Painter, et al., 1997). It gives useful information throughout the whole emulsification process and is of significant importance when calculating wear on the mixing installations.

The rheological properties of emulsions are complex and governed by droplet-droplet interactions. These interactions are in turn affected by factors as; dispersed phase fraction, continuous phase viscosity, droplet size distribution, droplet deformability, surfactant concentration, temperature, dispersion age and particle –particle interactions (Watson, et al., 2002) (Barnes, 1994).

In qualitative terms, the emulsions range from low viscosity, milk-like, Newtonian liquids, through thicker shear-thinning liquids, to thick creamy materials. The common element, in terms of microstructure, is the liquid continuous phase together with a liquid dispersed phase. (Barnes, 1994).

Well-understood quantitative theories of emulsion viscosity have not been developed. Probably because liquid state is an intermediate state of matter between gas and solid, and not easy to represent in terms of different characteristic properties of substances (Viswanath, et al., 2007). However, for suspensions of gas or solid particles in a liquid phase there are good models.

Theoretical models for viscosity estimations are suggested but are not yielding convincing results for general emulsions (Barnes, 1994). The simplified form of the so-called Krieger-Dougherty equation seen in 3-10, can closely describe the viscosity of a dispersion of particles (Barnes, 1994).

$$\boldsymbol{\eta = \eta_c \left(1 - \frac{\varphi}{\varphi_m}\right)^{-2}} \qquad 3\text{-}10$$

Here $\eta_c$is viscosity of the continuous phase and φ is the phase volume of the dispersed phase. As the dispersed phase fraction increases the dispersion rheology changes significantly due to increased interaction between the two phases. Especially at low fractions of dispersed phase, the continuous phase viscosity is the main factor determining the overall viscosity.

Under a steady macroscopic flow, the droplets of the emulsions are subject to two opposing effects. The viscous stress, of magnitude $\eta_c\dot{\gamma}$, which tends to elongate the droplets, as seen in Figure 9, and a stress of magnitude σ/R that tends to minimize the surface energy and maintain the droplet in a spherical shape. The equilibrium shape, referred to as the capillary number (N_{Ca}), is governed by the ratio of viscous stress to σ/r as seen in equation 3-11. r is the radius of the droplet, σ is the interfacial tension and $\dot{\gamma}$ is the shear rate. It the capillary number is low ($N_{Ca} \rightarrow 0$), the

deformation can be neglected and the droplets can be treated as spherical. (Pal, 2000).

$$\boldsymbol{N_{Ca} = \frac{\eta_c \dot{\gamma}}{\sigma/\mathrm{r}}} \qquad 3\text{-}11$$

In order to take into account the hydrodynamic interaction between neighbouring droplets when ($N_{Ca} \rightarrow 0$), Yaron and Gal-Or designed a cell model where λ is $\varphi^{1/3}$ and I (λ) is given by equation 3-12 (Yaron, et al., 1971).

$$\boldsymbol{I\,(\lambda) = \frac{5{,}5\,[4\lambda^7 + 10 - \left(\frac{84}{11}\right)\lambda^2 + \left(\frac{4}{\kappa}\right)(1-\lambda^7)]}{10(1-\lambda^{10}) - 25\lambda^3(1-\lambda^4) + \left(\frac{10}{\kappa}\right)(1-\lambda^3)(1-\lambda^7)}} \qquad 3\text{-}12$$

It follows that the viscosity can be calculated from equation 3-13 (Yaron, et al., 1971).

$$\boldsymbol{\eta_r = 1 + \mathrm{I}\,(\lambda)\varphi} \qquad 3\text{-}13$$

3.5.1 Cone and Plate Viscometer

The cone and plate viscometer is a rotational viscometer used for studying the rheological properties of both Newtonian and non –Newtonian fluids. In a rotational viscometer, the fluid sample is sheared as a result of the rotation of a cylinder or cone. The sharing occurs in a narrow gap between two surfaces, on stationer and on rotating (Kim, 2002). As can be seen in Figure 17, the gap where the sample is measured is a small space between an angled cone and a flat space. The shear rate of the fluid depends on the gap angle, α, and the linear speed of the plate. If the angle is less than 0,05 rad (3º) the rate of shear can be said to be uniform throughout the sample (Viswanath, et al., 2007).

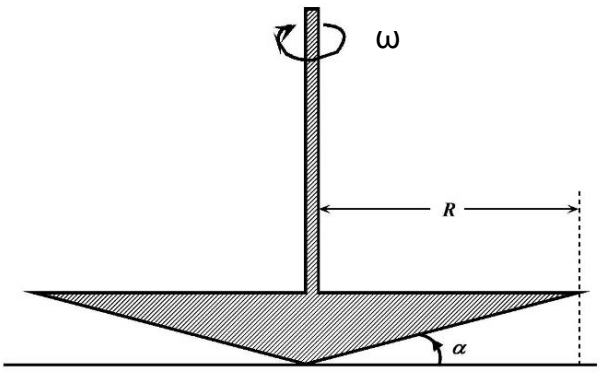

Figure 17: Cone and Plate Viscometer (Viswanath, et al., 2007).

The shear rate,$\dot{\boldsymbol{\gamma}}$, at a distance r from the axis, can be seen to be independent of r in equation 3-14.

$$\dot{\gamma} = \frac{r\omega}{r\alpha} = \frac{\omega}{\alpha} \quad 3\text{-}14$$

This independency of r, means that also the shear stress,τ, should be independent of r. The shear stress is defined as the force needed to keep a constant rotation speed. The total torque, M_{Tot}, can then be expressed as a function of the torque, M, and the area as seen in equation 3-15.

$$M_{Tot} = \int_0^R M\, r\, (2\pi r) dr = \frac{2\,\pi\, R^3\, M}{3} \quad 3\text{-}15$$

For a Newtonian liquid, the viscosity can then be obtained from equations 3-16 or 3-17 where the C is a constant provided by manufacturer (Viswanath, et al., 2007).

$$\eta = \frac{\tau}{\dot{\gamma}} \quad 3\text{-}16$$

$$\eta = \frac{3\, M_{Tot}\, \alpha}{2\,\pi\, R^3 \omega} = \frac{C\, M_{Tot}}{\omega} \quad 3\text{-}17$$

There are some possible errors associated with this type of viscometer. The effect of inertia forces and secondary flows are the two most important errors and modifications are made in order to account for these. However, in normal operations with well constructed and calibrated viscometers the errors are found to be minor (Viswanath, et al., 2007).

3.6 Nuclear Magnetic Resonance (NMR)

Measurement techniques based on Nuclear Magnetic Resonance (NMR) have become increasingly important and popular as a characterization tool in the field of emulsion technology (Peña, et al., 2006). The technique can be used to look at any stage of the emulsification, but has in this study been used for water droplet-size determination and to detect the inversion point.

NMR offer several advantages compared to the traditional droplet size determination techniques as microscope, Coulter-Counter and light-scattering. The emulsion can be tested in a non-destructive and undiluted state. This eliminates typical sources of error when measuring the droplet sizes with the mentioned techniques (Nordgård, 2009). All droplets are measured, which means that the droplet-size distribution is based on the whole distribution not only a statistical selection.

The method applied uses a combination of Puls-Field Gradient (PFG) NMR, Stimulated Echo (STE) and Carr-Purcell-Meiboom-Gill (CPMG) sequences. It measures diffusion, profiles and resolves oil and water signals for measuring attenuation that arises due to T_2 distributions. From these sequences, the droplet size distributions of water-in-oil emulsions can be found without making any assumptions on the shapes of the droplet shape distribution (Sørland, 2013) in Appendix B.

Extensive details about the NMR procedure and theory can be found in *Emulsion Stability Studied by Nuclear Magnetic Resonance (NMR)* (Opedal, et al., 2010), *Separation Profile of Model Water-in-Oil Emulsions followed by Nuclear Magnetic Resonance (NMR) measurements: Application Range and Comparison with a Multiple-light Scattering Based Apparatus* (Simon S, 2011) and in *Characterization of water in paint at different concentrations(Geir Sørland, 2013)* in Appendix B.

3.6.1 Water profile

The signal from the PFG – NMR sequence showed in Figure 18 contains contributions from both alkyd and water. The PFG – NMR technology utilizes the theory of restricted diffusion by studying the difference in relaxation time for oil and water in order to separate the signals (Opedal, et al., 2009).

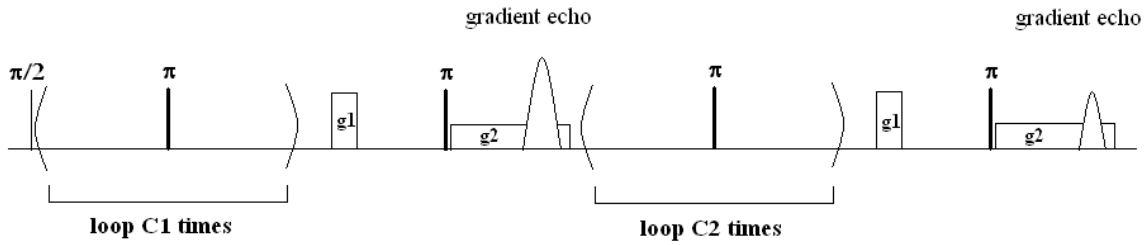

Figure 18: PFG-NMR sequence used for acquiring the water profile (Sørland, 2013) in Appendix B.

The alkyds have lower transverse relaxation time than water. The C1 loop in Figure 18 may therefore be used to supress the contribution from the alkyd leaving only the water contribution. The first gradient echo is from water only, and can be Fourier transformed into a water profile. The second echo, using longer observation time, returns a second water profile that can be used to correct for transverse relaxation of water. The profile obtained is proportional to the water content along the sample. A calibration, with a sample containing 100% water, make it possible to return the water amount along the length of the sample.

3.6.2 Droplet size distribution

In order to derive the absolute droplet size distribution the square of the average droplet radius,$\bar{r}^2$, needs to be found. This can be found by fitting diffusion measurements at long observation times to equation 3-18. It can be correlated to the average *(1/T_2)* distribution, found from Carr-Purcell_Meimboom-Gill (CPMG) (Palmer, 2012) measurements, trough equations 3-19 and 3-20 in order to find the droplet size independent relaxivity, ρ (Opedal, et al., 2009).

$$\frac{\mathbf{I}}{\mathbf{I_0}} \approx \mathbf{exp}^{-\frac{\gamma^2\delta^2 g^2 r^2}{5}} \qquad 3\text{-}18$$

$$\overline{\left(\frac{1}{T_2^2}\right)} \approx 9\rho^2 \overline{\left(\frac{1}{r^2}\right)} \qquad 3\text{-}19$$

$$\rho = \frac{1}{3}\sqrt{\overline{\left(\frac{1}{T_2^2}\right)}^2 \times \left(\frac{\overline{T_2^2}}{\overline{r^2}}\right)} \qquad 3\text{-}20$$

Assuming an independent relaxivity it can be used, in equation 3-21, to find a linear relation between T_2 and the volume to surface ratio. The droplet size distribution is derived from the volume to surface ratio, a measure of the droplet size given in equation 3-22. It is normalized by multiplication with the surface relaxivity and in absolute units.

$$\rho = \frac{1}{3}\sqrt{\left(\frac{\overline{1}}{T_2^2}\right) \times \left(\frac{\overline{1}}{r^2}\right)^{-1}} \qquad 3\text{-}21$$

$$T_2 \approx \frac{V}{S\,\rho} \qquad 3\text{-}22$$

3.6.3 Separation of signal

The most straightforward way of separating the water contribution from the contribution of alkyd is when the viscosity of the alkyd is much higher than of the water. The relaxation times will be significantly different, either in the longitudinal or in the transverse direction. The NMR signal may be stored for full recovery of the alkyd signal, back to the thermal equilibrium, while the water signal still can be measured. In Figure 19, the T_2 distribution of a water in oil emulsion system with short and long z-storage intervals. By increasing the duration of the z-storage the alkyd signal can be omitted. The two short interval tops correspond to the alkyd signal left (0,05), and the water signal right (0,7).

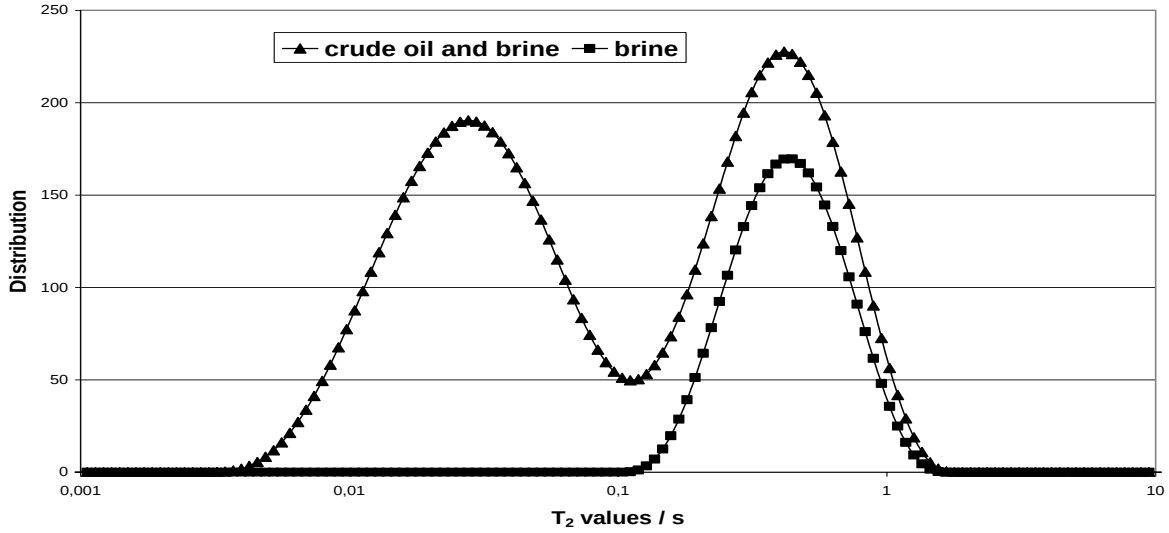

Figure 19: Z-storage of NMR signals and the effect of z-storage delay to obtain the T2 distribution of water alone. (Sørland, 2013) in Appendix B.

3.6.4 Alternative water profile method

The alternative method for acquiring water profiles is not yet published and will therefore not be described in detail. The technique supresses the part of the water that possesses high mobility. This represents water present in big droplets (>60 µm) or in a bulk phase.

3.6.5 Diffusion experiment

The water populations can also be investigated using diffusion experiments from the NMR instrument. Analysis of the behaviour of the two diffusion coefficients in the emulsions shows that the contribution of hindered diffusion increases relative to that of restricted diffusion with increasing energy input during production. Highly homogenized emulsions accordingly contain almost only hindered water (Berg, et al., 2004). These measurements have the possibility to reveal presence of different populations and also prove when inversion can take place. The inversion will take place at the water concentration where the water diffusivity is significantly enhanced compared to previous tests. The attenuation of the NMR signal can be plotted as a function of applied magnetic field gradient strength. The slope of the attenuation is then directly related to the diffusivity according to equation 3-23. Al parameters except the molecular diffusion coefficient D(***Δ***) and the gradient strength (g) is fixed. The slope of the signal is therefore only dependent on the diffusion (Sørland, 2013) in Appendix B.

$$I = I_0 e^{-2(\gamma^2\delta^2 g^2 D_{(\Delta)}(\Delta+\frac{3\tau}{2}-\frac{\delta}{6}))} e^{-2(\frac{\Delta}{T_1}+\frac{4\tau}{T_2})} \quad \textbf{3-23}$$

4 Experimental

The experimental procedure has been by Jotun As. A risk assessment has been performed and is provided in Appendix C.

4.1 Alkyd preparation

In the following emulsions long chain oil modified alkyds provided by Jotun AS are used. The viscosity of the alkyd resin is high (~3 Pa s) and a function of temperature. The sample needs to be preheated to a suitable temperature to ensure good mixing conditions. For the alkyd resins used in the following emulsions 60 ^{o}C is sufficient for mixing. The alkyds are heated to 60^{o}C overnight in order to ensure uniform temperature throughout the alkyd. After mixing, and before emulsification, the alkyd mixtures are cooled during continuous stirring to a suitable emulsification temperature, being 35^{o}C, 40 ^{o}C or 60 ^{o}C depending on alkyd and process equipment.

4.2 Surfactant preparation

Anionic and non-ionic polymeric surfactants, chosen by Jotun, are used in the emulsions. They are chosen based on trial and error, and the HLB values are not specifically considered. However, the HLB value of the standard non-ionic surfactant is reported by Jotun AS to be in the oil-in-water supporting region, HLB 8-18 in Table 1 in chapter 2.1.2. The anionic surfactant is chosen because it is oil soluble and often used as pigment wetter, dispersant for aqueous and non-aqueous dispersions, resin emulsifier and to ensure good compatibility. The polymeric surfactant is chosen as polymeric O/W emulsifier and dispersant, because it is considered to provide superior colloidal stability. It is tested to be excellent suitable for alkyd resin emulsification with minimum impact on film properties.

The polymeric surfactants are wax at room temperature and need to be heated overnight at 60 ^{o}C in order to be fully melted and compatible with the alkyd resins. The anionic surfactant and the neutralizer can be added at room temperature without compatibility problems.

4.3 Emulsification procedure

4.3.1 Preparations

The water needs to be tempered to 35 ^{o}C, 40 ^{o}C or 60 ^{o}C (+/- 2^{o}C) depending on the temperature for the emulsification. Details on temperatures for the different emulsifications can be found in Appendix D.

Alkyds, surfactants and neutralizer are weighed out in a reactor (2l, diameter 12 cm). The mixture is immediately put under stirring, and tempered to the desired temperature in a water bath.

The stirrer is either an u-shaped anchor impeller (diameter 8 cm) operated by an IKA^{R}-Werke Eurostar digital stirrer, with scale 50 – 2000 rpm or a jetstream mixer (diameter 6 cm) run at 4000 rpm. The ideal stirring, found experimentally for the anchor impeller, giving good circulation without pulling in air was 200 rpm – 600 rpm depending on the viscosity of the emulsion. The temperature should ensure that the viscosity of the alkyd resin is able to provide the shear stress necessary for the droplet size reduction to occur.

The temperature for ideal starting viscosity is respectively 35 ^{o}C, 40 ^{o}C and 60 ^{o}C for the alkyd resin mixtures used. A temperature and conductivity meter is positioned in the reactor in a position so that it alters the stream as little as possible. Good fluid movement is ensured to prevent water collection around the probe. Figure 20 shows a setup of the equipment used.

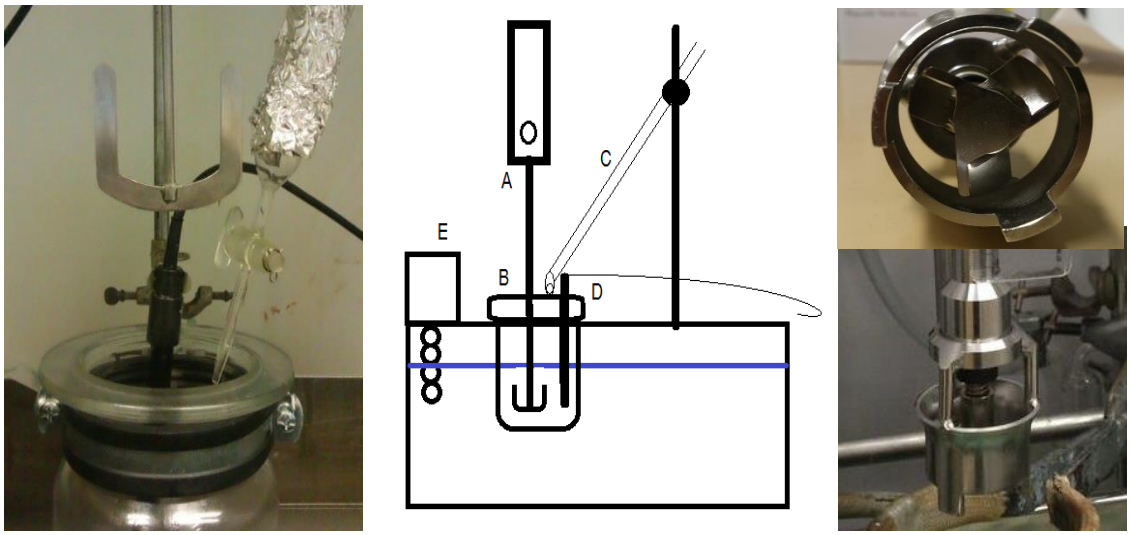

Figure 20: Left: Anchor stirrer. Middle: Emulsion equipment. A: Stirrer B: 2l reactor with u-style anchor stirrer C: Burette for addition of water D: Conductivity and temperature meter E: Heating devise for water bath. Right: Jetstream mixer

4.3.2 The emulsification

In order of making the emulsion a low shear u-shaped anchor impeller with powerful motor (IKA^{R}-Werke Eurostar digital stirrer), or a turbine Jetstream mixer (Ystral GMBH D-79282 Ballrechten) was used. The stirrer needs to be able to cope with high viscosity. A glass reactor (2l, diameter 12 cm), with temperature control either by double wall or by water bath, was used to hold the emulsion.

The water needs to be added at a certain dosage. A drip funnel was used for water addition and the dosage was approximately 20 mL/min. A stopwatch was started when the first drop hit the water, and the time, temperature, conductivity and water addition during the process was logged. The temperature should ideally be kept constant, within +/- 2 ^{o}C of emulsification temperature, so the temperature of the alkyd and the added water was logged as well. These data are available in the process reports in Appendix D.

The inversion point by mark of conductivity is approximated to occur after about 20-25 minutes or 400 mL – 500 mL of added water. The viscosity of the emulsion varies throughout the emulsion. Often it starts to thicken at around 10 minutes (200 mL) and keeps increasing until a maximum around 25 minutes (500 mL). From 25 minutes to approximately 30 minutes (600 mL) the mixture is at its most viscous and difficult to stir. After this maximum the viscosity decrease again and the emulsion ideally eventually becomes milky. This means that the agitation rate needs to be controlled dependently of the viscosity in order to ensure proper stirring and prevent foaming when the viscosity decreases again. Suggested guides to agitation control can be found in the process reports in Appendix D. After approximately 45-47 minutes, the water addition is stopped at 900 mL, and by 50 minutes, the emulsion should be finished.

The times are approximations and will wary from emulsion to emulsion depending on the process conditions, and the samples are logged, and referred to by water addition. The change into a milky fluid will not fully happen since the reactor is not big enough for addition of the last 120 mL of water that ideally will give it the milky consistency. Final emulsion needs to be filtered through a filter bag in order to remove any spare alkyd particles. Testing of the final droplet size in a Nanosizer is important as an indication control of the quality of the emulsion.

4.4 Testing procedure

The testing is important in order to get the best possible understanding of the process. In an earlier work; Alkyd emulsification: A screening of different analytical methods to gain knowledge of the inversion point during alkyd emulsification were performed in an earlier study (Lefsaker, 2012). The test were performed in order of mapping the different test possibilities available in the Ugelstad laboratory. The most promising tests were conductivity, E-critical cell and NIR, and these were deployed during this project together with a rheometer test revealing the viscosity.

It is of great interest to test the emulsion around the inversion point, and the pre and post conditions. There was conducted a series of introductory emulsification experiments to test the comparability of the emulsions made using the u-shaped anchor impeller and those made with the jetstream mixer. All measurements used in the results were made within 12 hours of emulsification in order to avoid major coalescence of the possible unstable mid-emulsification emulsions.

4.4.1 Droplet size

Samples of the emulsion is taken at different intervals during the emulsification process, the specific sample times can be seen in Appendix D. The samples were dissolved, approximately one droplet of emulsion in 200 mL of distilled water, for some minutes before measured in the Nanosizer. The SOP used is provided by Jotun, and three parallels are run on every sample. Samples where the emulsion droplets not fully dissolves, typically early tests 0-10 minutes, the are not tested.

4.4.2 Conductivity

The conductivity is monitored during the emulsification process. The interval of logging can be found for the individual emulsifications in Appendix D.

4.4.3 E-critical cell

The E-critical field measurements were performed on undiluted samples, and there was run at least three parallels of each sample dependent on correlation of the measurements. It was performed only on the first emulsions, which emulsions and the individual sample times can be seen in Appendix D.

4.4.4 Near Infrared Spectrophotometer (NIR)

The NIR measurements are performed directly in the sample compartment, using an empty sample compartment as reference. The OP used was provided by the apparatus responsible engineer at Ugelstad laboratory. The individual sample times can be seen in Appendix D.

4.4.5 Viscosity

The viscosity tests are performed in a Rheometer (Physica MCR 301, Anton Paar) using Cone and Plate geometry (spindle CP40-2/S). The geometry used has a diameter of 39,975 mm, Angle of 2,009 ^{o}, and Truncation of 170 µm. The conversion factor is provided as, Css = 59616,6 Pa/Nm. A sample of about 1 mL where placed on the plate, the share rate was kept constant at 10 [1/s] while the shear stress, and calculated viscosity were logged after 10 measurement points (10 sek). Emulsions are generally unstable and the viscosity can change when exposed to strain, so the start viscosity is considered the most correct to measure. The individual sample times for each emulsification can be seen in Appendix D.

4.4.6 Nuclear Magnetic Resonance

Anvendt Teknologi AS performed the NMR measurements on request from Jotun AS. A low field NMR spectrometer with magnetic field 0.48 T, capable to deliver a gradient strength of 4 T/m, was used. The sinusoidal gradient pulse was 0.8 ms and directed along the length of the tube. For testing 4 mL of emulsion was placed in 18 mm NMR sample tubes. The operation temperature was 33 ^{o}C.

Five samples from different times of the emulsification process were studied. Water concentrations were approximately 10%, 18%, 25%, 30% and 35%. Droplet size distribution, surface to volume ratio (S/V) and water profiles were recorded assuming water droplets < 100 µm. A set of diffusion measurements were also performed to verify bimodality. The full report with experimental and results can be found in Appendix B.

4.5 Uncertainty assessment

The procedure is not optimal and there are uncertainties associated with the mixing and uniformity of the emulsion when samples are collected. Visually there can be seen gradients and stream differences in the emulsion at different times during the emulsification process for both stirrers. The high viscosity of the emulsions in certain emulsifications also provides uncertainties when it comes to proper stirring during the process and uniformity when sampling for these emulsions. Water can be seen to float on top of the emulsion at certain times, making the amount of water included in the emulsion in precise at sampling times.

Experimental difficulties, particularly related to control of water addition by drip funnels, make it impossible to exactly control or estimate the water cut. The water cut at each time is also extremely difficult to calculate and predict due to the almost continuous gathering of samples. Further work needs to be performed, using other techniques, to fully determine water cut at all times.

The uncertainty in water addition can be estimated to about ± 20 mL / 2 min. The water uncertainty, however, does not influence the property development of the conductivity significantly. As can be seen in the reproducibility graphs in Appendix E, and in all the graphs describing the conductivity development in chapter 5, the difference in offset for the conductivity rise is within approximately ± 20 mL, unless other factors are influencing the properties. The other properties can be seen to relate to the conductivity, and is therefore considered insignificantly influenced by the uncertainty in the water addition.

The uncertainty in the water addition does not seem to be a factor affecting the final properties of the emulsification. As can be seen, in Table 7 in Appendix A, the final emulsification properties do not seem to be significantly affected by small shifts in property changes, rather than direct deviations from the general trend. As long as the trend is followed within the borders of the respective periods, defined in chapter 5, the uncertainty in water addition seems to be of no major significance for the final emulsification.

There are uncertainties related to the role of surfactants during dilution of the samples when measuring the droplet size during the emulsification process. Spontaneous emulsification, caused by a surplus of surfactants in the emulsion, may be affecting the results from the nanosizer.

5 Results and discussion

The results reflect the monitoring and sequential testing of alkyd emulsifications using the different techniques presented in Chapter 3. The presented results only include successful emulsifications or emulsifications that illustrate interesting theories describing the emulsification process. Table 2 displays the emulsifications discussed in results and discussion. An overview of all the performed emulsifications is presented in Appendix A, including representative results from an earlier study on testing methods for alkyd emulsification (Lefsaker, 2012).

Continuous monitoring of emulsification properties of alkyd emulsifications is not something that has ben published on a large scale. Most of the research done on similar emulsifications or methods are internal research kept secret by commercial interests. There is therefore not much to compare the data obtained in this research to.

Trends in the emulsification process are presented relative to approximate water addition at the time of sampling. The droplet size and droplet size distribution, represented by the poly dispersity index (PDI), is used as a measurement for determining the quality of the end properties of the emulsion. The lower the values the better emulsification result. A good stability criterion for an emulsion is to obtain a final droplet size, of alkyd in water, below 300 nm and a size distribution below 0,1. All the inverted emulsions where found to satisfy the size criterion, but reveal small differences in the quality of the emulsion results. When considering the PDI some of the emulsions have values indication a possible instability. As can be seen in Table 2, the reference system, System 1, is a robust system when it comes to change of the process parameters investigated. The quality, defined by droplet size and PDI, is good and not significantly altered considering the large standard deviation (STD) by changes in process parameters. The differences might be more evident in other alkyd systems, as can be seen from the emulsion without neutralizer or the alternative alkyd test. The complete results with respect to water addition and time (minutes) after emulsification start, are presented along with process comments, in

the process reports in Appendix D.

Table 2: List of emulsions providing interesting information on the emulsification process, with final emulsification results.

Emulsion Nr	System Nr	Variation	Droplet size [nm]	STD [nm]	PDI
EML 9	1	Reference emulsification from earlier study	188		0,07
EML 16	1	Reference emulsification jetstream mixer	182	55	0,037
EML 17	1	Performed NMR measurements	179	47	0,058
EML 18	1	Reference emulsification anchor stirrer	183	55	0,054
EML 19	3	Reduced surfactant amount, no inversion	-		-
EML 20	2	Less non-ionic, more anionic surfactants	216	47	0,014
EML 22	4	Without neutralizer	256	120	0,167
EML 24	5	Without non-ionic surfactant	-		-
EML 25	7	Alternative alkyd	227	91	0,095
EML 26	1	Rapid water addition after inversion	174	45	0,048
EML 27	1	Slow water addition from 200 mL – 500 mL	193	59	0,043
EML 28	1	Stop in water addition	183	51	0,045
EML 29	1	Water leak	193	90	0,063
EML 30	1	Break after 300 mL	188	80	0,169
EML 31	1	Break after 200 mL	183	40	0,052
EML 33	6	Alternative surfactant	239	71	0,128

The results from the NMR tests performed by Antek AS (Sørland, 2013) in Appendix B, on EML 17 are presented in Table 3. The modality tells something about the affinity relationship of the droplets. Monomodality refers to droplets present in a unique mode, while a bimodal emulsion have droplets present in two different modes. The NMR results is discussed and related to the general emulsification trend, by means of water addition and emulsification periods presented in chapter 5.1.

Table 3: Results overview of NMR tests performed by Antek AS, at five different stages of the emulsification (Sørland, 2013) in Appendix B.

NMR sample	Water addition	Percent water	Period	Modality
NMR 1	160 mL	~10 %	1	Monomodal
NMR 2	280 mL	~18 %	2	Bimodal
NMR 3	400 mL	~25 %	3	Bimodal
NMR 4	500 mL	~30 %	3	Bimodal
NMR 5	700 mL	~38 %	4	Monomodal

5.1 General emulsification trends

A plot of the results from the four different test methods, Conductivity, Near-Infra-Red Spectroscopy (NIR), Viscosity and E-critical field, as a function of the amount of added water, is presented in Figure 21. It shows the tests run on a reference emulsion (EML 16), and the results are related to the NMR results, seen in Table 3, by water addition. A table presenting the approximate water additions and approximate presents of water added to the emulsion is presented in Table 4. Due to the frequent sampling the loss alkyd is accounted for by subtracting ca. 20 g per sampling.

Table 4: Overview of water addition and percent of water in the emulsion at specific times.

Time [min]	Water addition [mL]	Percent water	Period
0	0	~0 %	1
5	100	~7 %	1
10	200	~13 %	2
15	300	~20 %	2
20	400	~25 %	3
25	500	~30 %	3
30	600	~34 %	4
35	750	~40 %	4
40	900	~46 %	4

The four test methods cover all stages of the emulsification process, from alkyd continuous, through intermediate stages to water continuous. The viscosity test covers the whole emulsification process, while the e-critical and NIR spectra gives useful information until the middle of period three and conductivity from the middle of

Period 2 until past inversion in Period 4. The conductivity is normalized (*10^-2) in order to be easier to compare to the other tests on the same scale.

The periods are defined according to changes in process parameters. Period 1 is the initiation period where no big impact on process parameters occur. Period 2 is defined in order to cover the first emulsification trend, covering the local maxima in conductivity, NIR and viscosity, and the local minimum in E-critical value.

The plots in Figure 21 reveal that the results from the four different tests correspond, and display a clear trend regarding emulsion property changes. The viscosity maximum occurs later, but still follow the same trend. All the trends are reproducible and further results are presented in Appendix E.

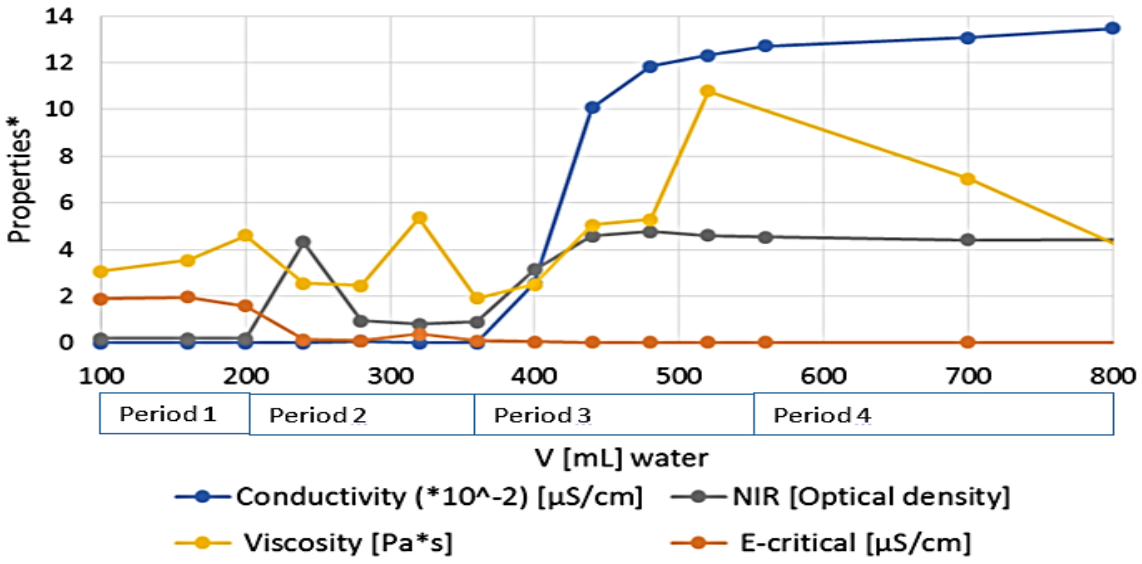

Figure 21: The properties of the emulsification process showed by: *Conductivity (*10-2), NIR, Viscosity and E-critical cell values as functions of water addition [mL]. The results presented are from the reference emulsion for jetstream mixer, EML 16.

The emulsion property trends can be divided in four periods as seen in Figure 21.

- Period 1, 0 mL – 200 mL of water, represents an introduction period where no major change in conductivity, NIR, e-critical value or viscosity occurs.
- Period 2 , 200 mL – 350 mL of water, covers the first trend in properties. It shows a local maximum in conductivity and NIR coinciding with a local minimum in the e-critical value.
- Period 3, 350 mL – 550 mL of water, includes the proposed inversion point marked by a significant increase in the conductivity followed by an increase in both NIR and viscosity coinciding with a breakthrough of the E-critical value.
- Period 4, 550 mL – 900 mL of water, represents the stabilization period where all the properties have stabilized.

As can be seen when examining the periods, especially Period 2 and Period 3 in Figure 22, the trends in the development of the four different properties coincide. In Period 2 there can be seen that the conductivity and NIR have local maximums at the same time as the E-critical value have a local minimum. The viscosity can be seen to follow the trend by having a local maximum shortly after the two other. In the same way the properties can be seen to develop in Period 3. The trend shows that a rapid rise in conductivity and NIR, coincides with a breakthrough, fall to zero, of the E-critical value. The viscosity also here follows with a maximum shortly after the conductivity and the NIR value have stabilized at their final values.

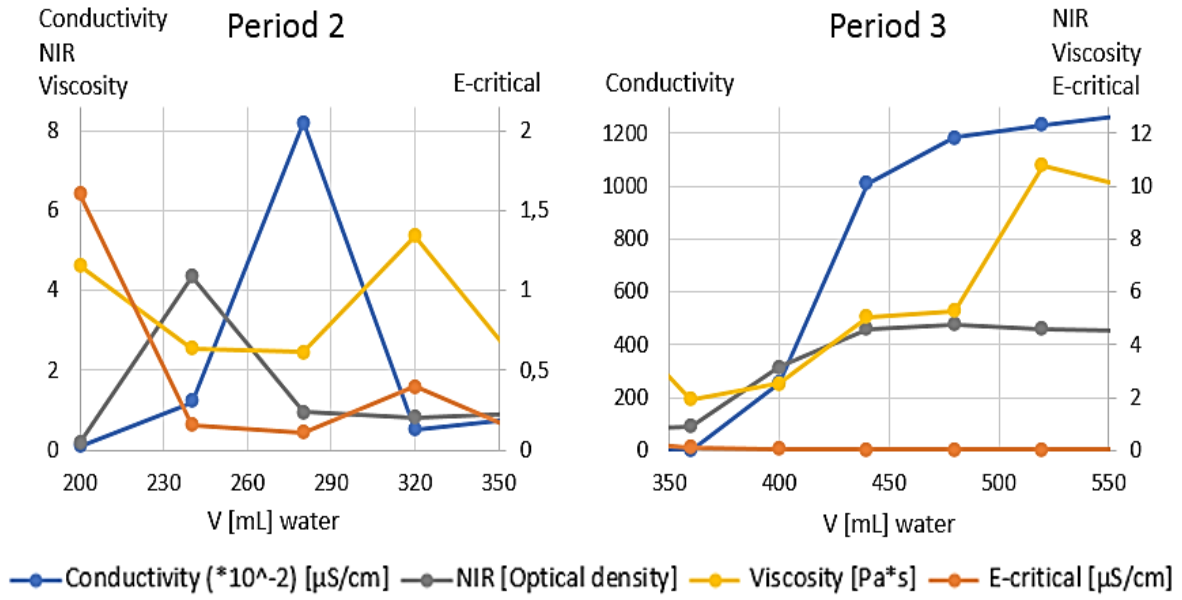

Figure 22: Detailed graphs of a) Period 2 and b) Period 3. The plots shows the process properties, Conductivity, NIR, Viscosity and E-critical value as functions of the water addition [mL] for the jetstream emulsification reference, EML 16.

Period 2 starts at a water addition of approximately 200 mL, and ends after approximately 350 mL. There is a small reduction in the viscosity in this period, followed by a local maximum after adding 320 mL. The details can be seen in Figure 22 a).

The shifts in the emulsification properties may be related to a redistribution of the surfactants in the mixture. Before addition of water, the polarity is mainly due to neutralized carboxylic acid groups on the alkyd. At this point, the anionic surfactants might be attached to the oxygen on the non-ionic surfactants in addition to the polar groups on the alkyd.

As more water is introduced to the system, the anionic surfactant will move over to the polar water molecules and this shift in charge might influence the conductivity. When the non-ionic surfactants are free of the anionic surfactants they may connect to each other through the water droplets as suggested in Figure 5 in chapter 2.1.3. Emulsions. The mobility of the droplets will decrease, decreasing the conductivity

and increasing the viscosity. The high viscosity may indicate a larger amount of small water droplets in the alkyd, or maybe even a sort of bi–continuity with the water.

Another factor influencing the viscosity may be the surfactants ability to form micelles having the possibility of increasing the viscosity. As can be seen in Figure 3, in the surfactant theory different aggregation structures, especially reversed hexagonal, can arrange in order to make a transfer of a current possible. The bilayer structure may also make it possible to transfer current, as well as contribute to a high viscosity.

The NMR tests performed on samples taken in Period 1 and late Period 2 indicates that an inversion process may have started during this period. In Period 1, NMR results indicate that the droplet size distribution is monomodal, with water droplet sizes varying from 1 to 40 µm. In Period 2 the distribution was found to be bimodal. In the bimodal distribution, about 5% of the water was present in small droplets. The larger droplets had droplet sizes increasing with increasing water concentration (Sørland, 2013) in Appendix B. The increase in droplet size, mainly observed for the initially large droplets, may indicate a triple emulsion, with small droplets of water present within droplets of oil that again are present within increasing droplets of water (w/o/w/o). The triple emulsion is illustrated in picture two, in Figure 23.

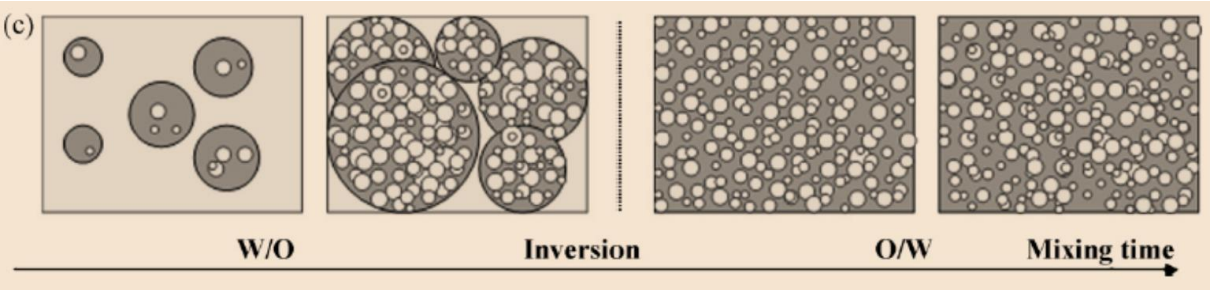

Figure 23: A schematic presentation over the time evolution of droplet size and morphology with mixing time before and after inversion of an emulsion. c: high [surfactant] low HLB (Jahanzad, et al., 2009)

Another alternative is that the large droplets grow due to Ostwald ripening or similar molecular diffusion processes, whereas the smallest droplets remain stable either due to the high viscosity of the oil, or due to a thick interfacial film stabilizing the droplets. The likelihood of colliding with large droplets are higher and the small droplets are more stable due to surface stabilization and higher Laplace pressure, making them less susceptible to additional water (Sugiura, et al., 2001). This can result in two distinct populations of droplets having different sizes. The surfactants are more effective in making o/w emulsions, and have therefore a saturation limit for stabilized water droplets. This means that the water will add to the already water rich phases, and only the stirring hinder a visible bi-phase.

A third possible reason for the bimodal droplet size distribution is the instability scenario of coalescence. With increasing concentration of the dispersed phase, there is generally higher coalescence rate, possibly higher rate of coalescence than break-up of droplets. This scenario can give increased droplet size for the large droplets

coalescing but will not affect smaller stabilized droplets. The increase of the larger droplets reduce the viscosity before it reaches a concentration where the coalescence scenario may be the reasons for the catastrophic phase inversion (CPI) (Nienow, 2004). The CPI will result in a creation, and release of a large amount of small alkyd droplets increasing the viscosity rapidly.

The hypothesis of a transformation into a triple emulsion can also be supported by the small maximum in conductivity and minimum in e-critical value. These small changes in the process parameters indicate a small period where the emulsion to a certain degree is able to transfer a current and the droplets easily line up to conduct a current when put under pressure. The large water droplets, may even be water pockets, will be mobile and may orient themselves so they have only a thin alkyd membrane between them, making the transfer of a current possible despite the alkyd continuous phase. This will last until the amount and size of the water droplets saturate the emulsion and create a viscosity rise due to a grid of droplets having higher interfacial tension. The loss of mobility of the water droplets may affect their ability to conduct a current, and in turn lower the conductivity.

The maximum in NIR and late maximum of viscosity also support the possibility of a transformation. The NIR gives information about the sizes and amounts of droplets, or flocs of droplets, which will be large around this transformation stage. The late increase of viscosity can be influenced by the fact that more or bigger droplets, with double emulsions inside, increase the friction and inter droplet repulsion, in the same way as for flocs, and hence increase the viscosity.

Period 3 starts after adding approximately 350 mL of water, and ends after 550 mL of water. The details can be seen in Figure 22 b). The viscosity and e-critical value taper off and starts this period at a local minimum. This is followed by a rapid increase of the NIR and the conductivity. The decrease in the e-critical value and the rapid increase of the conductivity indicates an inversion from alkyd continuous to water continuous phase.

After 400 mL, in the middle of Period 3, the NMR 3 test shows that the emulsion has two water populations. Some of the water is present in a continuous phase and some as small droplets with in an alkyd phase. This strengthens the hypothesis that there was a triple emulsion, with water within oil droplets, before inversion. As illustrated in Figure 24 this is possible to measure, by considering the diffusivity of the water and only count the amount present in small droplets through the height of the sample (0 - 25 mm).

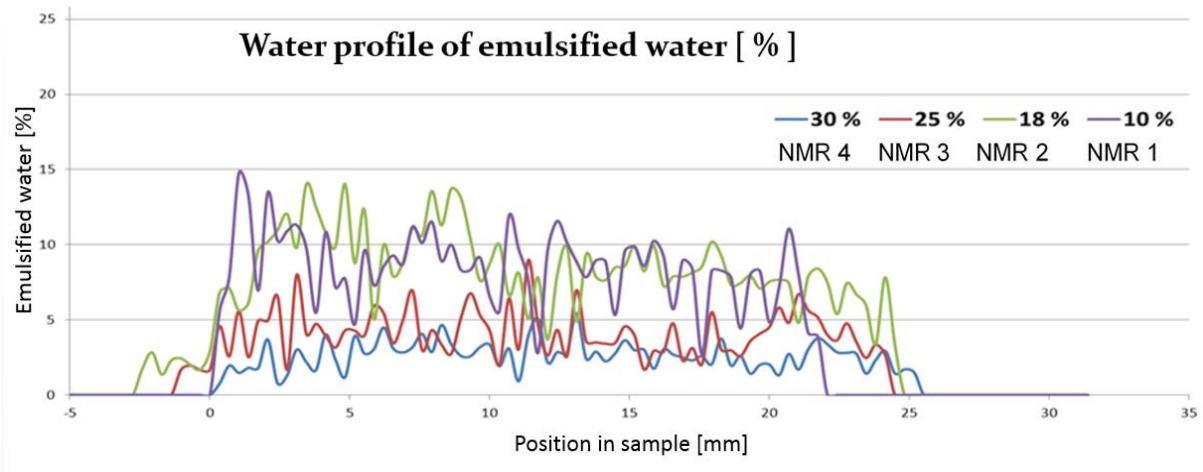

Figure 24: Water profiles, measured by NMR, of water present in smaller droplets along the sample for emulsification EML 17.(~5-10 um) (Sørland, 2013) in Appendix B.

Figure 24 shows that the sample is quite stable and that the amount of water is evenly distributed form the bottom to the top (0-25 mm). When comparing the amount of water present to the total amount of water added, there can be seen that the amount present in small droplets corresponds to approximately 100% of the total amount of water added, for NMR 1. The amount is reduced for the possible triple emulsion present at NMR 2. For NMR 3 the amount of water present in small droplets is only about 5 %. The remaining 20% is present in a continuous phase, in large droplets or as water pockets. The large amount of water with high mobility supports the conductivity indication of water as the continuous phase at this stage of the emulsion.

The rapid increase in the optical density indicates a larger amount of droplets present, increasing the optical density of the emulsion. This might be because water droplets adsorb the non-ionic surfactants, resulting in a stabilisation failure and an inversion of the emulsion. At the inversion numerous amounts of alkyd droplets may be released in the water phase, replacing large double emulsified water droplets. The inversion and release of numerous amounts of alkyd droplets is also supported by the decrease and following increase in viscosity. In the time prior to the inversion, there will be large droplets of water reducing the droplet-droplet interface, hence reducing the viscosity. When the interfaces between the water droplets break, and release numerous smaller alkyd droplets into the continuous water, the droplet-droplet interface increases again. This results in an increased droplet-droplet interaction and a rapid increase in the viscosity.

After a water addition of approximately 500 mL, the inversion period can be said to be over and Period 4 starts. The conductivity and NIR values have stabilized on a maximum value, and the e-critical measurements fail due to instant breakthrough of the current. However, the viscosity keeps increasing for a short period and the NMR 4 tests shows that the water amount present in small droplets is at the same amount as for NMR 3. This indicates that there still is a double emulsion, w/o/w, present. The high viscosity indicates that there still is larger amounts of small alkyd droplets

present in the water and that they are present in a three-dimensional grid, or that the distance between these are low and gives friction, resulting in high viscosity.

When more water is added the distance between the alkyd droplets increases and the droplet-droplet interaction decreases, resulting in a rapid decrease in viscosity. After a water addition of 700 mL, the NMR 5 results show a lower, almost insignificant, amount of water present in the small droplets. This indicates a full inversion to an alkyd in water emulsion having a monomodal droplet distribution of water present as the continuous phase.

5.2 The emulsification process

The main system of the emulsification testing is the reference system, System 1, which is identical to the system investigated in an earlier study (Lefsaker, 2012). When a low concentration of immiscible phase is dispersed, break-up in the impeller region controls the droplet size (Nienow, 2004). It is therefore interesting to test the effect of different impellers. System 1 is emulsified, using both an anchor impellor and a jetstream mixer, at alkyd temperatures between 35 ^{o}C and 40 ^{o}C. For this system, and under these conditions, the emulsification was easy to perform and, as can be seen in Figure 25, followed the same trend independent of stirring technique.

It is interesting to test different stirring techniques since they may have an important impact on the process and the result. The anchor stirrer results in low shear and a large contact surface against the alkyd. The jetstream stirrer results in almost no shear, and has a low contact surface. However, the jetstream mixer has proved to have a good and different stirring effect, after testing by Jotun on other systems.

Figure 25 shows a comparison of the emulsification process performed with a jetstream mixer (EML 16) and an anchor stirrer (EML 18) for system 1. The e-critical test was not performed for emulsifications performed after EML 16, because it was considered not to provide any additional information beyond the conductivity. The e-critical trend is therefore compared to values from EML 9 from the pre project (Lefsaker, 2012). The lower e-critical and conductivity value observed for the jetstream mixer may be due to better stirring. The different stages of the emulsion seams to be easier to identify with anchor stirring, considering the observed effect on emulsion properties. This is observed especially for the viscosity, but also as mentioned for the e-critical and conductivity values. The trends however, are the same.

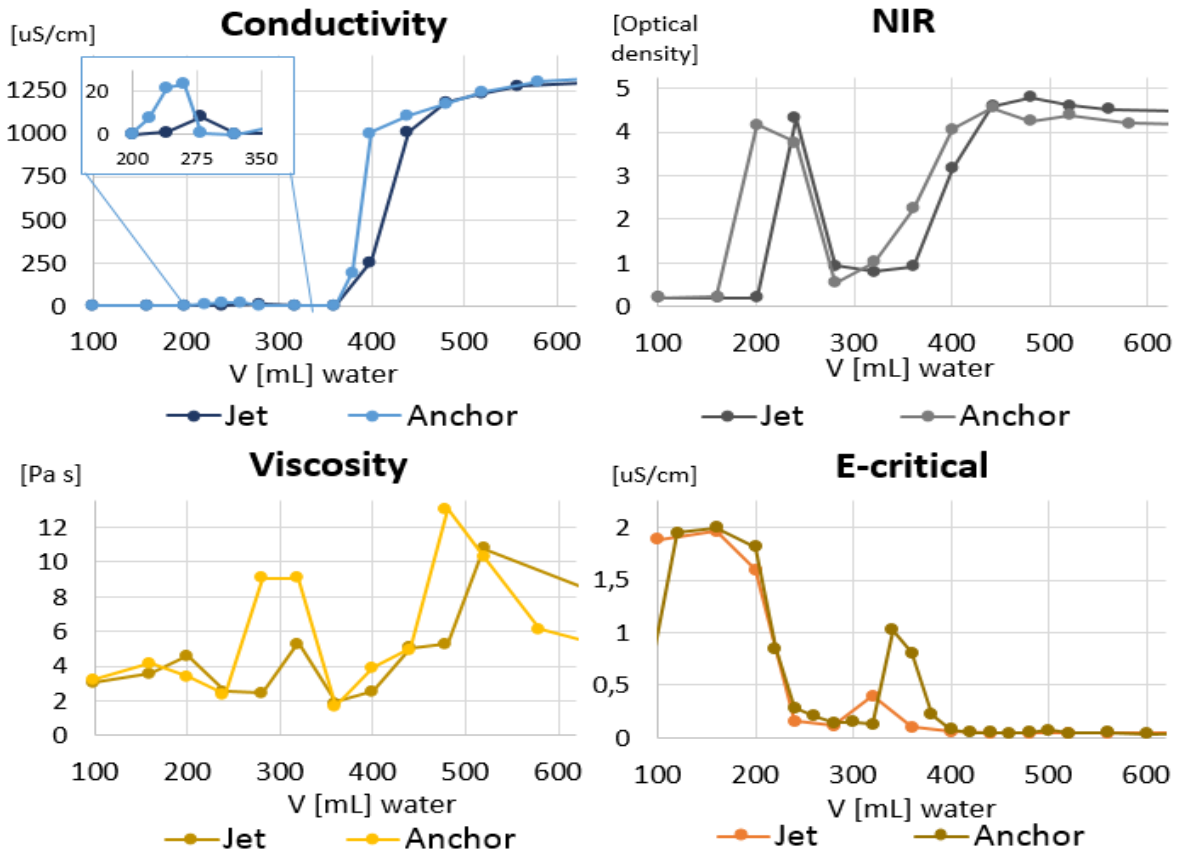

Figure 25: Emulsification trends for the four different process parameters, conductivity, NIR, Viscosity and E-critical cell as functions of water addition [mL]. The graphs shows a comparison between the results from the jetstream mixer reference, EML 16 and the anchor stirrer reference, EML 18.

The identification of property changes makes the anchor stirrer possibly more suitable for looking at the different process stages for further tests. The end properties, represented by the final droplet size, of the two different methods are also comparable. They are 188 nm, 182 nm and 183 nm for EML 9, EML 16 and EML 18, respectively. System 1 has proved to be a robust system, independent of stirrer, and a larger impact on the process and end-results may be expected on other systems.

5.3 Droplet size distribution

The average droplet size [nm] distributions for the emulsion were estimated for some of the introductory emulsifications using the Malvern Naonosizer. A good stability criteria for the droplet size distribution is Z avg < 300 nm, and PDI < 1. The development of the droplet size distribution are shown for emulsion EML 17, as reference of jetstream, and emulsion EML 18 as reference for anchor impeller in Figure 26.

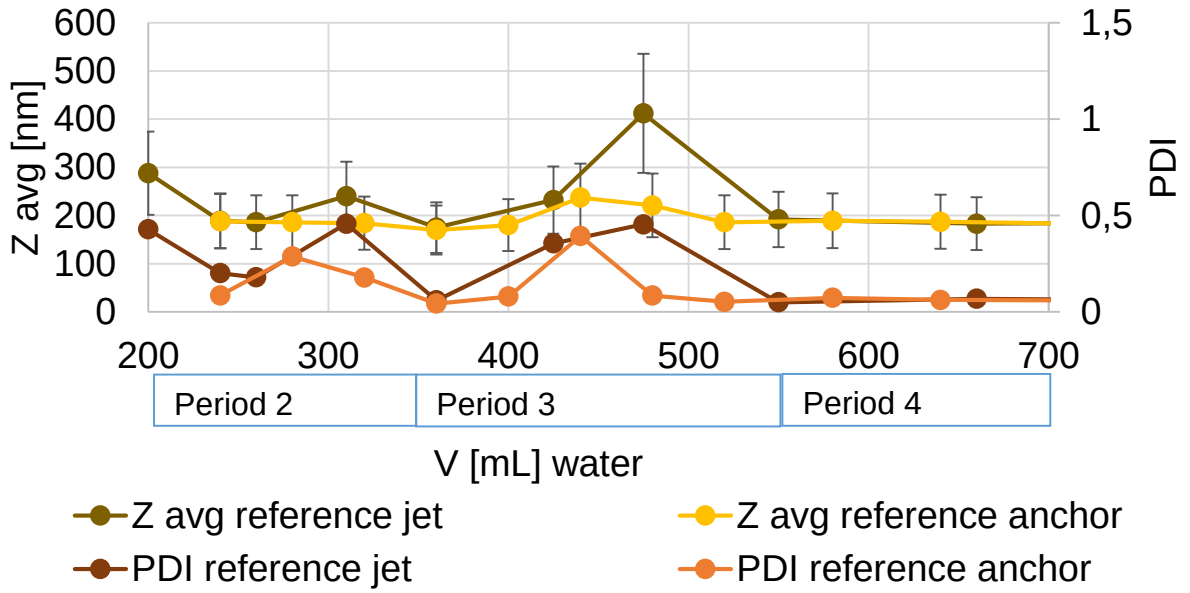

Figure 26: Droplet size and poly dispersity development for emulsifications EML 17, reference of jetstream mixer, and emulsion EML 18, as reference for anchor impeller as a function of water addition [mL].

The emulsions has been dissolved or diluted in water, depending on the continuous phase, in order to be able to measure the droplet size. The poly dispersity index (PDI) is plotted together with the droplet sizes in order to have a feeling of the size distribution. The deviation is estimated to be approximately 30% based on the standard deviations of the en emulsion seen in Table 2. Despite the high deviation most of the droplet distributions satisfy the requirement of max 300 nm. This trend was also observed in an earlier study (Lefsaker, 2012) and plot showing reproducibility is provided in Appendix E.

It can be seen that the surfactants are well suited for solving the alkyd mix and stabilizing droplets around 200 nm in diameter independent of the continuous phase. This might be due to a surplus of surfactants spontaneously emulsifying the alkyd when diluted in water. However, the droplet size distribution and PDI have local maxima around 450 mL into the emulsification. This change in droplet size can be seen to coincide with the property changes occurring in Period 3, defined in Chapter 5.1, and may have something to do with the inversion of the emulsion. It might for example indicate a bimodality affecting the surfactants ability to instantly form small droplets at solvation.

5.4 Surfactant variation

As seen in Table 2, the effect of surfactant variations are investigated in EML 19, EML 20, EML 24 and EML 33. An overview is given in Appendix A and a more through description is to be found in the process reports in Appendix D. A reduced amount of surfactant resulted in an emulsion that did not invert. The most likely reason for this is that there is simply not enough surfactants in the mixture to allow for a proper emulsification of the two liquids in the first place. This will mean that the sizes and amounts of water droplets supported in the alkyd mixture is restricted by the amount of surfactants available to support them. Therefore only few and large droplets, within a surface limit large enough to be supported by the surfactants, will be formed.

An emulsions ability to invert and stay stabile is affected by the HLB value. When altering the relation between anionic and non-ionic surfactants the HLB value of the surfactant mixture is changed. A shift in the surfactant amount to more anionic and less non-ionic surfactant resulted in an unstable emulsion. An emulsion is stable, from a kinetic point of view, only when the number, droplet size distribution, and arrangement of droplets do not undergo any discernible change over a certain storage time (M. C. Sanchez, 2001). The non-ionic surfactant is often used as a stabilizing agent in w/o emulsions because their physiochemical properties are not affected by electrolytes (Holmberg, et al., 2003). The neutralization of the alkyd solution creates a salt, making the emulsion electrolytic when water continuous, in turn affecting the stabilizing effect of the two different surfactants. Both can be seen, compared to the reference EML 18, in Figure 27.

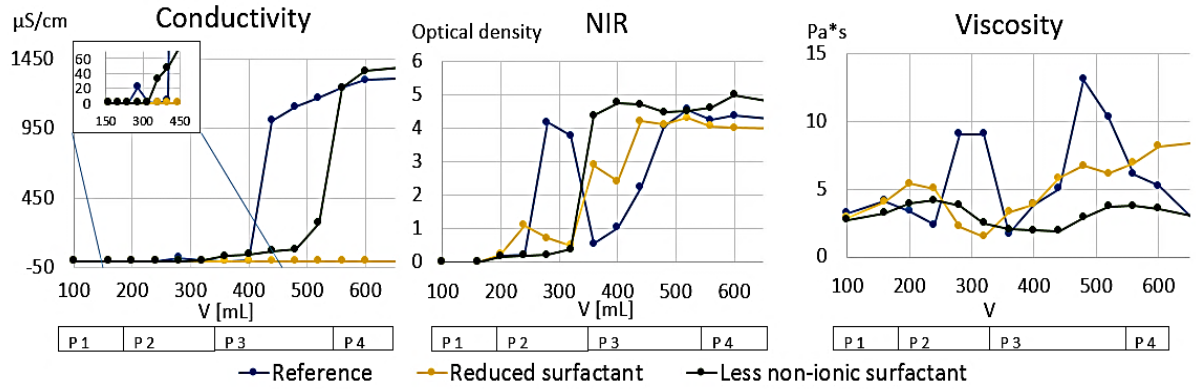

Figure 27: Effects of surfactant variation for conductivity, NIR and viscosity as a function of water addition [mL] for the anchor-emulsified reference, EML 18, emulsion EML 19 having a reduced amount of surfactant and emulsion EML 20 having the same amount of surfactants as the reference but in a ratio favouring the anionic surfactant.

When comparing the results in Figure 27, it seems obvious that the process development between 200 mL and 400-500 mL of water addition, Period 2 and Period 3, is critical for the final emulsion properties. This is firstly when the water is dispersed in the alkyd and secondly when the emulsion inverts and become water continuous. Both the failing emulsifications lack the local conductivity, NIR and viscosity maxima in the start of this area.

For the emulsion with reduced surfactant amount, the deviations can be because of the restrictions on the size of the surface supported by the surfactants. There may not be created a triple emulsion with high mobility droplets having the capability of lining up and conducting a current, or it may not be enough surfactants for the rearranging of surfactants to occur, initiating a shift in charge making the conductivity possible. The lack of the NIR maximum also indicate fewer and larger droplets. The droplets may not affect the optical density as much as if they were filled with a double emulsion, or surrounded by smaller droplets scattering the light. The low amount of large water droplets can also explain the low viscosity. They are formable, have a low total surface area and are relatively fare apart, not creating that significant inter droplet friction. However, there can be seen tendencies to a conductivity rise and a viscosity maximum, in the start of Period 2, indicating that some rearranging of surfactants alternating the interfacial tension was supposed to happen at this time.

For the emulsification with shifted surfactant concentrations, to more anionic and less non-ionic surfactant, the lack of the NIR, conductivity and Viscosity tops does not seem to have that big influence on the inversion process of the emulsion. A small conductivity rise occurs at the same time as for the reference, but keeps rising slowly until an assumed inversion at around 520 mL, Period 4. This reaction may support the hypothesis stating that a rearranging in the surfactants makes the conduction of a current possible and that the high viscosity again hinders it. The high viscosity is not a factor in this emulsification and the conductivity may therefore develop steadily until the inversion to a water continuous emulsion. There can be seen that the shift in surfactants has a significant impact on the viscosity. The non-ionic surfactant seems to have an important influence on the viscosity. It is known to act as an emulsion thickener due to good capability of filling the free volume between the polymer chains. A reduction in the concentration of this surfactant may therefore be the reason for the lack of viscosity in the emulsion.

The distinct tops in viscosity for the reference became more visible when compared to systems containing less non-ionic surfactant. Interestingly this strengthen the hypothesis further in that the viscosity is significantly influenced by the surfactant combination. The ethylene oxide segments of non-ionic surfactants is suggested, in literature (Kientz, et al., 1994), to connect via hydrogen bonds in water molecule, as shown in **Feil! Fant ikke referansekilden.**

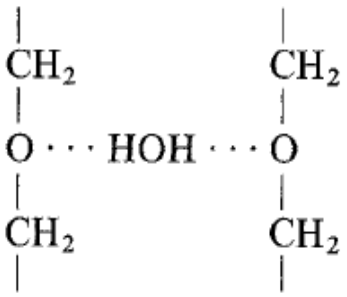

Figure 28 : A suggested hydrogen bonding between the ethylene oxide segments of non-ionic surfactants via water (Kientz, et al., 1994)

The first viscosity tops, seen for the reference in Figure 27, may therefore be due to surfactants added to the different alkyd chains by hydrogen bonds, thereby increasing the steric hindrance and the viscosity. Addition of more water may result in larger droplets of water surrounding the alkyd polymer chains, almost as a bilayer, reducing the droplet-droplet interface, hence reducing the viscosity. When the water-water interfaces break and release numerous smaller alkyd droplets in the water, the droplet-droplet interaction increases again and the viscosity increases. The viscosity increases close after the believed inversion to water continuous, at the same time as the NIR rises from a local minimum, indicating a release of multiple small alkyd droplets with high optical density and interfacial tension.

The amount of non-ionic surfactant also seems to be important for the stability as well. The emulsion with shifted amount of surfactant, less non-ionic surfactant, has approximately the same amount of surfactant as the reference, but in different ratio between anionic and non-ionic surfactant. The one with a lower amount of non-ionic surfactant was visibly separated after one month, while the reference maintained the original droplet size. As mentioned, this might be due to the nature of the anionic versus the non-ionic surfactant in terms of effect in an electrolytic water solution. The emulsification lacking non-ionic surfactant, EML 24, showed no reaction, and did not invert. As can be seen in Figure 29, all the curves are flat. This confirms, what has been seen in the previous surfactant investigating emulsions that the non-ionic surfactant is of significant importance when performing an emulsification of alkyd. The constantly high NIR and viscosity indicates a large number of droplets having a high optical density and a certain amount of droplet interaction. In a system with only one type of surfactant, no rearranging of surfactants are possible, and this seems to affect the emulsions ability to invert as well. This may be due to the anionic stability of the polar water droplets, and the lack of viscosity-induced shear needed to break them up.

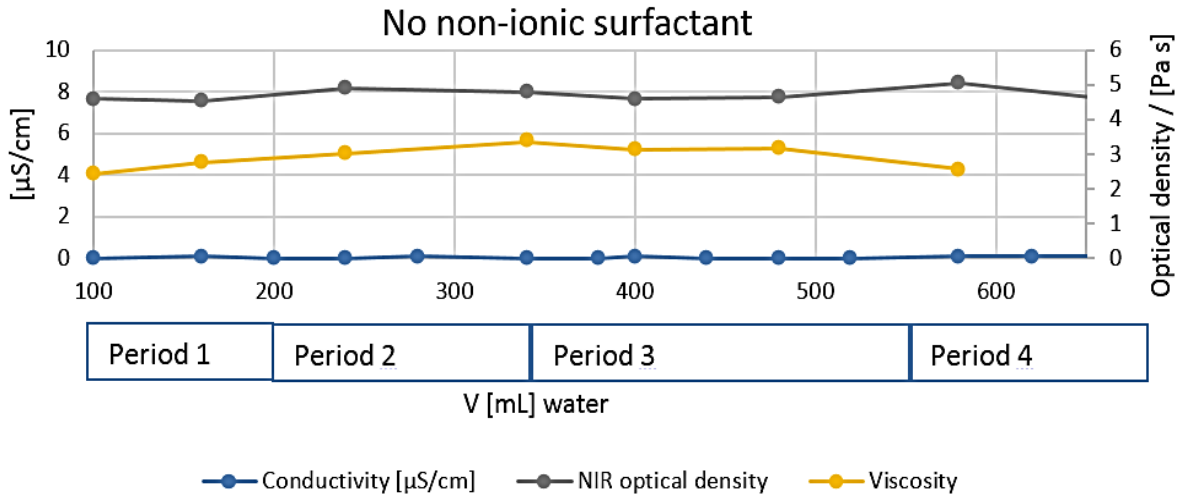

Figure 29: The process properties conductivity, NIR and viscosity as functions of water addition [mL] for an emulsion without non-ionic surfactants, EML 24.

Two alternative surfactants, one non-ionic and one anionic, where tested in EML 32 and EML 33. The first test did not invert, most likely due to problems with the neutralizer, but the second emulsification test inverted resulting in an emulsion with slightly higher droplet size, i.e. 239 nm. A comparison with the reference, EML 18, is shown in Figure 30.

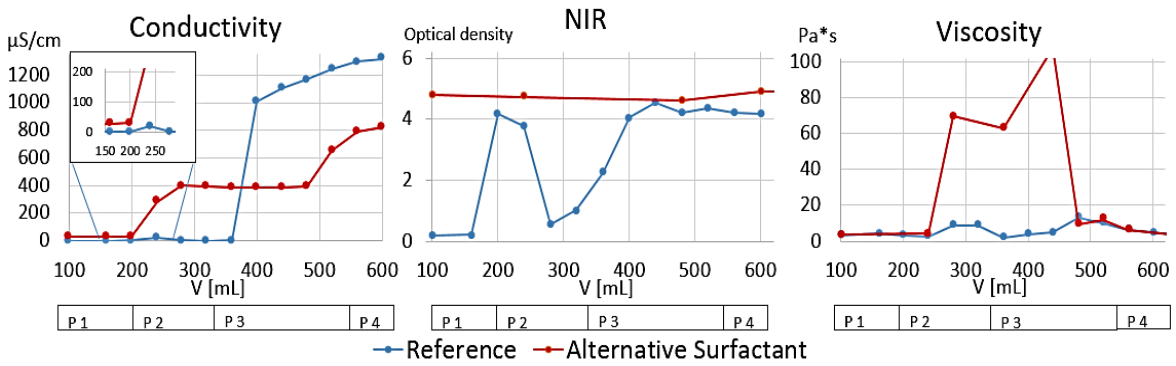

Figure 30: The effect of an alternative surfactant on the a) conductivity, b) NIR and c) viscosity as functions of the water addition [mL]. The emulsions shown are the anchor reference, EML 18, and an emulsion containing an alternative surfactant, EML 33.

It is interesting to observe the significant difference in process properties, seen in Figure 30. Despite having the same ratios of non-ionic and ionic surfactants, the properties are significantly different. This might be due to a difference in the HLB value of the surfactant mixture. When looking at the conductivity the alternative surfactant emulsion seems to have two inversion steps, with the first in Period 2, around 200 mL, and the second in Period 3, around 500 mL. At the same time as the second inversion step, the viscosity decreases. The first increase in conductivity sets off an extensive increase in viscosity, which makes the emulsion ductile and difficult to stir. The high viscosity might be due to a stronger thickening effect of the alternative non-ionic surfactant than the original non-ionic surfactant.

The high viscosity is observed to hinder the inclusion of water, and may therefore kinetically hinder further inversion. The result may be that the conductivity levels out. After 500 mL of water, most of the water is included, and the viscosity drops rapidly. The conductivity starts rising again and the centre of the emulsion inverts. However, the reactor obtains a coating of un-inverted alkyd, which results in a lot of time-consuming cleaning and loss of product. The optical density, NIR, was constantly high indicating a large amount of particles scattering already from the start. It is an interesting observation the surfactants in itself can have such large effect on the viscosity, and this strengthen the possible theory of the variations in the thickening effect of non-ionic surfactant.

5.5 Neutralization

The significance of neutralization of the carboxylic acid groups on the alkyd, and the introduction of a carboxylic acid salt, is investigated in EML 21 and EML 22. It is interesting to see which effect the neutralization might have on the emulsification process, but also to get the opportunity to discover signs of missing neutralization in large-scale production. The neutralization increases the pH by reducing the acid groups from COOH to COO^-. The neutralizer is a small, mobile and positive molecule with a charge that will contribute to the conductivity of the emulsion and affect the efficiency of the surfactants.

As can be seen in Figure 31, EML 22 inverts, but has a low conductivity. The low conductivity may be due to the lack of ions reducing the electrolytic effect of the alkyd in the emulsion. The non-neutralized emulsion has the local maximum in conductivity around the same point (~240 mL) as for the reference but it is significantly higher and does not return to zero conductivity, before rising again. This may be because the non-ionic surfactant act as a more effective thickening agent in a non-neutralized emulsion. The positive ammonium form the neutralization will possibly stabilize the oxygen on the non-ionic surfactant reducing its ability to bind to water.

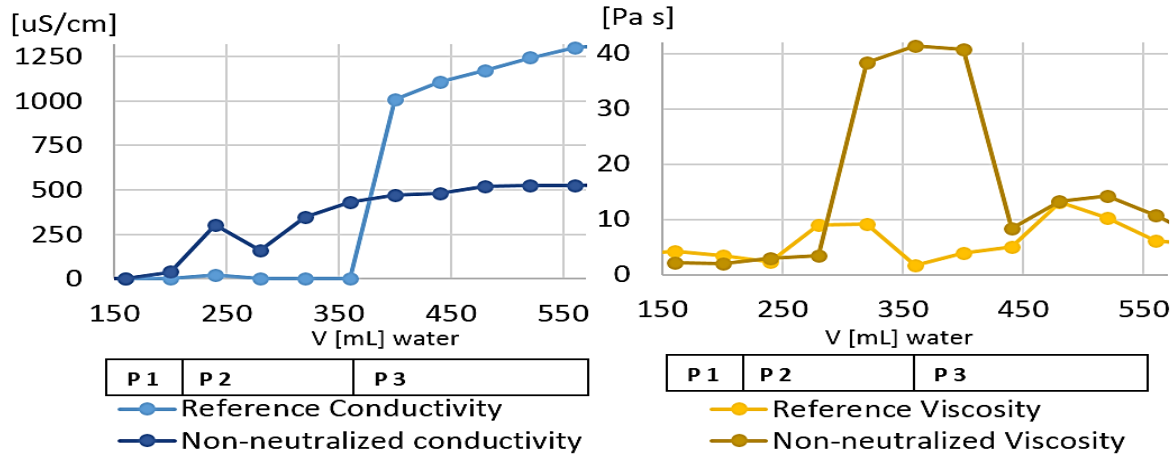

Figure 31: The effect of the use of neutralizer on the a) conductivity and b) viscosity as functions of water addition [mL]. The emulsification shown are the anchor reference emulsion, EML 18 and an emulsion without neutraliser, EML 22.

The viscosity has a very high maximum, which made it impossible to take samples for NIR. As can be seen in , the viscosity was four times higher than the reference, which gave made proper stirring difficult to conduct. The viscosity rise is also here occurring slightly after the first rise in conductivity. Neutralisation of the acid groups adds charge to the alkyd, making it more receptive towards surfactants and reducing the interfacial tension. The lack of neutralisation may give a high interfacial tension between the non-neutralized carboxyl groups, resulting in the high viscosity.

5.6 Alternative alkyd

An alternative alkyd was tested in EML 23 and EML 25 using the same surfactants as in the reference system, EML 18. Different alkyds can affect the emulsification process due to differences in structure and acid number among others. When comparing the conductivities, in Figure 32, the alternative alkyd emulsion can be seen to invert quite early in the process. It inverts without showing any signs of the local maximum, and the value of the conductivity is also significantly lower than for the reference emulsion. The low conductivity and lack of local minimum might be due to the difference in acid number between the two alkyds. If the alternative alkyd has a lower acid number it has less carboxylic acid groups that can be neutralized and contribute to the conductivity. It might also be due to different amounts of neutralization amount compared to the acidity of the alkyd.

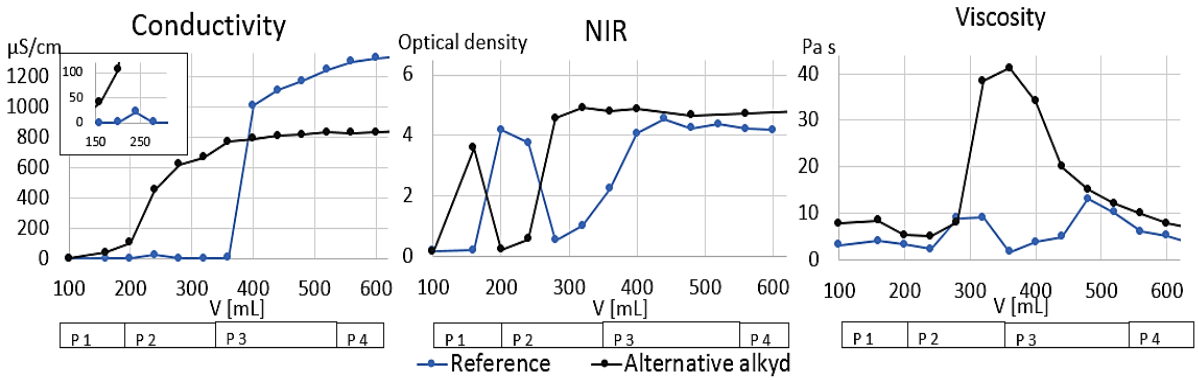

Figure 32: The effect of an alternative alkyd mixture on the properties a) conductivity, b) NIR and c) viscosity as functions of water addition [mL]. The emulsions presented are the anchor reference emulsion, EML 18, and the alternative alkyd emulsion, EML 25.

As for the emulsion without neutralizer, and the emulsion with alternative surfactant, the viscosity maximum is more than four times higher and lasts for almost the entire inversion period of the reference. This makes the emulsification difficult to stir and, from an industrial perspective, this is an undesired situation.

It can also be seen that the high viscosity follows the early rise in conductivity, indicating that the viscosity is due to alkyd droplet interaction. The common high viscosity may indicate a relation between acidity, neutralization and surfactant types and conductivity and viscosity. The emulsion had a final droplet size of 226 nm, but was found to be unstable after one month. The instability might also be connected to a difference in acid number. Less neutralized acid groups result in a less polar alkyd that are less soluble in water, resulting in a less stable emulsion. More surfactants could have been added, in order to increase the stability, however, this might in turn increase the already high viscosity.

5.7 Process parameters

Process parameters, like rate of water addition, stirring or water failures, might be of importance for the emulsification process. It might be of interest to tests scenarios that are especially relevant for industrial production, and the effect on the emulsification process, result and stability.

5.7.1 Rate of water addition

In other studies of emulsifications made by CPI, the droplet size distribution has been found to depend on stirring speed and rate of water addition (Brooks, et al., 1994). The effect of the rate of water addition was therefore interesting to test. It is tested in EML 26 and EML 27. The effect of rapid water addition, immediately after the change in conductivity, was tested in EML 26 and the effect of slow water addition in Period 2 and Period 3, between 200 mL and 500 mL, was tested in EML 27. The results are compared to the reference, EML 18, in Figure 33.

As can be seen the only visible effect of adding water faster after the inversion point is a lower viscosity maximum. The droplet size was also slightly smaller for the rapid water addition than for the reference, 174 nm versus 183 nm respectively. This, along with droplet size differences (50-70 µm) between emulsions having a long period of high viscosity (viscosity > 40 Pa*s) and emulsions having lower viscosities (viscosity < 12 Pa*s), indicates that the droplet size may be slightly dependent on the viscosity maximum and the duration of high viscosity. However, the amount of results available, and the extent of differences versus the uncertainty is not conclusive enough to state this.

The slightly higher droplet size may also be due to the time the emulsion gets to flocculate during the high viscosity, before it is stabilized by enough water. The lower viscosity also indicates that it might be possible to reduce the viscosity in the emulsification process compared to the reference, making the process less expensive and tearing for the process equipment.

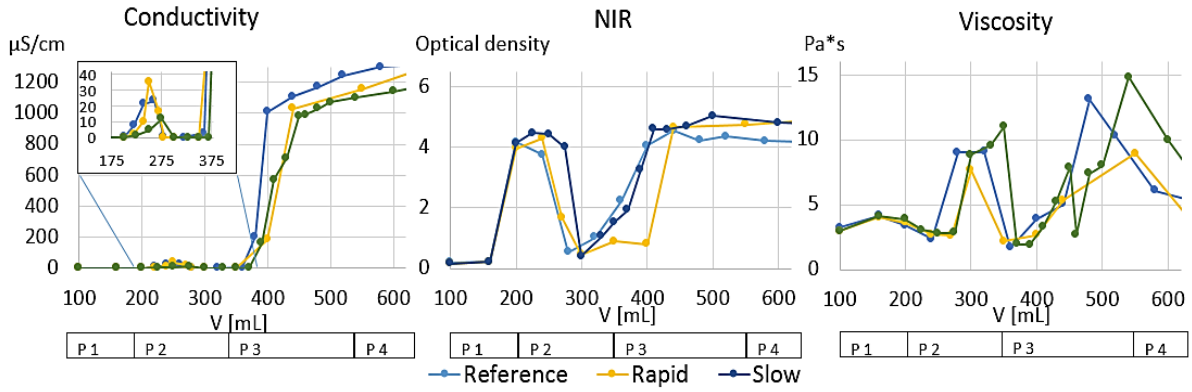

Figure 33: The effect of rate and time of water addition on the parameters a) conductivity, b) NIR and c) viscosity as functions of water addition [mL] for system 1. The reference is the anchor reference emulsification, EML 18. The rapid water addition represents an e emulsion where the water addition is increased after inversion, EML 26. The slow water addition is represented by an emulsion where the rate of water addition is lowered between 200 mL and 500 mL, EML 27.

In order investigate the main area of interest, between 200 mL and 500 mL, the rate of water addition in this area was reduced from 20 mL/min to 10 mL/min. Twice as many test points in the investigated area confirmed the trend, but showed no other significant effect on the emulsification process. The viscosity after 500 mL showed an increase that in light of the above theory might explain the slightly higher droplet size of 193 nm. Other research also indicate that a longer emulsification time leads to a longer bimodal period and slightly higher droplet size (Sanchez, et al., 2001).this might be because the surfactants can have an ability to act as both emulsifying and depleting agent.

5.7.2 Water failures

Another process parameter which is interesting to test is water failure, either as a stop in the water addition or as a failure in the dosing resulting in a sudden leak or spill of water in a large amount. This is tested in EML 28 and EML 29, respectively, and compared to the reference, in Figure 34. A stop in the water addition, for about 30 minutes after an addition of 300 mL, gives no process problems as long as the stirring is kept constant. The inversion point occurs slightly later than in the reference but the droplet size, 183 nm, NIR and viscosity are ale comparable to the reference seen in Figure 34.

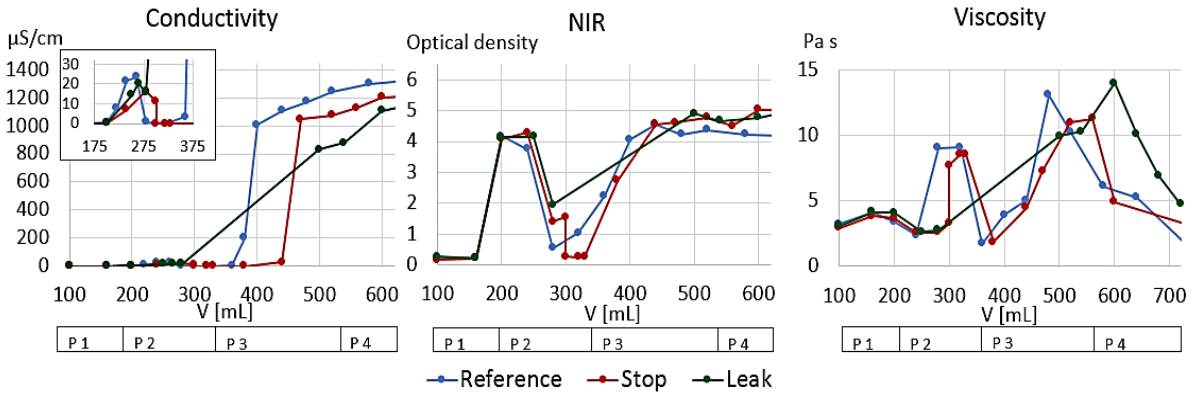

Figure 34: The effect of water failure on the process parameters a) conductivity, b) NIR and c) viscosity as functions of water addition [mL]. The anchor emulsification reference, EML 18 is compared to an emulsion where the water stops after about 300 mL of water, EML 28, and an emulsion where 200 mL of water leaks of into the emulsion after about 300 mL of water, EML 29.

A sudden leak in the addition off water, adding 200 mL at once, after a water addition of approximately 300 mL, kick starts the inversion around the top of the local maximum of conductivity. This early start of inversion sets off the increase in viscosity as well, further strengthening the theory of the viscosity following the conductivity as seen for the alternative alkyd, surfactant and the emulsion lacking neutralizer. The inversion, however, is carried out during a longer period than for the reference, and so the viscosity uses longer time reaching a slightly higher maximum. The conductivity development might be due to problems with water inclusion and inhomogeneity because of the sudden water leak.

5.7.3 Stirring failure

The last process parameter to be investigated is a stop in stirring. This is selected to be investigated together with a lid of top water, due to the unlikely ability to stop the water addition at the moment the stirrer fails. The stirring is stopped after 300 mL and 200 mL, in EML 30 and EML 31, respectively. A lid of 200 mL and 150 mL of water is added on top of the two emulsions, and left for 30 minutes, before recommencing the stirring. The top water is selected both because it is difficult to stop water immediately as the stirring fails, and because industrial experience tells that a top lid of water hinders diffusion of water from the emulsion and the formation of skin on top as the alkyd reacts with air. The water addition starts after one minute, when most of the top water is included in the emulsion.

The two emulsion points of stirring failure was chosen carefully in order to investigate the possible formation of small water droplets in the local maximum occurring around 240 mL of added water. This points in the emulsion, before and after 300 mL of added water, is also when the emulsion is most likely to stop due to overheating and local viscosity rise as can be seen from the introductory tests, EML 11 – EML 16, seen in the process reports in Appendix D.

As can be seen in Figure 35, in comparison with the reference EML 18 a stop in the stirring after this local maxima occurring at 240 mL, results in an instant inversion when stirring is recommenced. At this point a total of 500 mL is added, 300 mL prior to stop and 200 mL as top water. The NIR follows the reference, while the viscosity seems to skip the local minimum, level out during the break, and continue the rising when the stirring starts and the inversion continue. The viscosity reaches its top when the inversion, according to the conductivity, is completed.

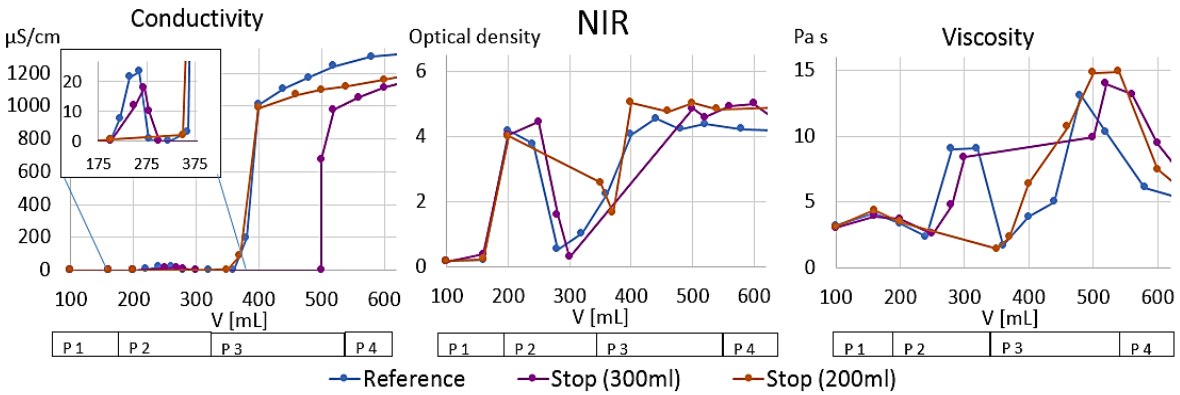

Figure 35: The effect of stirring failure on the a) conductivity, b) NIR and c) viscosity as functions of water addition [mL]. The emulsions presented are the anchor reference emulsion, EML 18, compared to an emulsion with stirring failure after 200 mL, EML 30, and an emulsion with stirring failure after 300 mL, EML 31.

The stop in stirring after 200 mL prior to any reaction does not show any signs of a local maximum in conductivity. This, however, might be because the 150 mL of added water, for where the local maxima occur, is added as top water during the

break. The result is that the inversion starts when the stirring is restarted, at the same amount of water as for the reference. The NIR and the viscosity show a slight decrease during the break and initial stirring start up, before picking up and following the reference values quite close. The viscosity is slightly higher and the duration of high viscosity is longer. The final droplet size, however, is still small, i.e. 183 nm. This contradicts the theory that the end-result might be this dependent of the viscosity for situations that are not extreme.

To sum up, it can be seen that for the robust reference system, system 1, the emulsion will not be lost by minor failures in the process parameters investigated. From section 5.4 and from section 5.5 it can be observed that there is possible to discover whether the system lacks surfactant or neutralizer by looking at the viscosity.

6 Suggestions for further work

There are several suggestions to be made in order to further investigate the emulsification process of alkyd in water by catastrophic phase inversion. Emulsification characterisation by NMR seem to be an interesting method for looking at especially pre-inversion properties. The NMR method of looking at water droplets in emulsion, showed to have several opportunities concerning modality of droplets and determination of the emulsion inversion point. It would be interesting to perform NMR tests on less stabile systems, and systems that does not invert. The differences in results for these systems, compared to the reference system, may offer further information of the meaning of the multiple droplet size modalities fund for the reference system. More work can also be done on development of NMR methods for investigating the different droplet size distributions and multimodality.

The NIR results can be investigated in order to look at the differences in peaks indicating molecular bonds within the emulsion, as can bee seen in Appendix F. This might provide deeper insight in to what kind of bonds the surfactants make with the alkyd and water.

The viscosity and the significance of it could be interesting to investigated further. Measurements and evaluations of stress, strain and modulus might offer more information of the differences in the viscosity during the emulsification. A picture of the stress-stain curve, measured for emulsification EML 12, is shown in Appendix G. Time dependent viscosity might provide information of the degree of shear thinning/thickening effects and viscoelasticity affecting the droplet breakup and coalescence.

The viscosity and strength of the interface can be investigated through measurements of interfacial tension. The strength of the surface tension can have an impact on the droplet size distribution of the final emulsion due to its effect on the coalescence rate versus reversible flocculation.

The possibility of adding fluorescent dye to the interfaces in order to look at the droplets in a microscope, as seen on the cover photo, is a possible way to try and further investigate the theory of triple emulsions prior to inversion.

Work should also be performed on several other alkyd and surfactant systems in order to verify the general trend of a successful inversion emulsification. It would be a good idea to test the development of properties for less stable systems and their impact of the final emulsification quality.

The general relation between alkyd and surfactant amount is also interesting to investigate further. The possibility of micelles formed by surplus surfactants, influencing the viscosity, and surplus surfactants inducing a spontaneous emulsification at highly diluted emulsions affecting the validity of the droplet size distributions measured for final emulsions. The effect of emulsification dilution in order to measure the final droplet size distribution could also be investigated further. For example by an investigation of stability of diluted emulsion over time. Surfactant mixtures designed on the basis of theoretical HLB calculations would also be interesting to explore.

It would be a good idea to develop of a secondary quality control criteria that don’t demand dilution or other alternation of the emulsification. This would be a good way to account for and investigate the uncertainties concerning dilution of emulsions. Finally, further work should be performed, using other techniques, to fully determine water cut of the emulsion at all times.

7 Conclusion

Properties that affect the emulsification process of alkyd in water have been investigated, and a general trend in property development has been observed. The test methods used are conductivity measurements, Near-infrared spectroscopy, viscosity measurements and E-critical cell evaluations. The general trend coincides for the test methods used, and are presented as functions of water addition. The trends were also confirmed by 5 NMR samples investigated by Antek AS.

The techniques used for testing the properties covers all the four periods, and the trends found for the different properties can be seen to coincide both pre and post inversion. The possible point of inversion is marked by a simultaneous rise in the conductivity, NIR and viscosity values, together with a breakthrough in the E-critical value.

In comparison to emulsifications performed on other systems and with different process conditions, the trend in the development of the properties appeared to be important for the final quality.

The trend in the development of the properties can be divided in four periods, defined by the different stages of the emulsification process. Period 1 and Period 4 were an introduction period and an emulsion stabilization period, respectively. No significant property changes took place in these periods. Period 2 and 3, however, were pre inversion periods, with significant changes in properties, and an inversion period containing large significant property changes indicating an inversion.

Period 2 lasted from around 200 mL to 350 mL of added water, and included a local maximum of conductivity and NIR, a local minimum in the e-critical value and a delayed local maximums of the viscosity. This, along with NMR samples showing a bimodal droplet size distribution of the water droplets, indicates that the emulsification process has started and that there might be created triple emulsions of w/o/w/o emulsions during the process.

Period 3 lasted from around 350 mL to 500 mL and covered a rapid and simultaneous increase in conductivity and NIR. These coincides with a zero in e-critical value indicating the inversion from alkyd continuous to water continuous. The following rise in viscosity also indicated that the amount of large water droplets had been replaced by a large amount of alkyd droplets at this stage of the emulsification.

Different process parameters and variations of the reference system, system 1, were tested. The emulsion process of the reference system was found not depend on the stirrer. It was tested for an anchor impeller and for a jetstream mixer. Except from slightly smaller droplets in the product when using jetstream mixer and clearer trends which respect to properties for the anchor impeller, there were no significant differences in the trends.

Variations of system 1 included surfactant variations. These variations represent combinations that are known from experience to have an unstable end-result, and variations known to fail to invert. These were tested, and the result showed that the local min/max in conductivity, NIR, e-critical value and viscosity in Period 2 might be a part of a critical development stadium in the formation and stability of the emulsion.

The relation between non-ionic and anionic surfactant, as was altered in favour of anionic surfactant in the instable emulsion, showed that the non-ionic surfactant had a big influence both on the viscosity development, and on the stability of the emulsion. Without the non-ionic surfactant, there was no rise in viscosity and no inversion of the emulsion. For an alternative surfactant mixture based on the same amount of non-ionic and anionic surfactants the viscosity was significantly higher than the reference, but the end results proved to be within the stability criteria.

The neutralization is of great importance for the emulsification properties. Without this, the viscosity gets high, and stay high for a long period, the conductivity and the end properties are not as good. The neutralisation was also critical for the conductivity of the emulsion in terms of electrolytic properties of carboxyl salts. The acid groups present on the alkyd may influence the viscosity in terms of surfactant interaction if not neutralized.

A test of an alternative alkyd with the same surfactants as in the reference shows that the trend applies to more than just the standard system. It reacts earlier and does not reach the same end conductivity or droplet size. The viscosity is high, which gives problems with the stirring, and might reduce the quality of the product. The viscosity development might be critical for the final emulsion properties. Three of the emulsions with higher droplet sizes show significantly higher viscosity than the reference emulsion. It can look like they lack a transition period, whit a viscosity drop, prior to the inversion.

The rate of water addition has also an influence on the viscosity. An increased rate of water addition, following the inversion point by conductivity, can decrease the viscosity top without compromising the end properties. Slower water addition in the critical area, between 200 mL and 500 mL, does not improve the end properties, but rather increases the viscosity and the duration of high viscosity.

Process failures as a stop in water or a big water leak do not have big influences on the final product as long at the stirring is kept constant. The water leak, however, will initiate the inversion early, and this might make the inversion period take longer time, and result in a slightly higher viscosity. A stop in stirring prior, or post, Period 2 does not have any significant influence on the end properties as long as the stops are kept shorter than 30 minutes, and the emulsion has a limited but present top water layer.

Bibliography

Aserin, Abraham. 2008. *Multiple emulsions.* Hoboken : John Wiley & Sons, Inc., 2008. ISBN: 9780470209257.

Aske, Narve, Kallevik, Harald and Sjöblom, Johan. 2002. Water-in-crude oil emulsion stability studied by critical electric field measurements. Correlation to physico-chemical parameters and near-infrared spectroscopy. *Journal of Petroleum Science and Engineering.* 2002, pp. p 1-17.

Autoclave, Ilshin. 2013. Suflux. *Ilshin Autoclave.* [Online] Ilshin Autoclave Co. ltd, 2013. [Cited: 24 05 2013.] http://www.suflux.com/eng/products/autoclave4_02.html.

Bancroft, W.D. 1913. The theory of emulsification. *journal of Phys Chem.* 1913, Vol. 17, 501.

Barnes, Howard A. 1994. Rheology of emulsions - a review. *Colloides and surfaces.* 91, 1994, Vols. 89-95.

Berg, T., et al. 2004. Insight into the structure and dynamics of complex W/O-emulsions by combining NMR, Rheology and Electron microscopy. *Colloids and Surfaces: A Physiochem.* 238, 2004, Vols. 59-69.

Bjerve, F. 1995. Aklyder, en kort introduksjon. s.l. : Kursmateriell Jotun, 1995.

Brooks, B.W and Richmond, H.N. 1994. Phase inversion in non-ionic surfactant-oil-water systems-||: drop size studies in cathastrophic inversion with turbulent mixing. *Chem. eng. Sciense .* vol.49, 1994, Vol. no.7, p. 1065-1075.

Can, Conv. 2010. Chemicals and polymers. *Environment Canada.* [Online] Canada.gc.ca, 02 03 2010. [Cited: 05 06 2013.] http://www.ec.gc.ca/subsnouvelles-newsubs/default.asp?lang=En&xml=789412CA-8061-9879-70ED-A51080B911AA.

Chen, S. 2006. *"Rheological Properties of Water in Oil Emulsions and Particulate Suspensions".* Trondheim : NTNU , 2006.

Elementis Specialties. 2011. Specialty Surfactant Products. The Netherlands : Elementis Specialties Inc., 2011.

Galindo-Alvarez, Johanna, et al. 2011. Viscous Oil Emulsification by Catastrophic Phase Inversion: Influence of Oil Viscosity and Process Conditions. *Industrial & engineering chemistry research.* 50, 2011, Vols. 5575-5583, ACS publications.

Garti, N., Benichou, A. and Sjöblom, J. 2001. *Encyclopedic handbookk of emulsions technology.* New York, : s.n., 2001.

Gooch, Jan W. 2002. *Emulsification and Polymerization of Alkyd resins.* New York : Kluwer Academic /Plenum Publishers, 2002. ISBN: 0-306-46717-8.

Guren, Heidi. 2008. Alkyd technology. s.l. : Jotun Coating, 2008.

Holmberg, K, et al. 2003. *Surfactants and polymers in aqueous solution, 2nd ed.* Chichester : John & Sons, Ltd, 2003. ISBN-13: 978 0 471 49883 4 hbk.

Jahanzad, F, et al. 2009. Catastrophic phase inversion via formation of multiple emulsions: A prerequisite for formation of fine emulsions. *Chemical engineering research and design.* 87, 2009, p. 492-498.

Kerker, M. 1969. *The Scattering of Light: and Other Electromagnetic Radiation, 1 ed.* New York : Academic Press, 1969.

Kientz, E. and Holl, Y. 1994. Interactions in solution between a hydriphobic polymer and various kinds of surfactants. *Colloid Polymer Sci.* 272, 1994, 141-150.

Kim, Sangho. 2002. *A study of non-newtonian viscosity and yield stress of blood in a scanning Cappilary-tube rheometer.* s.l. : Drexel University, 2002.

Lefsaker, Martine. 2012. Alkyd emulsification: A screening of different analytical methods to gain knowledge of the inversionpoint during alkyd emulsification. *Alkyd emulsification: A screening of different analytical methods to gain knowledge of the inversionpoint during alkyd emulsification.* Trondheim : NTNU, 2012.

M. C. Sanchez, M. Berjano, A. Guerrero, C. Gallegos. 2001. Emulsification Rheokinetics of Nonionic Surfactant-Stabilized Oil-in-Water Emulsions. *Langmuir .* 17, , 2001, Vols. 5410-5416.

Malvern Instruments. 2004. Zetasizer nanoseries user manual. s.l. : Malvern Instruments, 2004.

McCutcheon. 1977. McCutcheon's Detergents and Emulsifiers. Glen Rock, -NJ : McCutcheon Division, MC Publiching Co., 1977.

Mullins, O.C. 1990. *Analytical Chemistry.* 1990, Vol. 62, p 508-514.

Mørk, P.C. 1991. *Overflate og kolloidkjemi, 3 utg. .* Trondheim, Norway : Institutt for industriell kjemi, NTH, 1991.

NanoSight. 2012. Nanosight. *Nanoparticle-standards.* [Online] 2012. [Cited: 26 11 2012.] http://www.nanosight.com/applications/non-biological-nanoparticles/nanoparticle-standards.

Nienow, A.W. 2004. Break-up, coalescence and catastrophic phase inversion in turbulent contactors. *Advances in colloid and interface science.* 108-109, 2004.

Nordgård, Erland Løken. 2009. Model Compounds for Heavy Crude Oil Components and Tetrameric Acids. Trondheim : Norwegian University of Science and Tchenology, 2009. ISBN: 978-82471-1740-8.

Opedal, NIls van der Tuuk and Geir Sørland, Johan Sjöblom. 2009. *Methods for Droplet Size Distribution Determination of Water-in-oil Emulsions using Low-Field NMR.* s.l. : diffusion-fundamentals.org 9, 2009.

Opedal, Nils van der Tuuk. 2011. *NMR as a tool to follow destabilization of water-in-oil emulsions.* Trondheim : NTNU, NT-faculty, 2011. NTNU 2011:216.

Opedal, Nils van der Tuuk, Sørland, Geir and Sjöblom, Johan. 2010. Emulsion Stability Studied by Nuclear Magnetic Resonance (NMR). *Energy & Fuels.* 24, 2010, 3628-3633.

Painter, Paul C and Coleman, Michael M. 1997. *Fundamentals of Polymer Science.* s.l. : CRC Press, 1997.

Pal, Rajinder. 2000. Shear viscosity behavior of emulsions of two immiscible liquids. *Journal of Colloid and Interface Science.* 225, 2000, Vols. 359-366.

Palmer, A.G. 2012. NMR Spectroscopy: NMR Relaxation Methods. *Comprehensive Biophysics.* Columbia University, New York : s.n., 2012.

Patrick, Fernandez, et al. 2004. Nano-emulsion formation by emulsion phase inversion. *Colloids and surfaces A: Physiochem.* 251, 2004.

Pedrosa, S.M:C.P. and Nunhez, J:R:. 2000. The beavior of stirred vessels with anchor type impellers. *Computers & chemical Engineering.* 24, 2000, Vols. 1745-1751.

Peña, Alejandro A. and Hirasaki, George J. 2006. NMR Characterization of emulsions. [book auth.] Johan Sjöblom. *Emulsions and emulsion stability.* Boca Ralton : CRC Press, Taylor & Francis Group, LLC, 2006.

Sajjadi, S, Zerfa, M and Brooks, B.W. 2000. Morphological change in drop structure with time for abnormal polymer/water/surfactant dispersions. *Langmuir.* 16, 2000, 10015-10019.

Sanchez, M.C., et al. 2001. Emulsification Rheokinetics of Nonionic Surfactant-Stabilized Oil-in-water emulsions. *Langimuir.* 17, 2001, Vols. 5410-5416.

Sharma, Manju and Yashonath, S. 2007. *Size Dependence of Solute Diffusivity and Stokes-Einstein Relationship: Effect of van der Waals Interaction.* Bangalore , India : Institute of Sience, 2007.

Simon S, Pierrard X, Sjöblom J, Sørland GH. 2011. Separation Profile of Model Water-in-Oil Wmulsions followed by Nuclear Magnetic Resonance (NMR) measurements: Application Range and Comparison with a Multiple-light Scattering Based Apparatus. *Journal of Colloid and Interface Science .* 356, 2011, Vols. 352-361.

Sugiura, Shinji and Mitsutoshi Nakajima, Satoshi Iwamoto , and Minoru Seki. 2001. Interfacial Tension Driven Monodispersed Droplet Formation from Microfabricated Channel Array. *National Food Research Institute.* 17, 2001, Vol. 18, 5562-5566.

Sørland, Geir Humborstad. 2013. *Characterisation of water in paint at different concentrations.* Trondheim : Norwegian University of Science and Technology, Ugelstad Laboratory, Jotun AS, 2013.

Tuck, N. 2000. *Volume VI: Waterborne and Solvent based alkyds and their end user applications.* Chichester : John Wiley & sons Ltd, 2000. ISBN 471985910.

Ugelstadlab. 2009. ugelstadlab. *Ugelstadlab instrumentation.* [Online] 2009. [Cited: 26 11 2012.] http://www.chemeng.ntnu.no/research/polymer/ugelstadlab/instrumentation.htm.

Viswanath, Dabir S., Ghosh, Tushar K. and Prasad, Dasika H. L. 2007. VISCOMETERS. [book auth.] Tushar K. Ghosh, Dasika H. L. Prasad, Nidamarty V.K. Dutt, Kalipatnapu Y. Rani Dabir S. Viswanath. *Viscosity of Liquids - Theory, Estimations, Experiment, and Data.* s.l. : Springer Link, 2007.

Wang, L., Tiu, C. and Liu, T.J. 1996. Effects of nonionic surfactant and associative thickener on the rheology of polyacrylamide in aqueous glycerol solutions. *Colloid polmer Sci.* 234, 1996, 138-344.

Watson, David J. and Mackley, Malcom R. 2002. The rheology of aqueous emulsions prepared by direct emulsification and phase inversion from a high viscosuty alkyd resin. *Colloids and Surfaces A: Physicochemical and Engineering aspects .* 196, 2002, Vols. 121-134.

Weissenborn, P.K. and Motiejauskaite, A. 2000. Emulsification, drying and film formation of alkyd emulsions. *Progress in Organic Coatings 40.* 2000, pp. p.253–266.

WTW. 2004. Handheld meter Cond 315i. *Operating manual.* s.l., Germany : WTW GmbH, Weilheim, 03 2004.

Xylem Inc. 2011. globalw.com. *TetraCon 325 CONDUCTIVITY CELLS.* [Online] 2011. [Cited: 27 11 2012.] http://www.globalw.com/products/tetracon.html.

Yaron, I and Gal-Or, B. 1971. On viscous flow and effective viscosity of concetntrated suspensions and emulsions. *Rheologica acta.* 11, 1971.

Young and Freedman. 2007. *University Physics, Volume 2.* s.l. : Pearson, custom publishing, 2007.

Ystral gmbh. 2013. Ystral Machines, Jetstream mixer. *Ystral.de.* [Online] Ystral, 09 01 2013. [Cited: 24 05 2013.] http://www.ystral.de/Englisch/Machines/JetstreamMixer/jetstream_mixer.html.

Zhaoting, Zhang, et al. 2001. Studies on particle size of waterborne emulsions derived from epoxy resin. *European Polymer Journal.* 37, 2001.

Symbols

Table 5: List of symbols

Symbol	
W	Weight [g]
x	component
D	Diffusivity
R	Universal gas constant
T	Temperature
N_A	Avogadro constant
π	Pi
η	Viscosity [Pa s]
r_u	Radius of solute
κ	Electronic conductivity
ρ	Electrical resistivity
R_E	Electronic resistance [Ω]
V	Electronic potential [V]
I	Electric current [A]
G	Electrical conductance [S]
C_{cell}	Cell constant for a conductivity cell
S	Surface area [cm^2]
L	Length [cm]
E	Critical electric field [V/cm]
I_0	Intensity of wavelengths, initially (light & NMR)
I	Intensity of wavelengths, after absorption (light & NMR)
I/I_0	Transmittance
A	Absorbance
C	Concentration [mol/L]
ε	Molar absorptivity [L/mol cm]
$\sigma_{sc}/\sigma_{abs}/\sigma_{tot}$	Cross section of a particle/ cross sectional contribution form absorbance / total cross sectional of particle plus absorbance
r_p	Radius of particle
λ	Wavelength
n	Index of refraction
N	Number of particles
OD	Optical density
γ	Gyromagnetic ratio
$\dot{\gamma}$	Shear rate [1/s]
φ	Fraction of dispersed phase
ω	Relative angular velocity [rad/sec]
N_{ca}	Capillary Nr
r	Radius
M	Torque
C	Constant provided by producer
τ	Share stress
α	Angle
δ	Gradient pulse length

g	Strength of applied pulsed magnetic field
D(Δ)	Molecular diffusion coefficient
Δ	Z-storage delay
T_1 & T_2	Longitudinal and Transverse relaxation time
2τ	Inter echo spacing

Abbreviations

Table 6: List of abbreviations

Abbreviations	
NIR	Near infrared spectroscopy
NMR	Nuclear magnetic resonance
CPI	Catastrophic phase inversion
w/o	Water in oil emulsion
o/w	Oil in water emulsion
VOC	Volatile organic compounds
CMC	Critical micelle concentration
HLB	Hydrophilic lipophilic balance
DSD	Droplet size distribution
rpm	Rotations per minute
DLS	Dynamic light scattering
NIBS	Non-invasive back scattering
SOP	Standard operating procedure
OD	Optical density
PFG	Puls-field gradient
STE	Stimulated echo
CPMG	Carr-Purcell-Meiboom-Gill sequence
OP	Operating procedure
PDI	Poly dispersity index
EML	Emulsification
STD	Standard deviation

List of Figures

List of Tables

Appendix

Appendix A Performed emulsification tests

Temperature 35 ^{o}C and water addition 20 mL/min if nothing else is stated.

Table 7: Performed emulsifications

EML NR	Stirrer	Syst.	Z avg [nm] /PDI	Visk max [cP]	Testing	Conclusion
9	Anchor	1	188 / 0,07	-	Anchor reference from pre-project	Good emulsion
11	Jet	1	179 / 0,052	-	Introduction to Jetstream mixer. Jetstream vs. Anchor stirring comparison	Ok start, technical problems.
12	Jet	1	183 / 0,044	-	Jetstream vs. Anchor stirring comparison	Good relation between the processes from 9 and 12
13	Jet	1	177 / 0,062	1100	Optimising Jetstream mixing for NMR testing, comparing the Jetstream process vs. Anchor	Several short stops in stirring, problems with water on top.
14	Jet	1	178 / 0,063	1240	Optimising Jetstream mixing for NMR testing, higher water addition(30 mL/min)	Good emulsion, no stop in stirring. Problems with water on top and difficult to landand test quickly enough
15	Jet	1	183 / 0,086	1290	Optimising Jetstream mixing for NMR testing, better cooling, testing viscosity as well	Stop in stirring due to overheating of the motor at 37,5 ^{o}C.
16	Jet	1	182 / 0,037	1080	Optimising Jetstream mixing for NMR testing, better cooling	Stop in stirring due to overheating of the motor
17	Jet	1	179 / 0,058	1310	Jetstream higher temperature 40 ^{o}C, basis for NMR testing	Better stirring with warmer alkyd, not fully tested due to technical difficulties.

18	Anchor	1	183 / 0,054	1310	Anchor reference, system 1, moderate water addition	Good reference related to previous project results
19	Anchor	3	-	863	Half amount non-ionic, and reduced anionic surfactant, not expected to invert	Does not invert
20	Anchor	2	216 / 0,014	416	Less non-ionic, more anionic, not stabile over time	Never high viscosity, but not stabile over time
21	Anchor	4	297 / 0,178	2545	System 1 without neutralizer	Extremely high viscosity and poor end result
22	Anchor	4	256 / 0,167	4140	System 1 without neutralizer	Extremely high viscosity and poor end result
23	Anchor	7	227 / 0,095	3620	Alternative alkyd	High viscosity and poor end result
24	Anchor	5	-	3370	System 1 without non-ionic surfactant	Did not invert
25	Anchor	7	226/ 0,089	4120	Alternative alkyd, higher temperature	Extremely high viscosity and poor end result, not stabile
26	Anchor	1	174 / 0,048	894	Rapid water addition (40-60 mL/min) after addition of 440 mL and ensured inversion by conductivity. Max viscosity significance	Good results, low visk and good emulsion qualities
27	Anchor	1	193 / 0,043	1480	Slow water addition (10 mL/min) between 200ml and 500 mL (creamy condition)	No big improvement, higher and longer period of high viscosity
28	Anchor	1	183 / 0,045	1130	Water break but normal stirring for 30 min, after 300 mL	No big process problem
29	Anchor	1	193 / 0,063	1400	Water leak 200 mL/min, after 300 mL	No big process problem, but high viscosity
30	Anchor	1	188 / 0,169	1400	Stirring failure, with water addition for 10 min and 20 min full stop water on top. after 300 mL	No big process problem, but high viscosity over a longer period

31	Anchor	1	182,5 / 0,052	1490	Stirring failure, with 150 mL water addition, and 30 min full stop water on top. After 200 mL	No big process problem, and good result!
32	Anchor	6	-	250	Alternative surfactant, high temperature (45ºC)	No inversion, possible neutralization problem
33	Anchor	6	239 / 0,128	1080 0	Alternative surfactant, high temperature (45ºC)	Extremely high viscosity, almost rubber at maximum.

Norwegian University of Science and Technology

NTNU Trondheim Department of Chemical Engineering

Ugelstad Laboratory

Characterisation of water in paint at different concentrations

Geir Humborstad Sørland

Research contract for Jotun

February 2013

Report of Analysis **Date: 22.02.13**

Responsible: Geir Humborstad Sørland, Anvendt Teknologi AS

Technical Responsible: Geir Humborstad Sørland, Anvendt Teknologi AS

Services rendered at Ugelstad Laboratory, NTNU

Summary

5 samples were studied during an inversion process from water in oil into oil in water. Water concentrations were approximately 10%, 18%, 25%, 30% and 35%. At 10% we found mono-modal droplet size distribution of water in oil emulsion with droplet sizes varying from 1 to 40 um. For the other concentrations a bimodal distribution was found, with one ~5% phase of smaller droplets and the rest of increasing droplet size with concentration of water. At 35% the fraction of small water in oil droplets was of the order of 1%.

Introduction

The object of this contract work was to study the impact of adding water into a system of alkyd oil on droplet sizes and to see if an inversion could be detected.

Samples

Alkyd oil supplied by Jotun and water.

Experimental

Experimental procedure

Samples containing different amounts of water were studied by NMR. Droplet size distribution, S/V distributions and water profiles were recorded using an application that assumes water droplets < 100 um. As it became evident that there was a bimodal droplet size distribution, a set of diffusion measurements were conducted in order to verify this bimodality.

NMR – water profile

Figure 4.2.1 shows a NMR sequence used for measuring the water profile. Initially, the NMR signal contains a crude oil and water contribution. Because of a significantly lower transverse relaxation time for the crude oil, one may use the C1 loop to suppress the contribution from the crude oil. The first gradient echo is then from water only, and a Fourier transform of this echo yields a water profile. The second loop is used to measure a gradient echo at an even longer observation time, which gives another water profile. These two profiles may then be used to correct for transverse relaxation of the water signal, ending with a third water profile, which is unaffected by transverse relaxation processes. This profile is proportional to the water content along the sample, and by calibrating with a sample that contains 100% water, one can measure the water content along the length of the emulsion. C_1 is determined by measuring the signal for pure oil phase and determining at which C_1 value the entire oil signal has vanished.

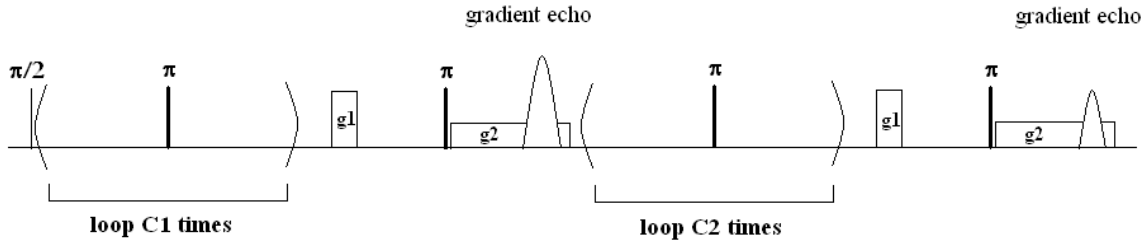

Figure 4.2.1: NMR sequence used for acquiring the water profile.

The NMR measurements were performed on a low field NMR spectrometer supplied by Anvendt Teknologi AS. The magnetic field is 0.48 T, capable of delivering a gradient strength up to 4 T/m. The duration of the sinusoidal gradient pulse is 0.8 ms, and the direction of the gradient is along the length of the tube. The NMR sample tubes of 18 mm diameter were filled with ~4 mL of the emulsion. The operating temperature was 33°C.

Details about the NMR procedure is given in Opedal et al. ”*Emulsion Stability Studied by Nuclear Magnetic Resonance (NMR)*”, Energy & Fuels, 2010, 24, 3628-3633 and in Simon et al. “*Separation Profile of Model Water-in-Oil Wmulsions followed by Nuclear Magnetic Resonance (NMR) measurements: Application Range and Comparison with a Multiple-light Scattering Based Apparatus*”, Journal of Colloid and Interface Science 356, 2011, 352–361.

In addition to this procedure we applied another method for acquiring water profiles that suppresses the part of the water with high mobility, either being preset in big droplets (>60um) or in a bulk phase. This method was applied because, as shown in section 5, there was a bimodal structure on the droplet size distribution. Details of this procedure are not available, as it has not been published yet.

Droplet size distributions (DSD) by NMR

There is a situation where the surface relaxation term is absent in the solution of the diffusion propagator, i.e. for diffusion within closed cavities and when the diffusing molecules have covered mean free path lengths >> cavity dimension [$(6 D_0 t)^{1/2} >> R_{cavity}$]. In such a situation the attenuation of the NMR signal from diffusion within the closed droplet can be simplified to

$$\frac{I}{I_0} \approx \exp^{-\frac{\gamma^2\delta^2 g^2 R^2}{5}} \tag{4.1}$$

where δ is the gradient pulse length, g is the applied gradient strength and R is the droplet radius. In a heterogeneous system a distribution in droplet sizes must be assumed. As long as [$(6 D_0 t)^{1/2} >> R_{cavity}$] holds for all sizes eq. (4.1) is valid also for a heterogeneous system. If ξ_i is the volume fraction of the droplets with surface to volume ratio $(S/V)_i$, eq. (4.1) can be expressed as

$$\frac{I}{I_0} \approx \sum_i \xi_i \exp^{-\frac{\gamma^2\delta^2 g^2 R_i^2}{5}} \tag{4.2}$$

When the exponent in Equation 4.2 is small for all *i*, we may expand the exponential functions using its two first terms:

$$\frac{I}{I_0} \approx \left(\sum_i \xi_i - \sum_i \xi_i \frac{\gamma^2\delta^2 g^2 R_i^2}{5}\right) = 1 - \frac{\gamma^2\delta^2 g^2 \overline{R^2}}{5} \tag{4.3}$$

Where $\overline{R}^2$ yields the average value of the square of the droplet radius. Measurements of the early departure from I_0 as a function of applied gradient strength may then result in a value for the average surface to volume ratio. This can be used in combination with a T_2 distribution to result in a droplet size distribution as shown in the following.
Assuming that the water molecules are probing the droplets within the sample, there is a simple relation between T_2 values and the droplet sizes

$$T_2 \approx \frac{V}{S\rho} \tag{4.4}$$

This couples the surface to volume ratio to the surface relaxivity, ρ, and makes it difficult to assign the T_2 distribution directly to a (V/S) distribution. However, if we make the assumption that eq. (4.4) holds for any droplet size, with ξ_i being the

volume fraction of pores with surface to volume ratio $(S/V)_i$ and corresponding relaxation time T_{2i} , we may write

$$\sum_i \xi_i \frac{1}{T_{2i}^2} = \sum_i \xi_i \rho_i^2 \left(\frac{S}{V}\right)_i^2 = 9\sum_i \xi_i \rho_i^2 \left(\frac{1}{R_i^2}\right) \approx 9\rho^2 \overline{\left(\frac{1}{R^2}\right)} \tag{4.5}$$

Here we have made the assumption that the surface relaxivity ρ is independent of droplet size. The left hand side of eq. (4.5) is the harmonic mean $\overline{1/T_2}$ of the T_2-distribution weighted by the fraction ξ_i of nuclei with relaxation time T_{2i} and n is the number of subdivisions of droplet sizes. This average can be calculated from the T_2-distribution obtained in a CPMG measurement where the magnetization attenuation $M^{obs}(t)$ is converted to a T_2 distribution by solving an inverse problem using e.g. an Inverse Laplace Transform (ILT) routine. Then the surface relaxivity ρ can be calculated from eq. (4.5)

$$\rho = \frac{1}{3}\sqrt{\left(\overline{\frac{1}{T_2^2}}\right) \times \left(\overline{\frac{1}{R^2}}\right)^{-1}} \tag{4.6}$$

$\left(\overline{R^2}\right)$ is the quantity that we are able to measure according to equation 4.3. $\left(\overline{\frac{1}{R^2}}\right)^{-1}$ is a parameter that we have to find an expression for based on measurable quantities in order to find a value for the surface relaxivity. Again denoting *(S/V)* as *(3/R)*, as for spherical droplets and assuming the surface relaxivity to be independent of droplet size we have the following relations

$$\left(\overline{\frac{1}{T_2^2}}\right) = 9\rho^2\left(\overline{\frac{1}{R^2}}\right), \quad \overline{T_2^2} = \frac{\overline{R^2}}{9\rho^2}, \text{ and } \left(\overline{\frac{1}{T_2}}\right) = 3\rho\left(\overline{\frac{1}{R}}\right) \tag{4.7}$$

From these expressions it's straight forward to deduce the following expression:

$$\overline{\left(\frac{1}{R^2}\right)} = \overline{\left(\frac{1}{T_2^2}\right)}\left(\frac{\overline{T_2^2}}{\overline{R^2}}\right) \tag{4.8}$$

Substituting this in the equation for ρ we finally get

$$\rho = \frac{1}{3}\sqrt{\overline{\left(\frac{1}{T_2^2}\right)}^2 \left(\frac{\overline{T_2^2}}{\overline{R^2}}\right)} \tag{4.9}$$

Finally, the measured T_2-distribution can be transformed into an absolute droplet size distribution (V/S) by means of the relationship inherent in eq. (4.4). To sum up, the procedure for deriving absolute droplet size distributions is as follows:

- The square of the average droplet radius is found from fitting eq. (4.1) to a diffusion measurement at long observation times.

- The square of the average droplet radius can be correlated to the average ($1/T_2$) found from a CPMG experiment. From eq. (4.7) eq. (4.6) can then be written as

$$\overline{\left(\frac{1}{T_2^2}\right)} \approx 9\rho^2 \overline{\left(\frac{1}{R^2}\right)} \quad \Rightarrow \quad \rho = \frac{1}{3}\sqrt{\frac{\overline{\left(\frac{1}{T_2^2}\right)}^2}{\left(\frac{\overline{T_2^2}}{\overline{R^2}}\right)}} \qquad (4.10)$$

hence we find the relaxivity, ρ, which then is assumed to be droplet size independent.

- Under the assumption of droplet size independency of the relaxivity the value of ρ can then be used in eq (4.6) thus resulting in a linear relation between T_2 and the volume to surface ratio which is a measure of the droplet size. By multiplying the T_2 distribution by the calculated surface relaxivity the distribution is normalized to a droplet size distribution in absolute length units

Separation of high viscosity oil and water signal

There are several ways to separate the NMR contribution of the oil and water components. The most straightforward way is when the viscosity of the oil is much higher than that of the water phase. Then the longitudinal and/or the transverse relaxation times will be significant different, and one may store the NMR signal for full recovery of the crude oil signal back to thermal equilibrium while the water signal still can be measured on. In figure 4.1 we have displayed the T_2 distributions of water in oil emulsion system for short and long z-storage (Δ) intervals. By increasing the duration of the z-storage one can thus omit the oil signal. The two peaks at short Δ correspond to the oil signal (left peak) and water signal (right peak), which is the strategy used by Opedal et.al.

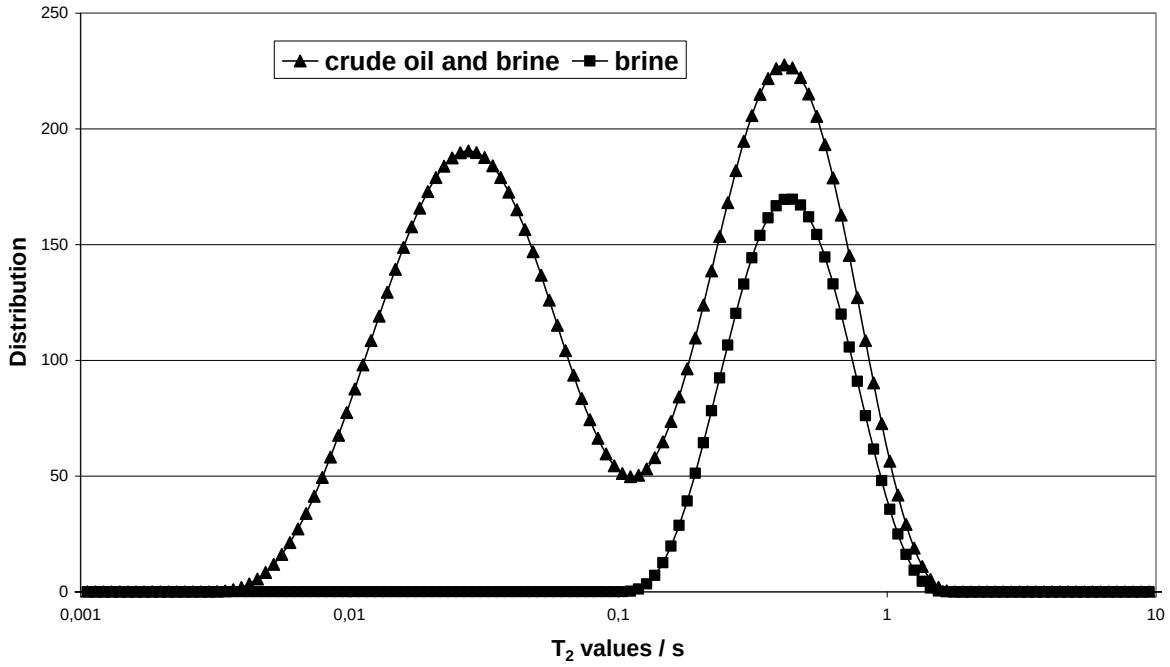

Figure 4.1: The effect of using z-storage delay Δ to obtain the T_2 distribution of water alone.

As the alkyd oil is a high viscous liquid it turns out that this is the best way of resolving the water signal from the oil signal. Further details and references may be found in Sørland et.al (*http://www.uni-leipzig.de/diffusion/pdf/volume18/diff_fund_18%282013%291.pdf)*

Results and discussion

Reproducibility

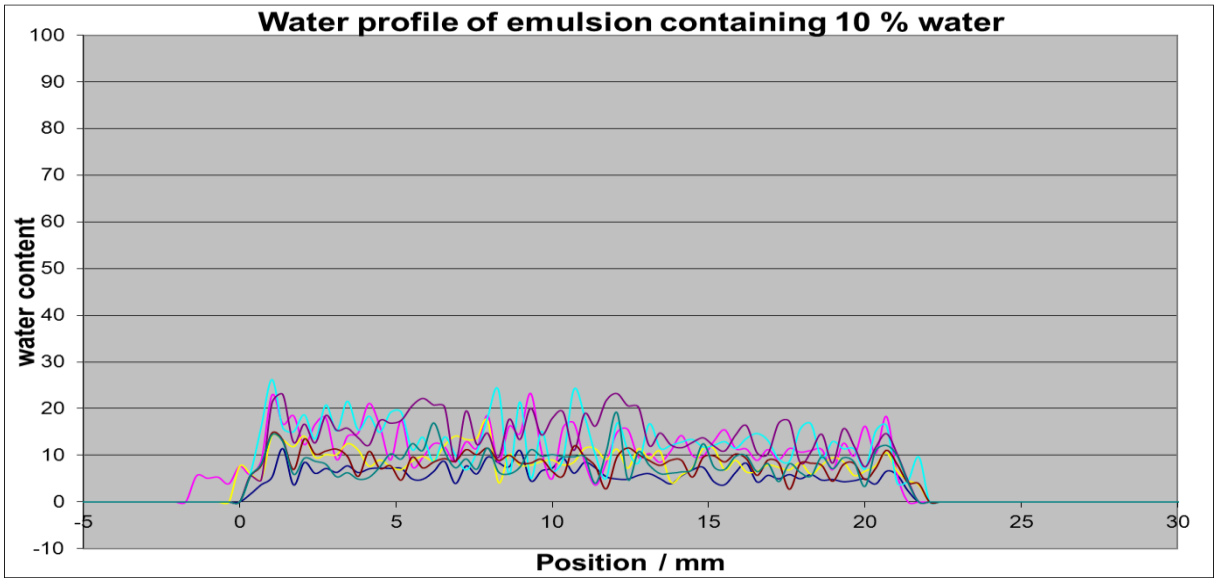

Figure 5.1: Reproducibility of water profile

In figure 5.1 we show the 7 brine profiles acquired on the same sample containing approximately 10% water. The relatively large uncertainty in the experiment is due to the need for long waiting time to suppress the oil signal. Thus much of the water signal has also vanished and resulting in the noise as shown in figure 5.1.

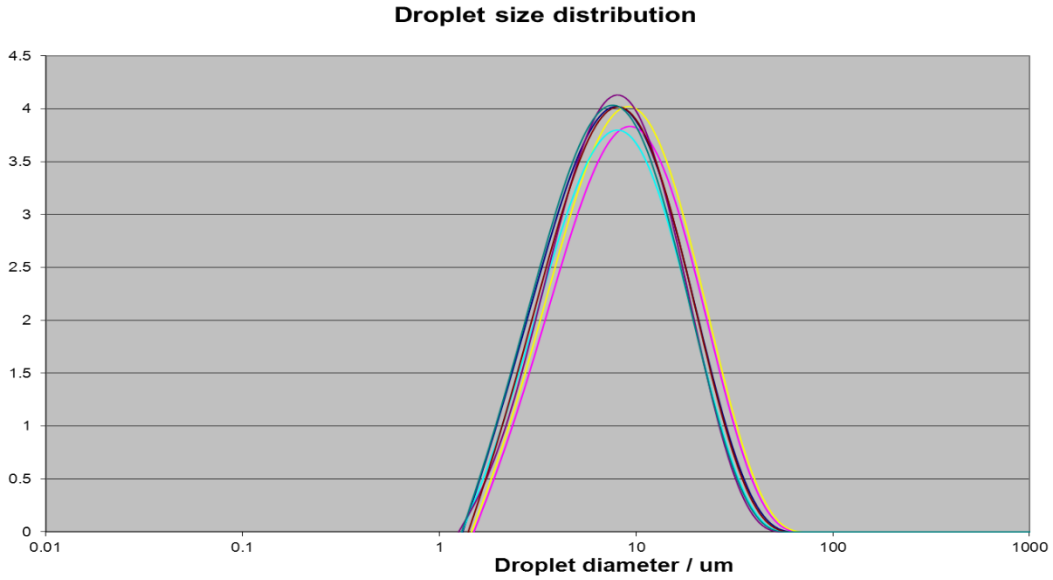

Figure 5.2: Reproducibility of droplet size distributions (DSD)

In figure 5.2 we show the 7 droplet size distributions on the same sample containing approximately 10% water. This reproducibility is acceptable and all together it seems feasible to characterize the emulsions containing alkyd oil and water from 10% water

content and upwards. However, it should be noted that one could reduce the noise in the brine profile significantly by lowering the temperature at which the measurements were conducted, for example down to 20 C instead of 33 C.

Results

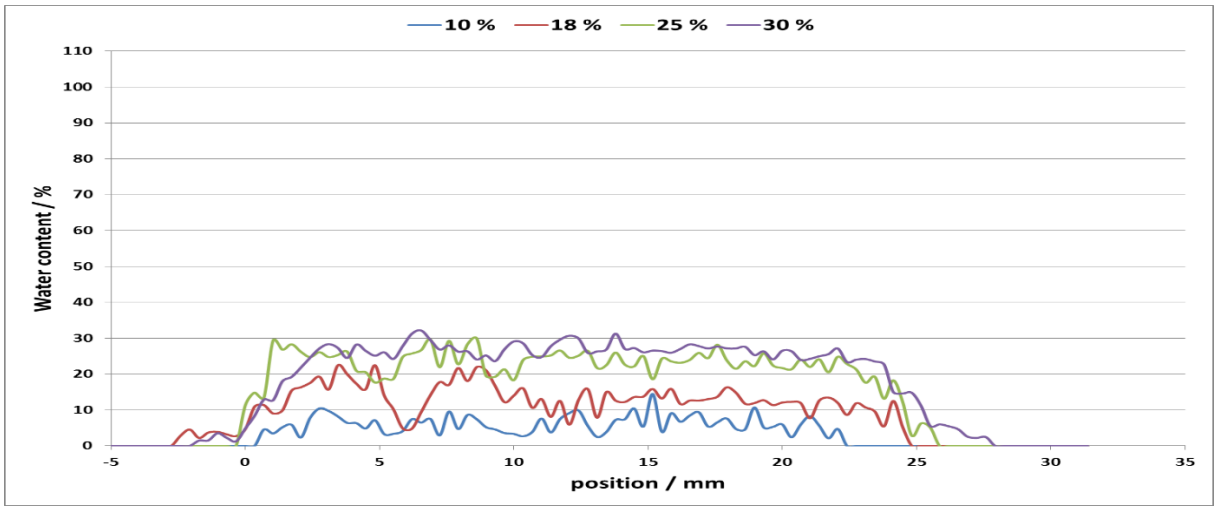

Figure 5.3: Water profiles from 4 of the 5 samples

Figure 5.3 shows the recorded water profiles. The different length of the profiles is due to slightly different filling of the emulsion into the NMR tube. Besides being close to the actual water content the profiles show that the water is relatively evenly distributed along the direction of the NMR tube (from 0 to 25 mm). The last sample, 35%, is not shown here, but had water content as expected.

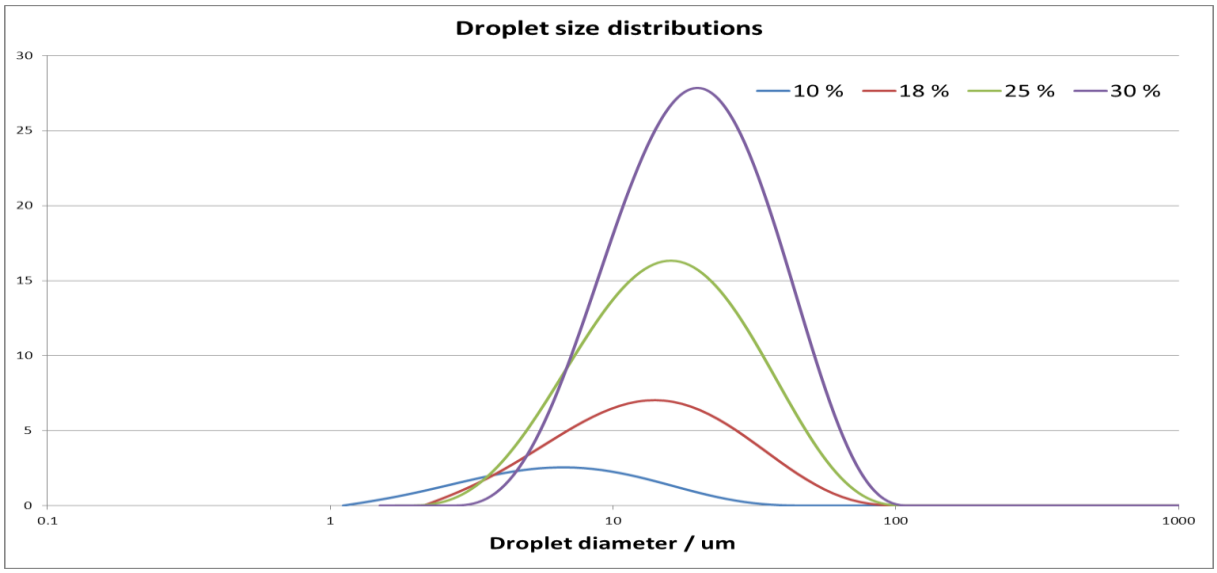

Figure 5.4 DSD assuming a mono-modal distribution

Figure 5.4 shows the distributions arising from the total NMR signal left after suppression of the oil signal (in accordance with the water profiles in figure 5.3) As expected the intensity of the distribution and the droplet sizes increases as the amount of water increases.

However, when starting to look for inversion within the systems from 35% and downwards, I realized that there was no simple picture describing the inversion point. From the experiments conducted it apparently seemed to be inverted at 35% as well as at 30% and 25 %. This was manifested in the profiles shown in figure 5.5, which are supposed to be the water profiles when the bulk water was suppressed. Surprisingly the water content then remained very low and more or less constant irrespective of how much water that was added (there might be a trend of a reduced fraction of this component as a function of water content, but there is not enough statistics to conclude with this). These profiles were recorded with an NMR experimental set-up that suppresses the water present in larger droplets (>60 um) or in a bulk phase. In figure 5.6 the droplet size distributions arising from these profiles are shown. In contrast to the increasing DSD's in figure 5.4, the DSD's of the 3 systems measured remained constant or slightly reduced in size (with 10% as the reference). All together there seemed to be two populations of DSD's that behaved differently as a function of water content. It should also be noted that while the DSD's in figure 5.6 are the actual DSD's, there is a weighting between the two populations in figure 5.4. thus the DSD's for the population with bigger droplets will definitely be larger than displayed in figure 5.4, or it could even be an inverted phase present.

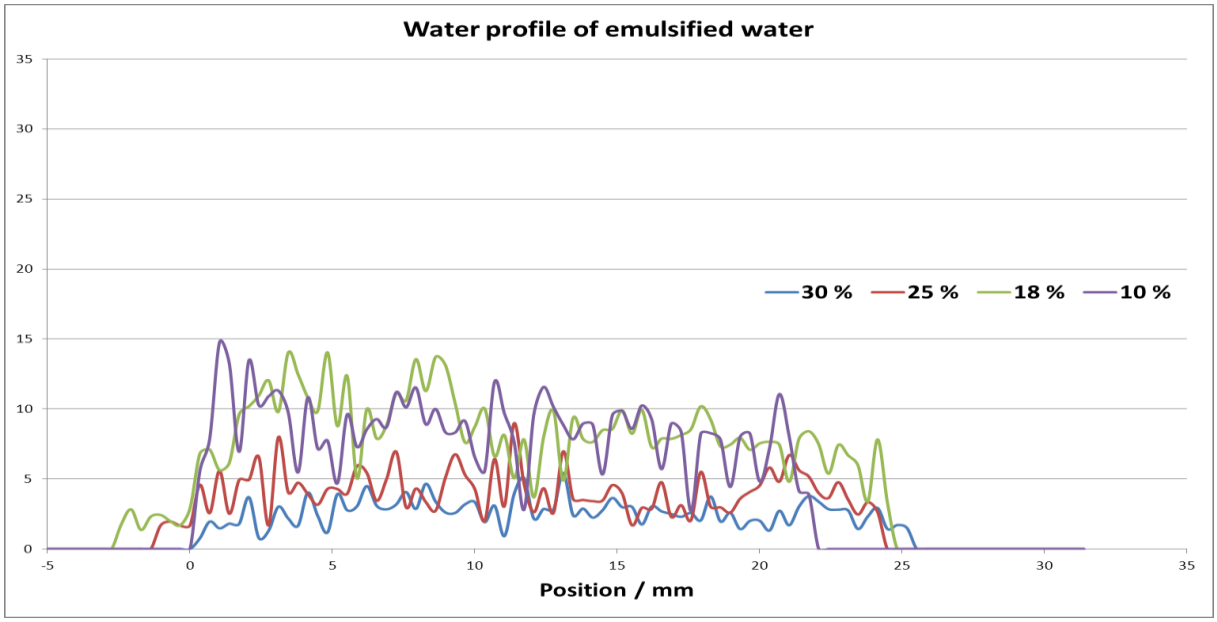

Figure 5.5: The water profile of the water present in smaller droplets (~5-10 um)

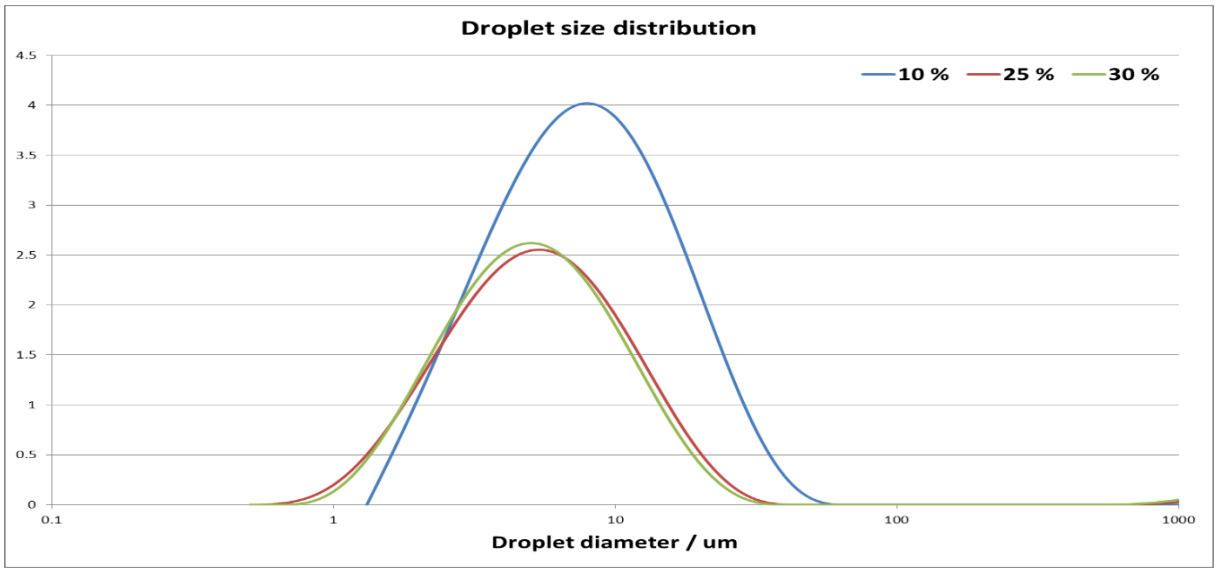

Figure 5.6. The droplet size distributions from the part of the water which is found in the smaller droplets.

In order to investigate the presence of the two populations further, I decided to perform an extra set of diffusion measurements on the 5 systems. These measurements will not only reveal the presence of the two populations, but also probe when inversion is taking place, i.e. at the concentration where the water diffusivity is significantly enhanced compared to the previous experiments.

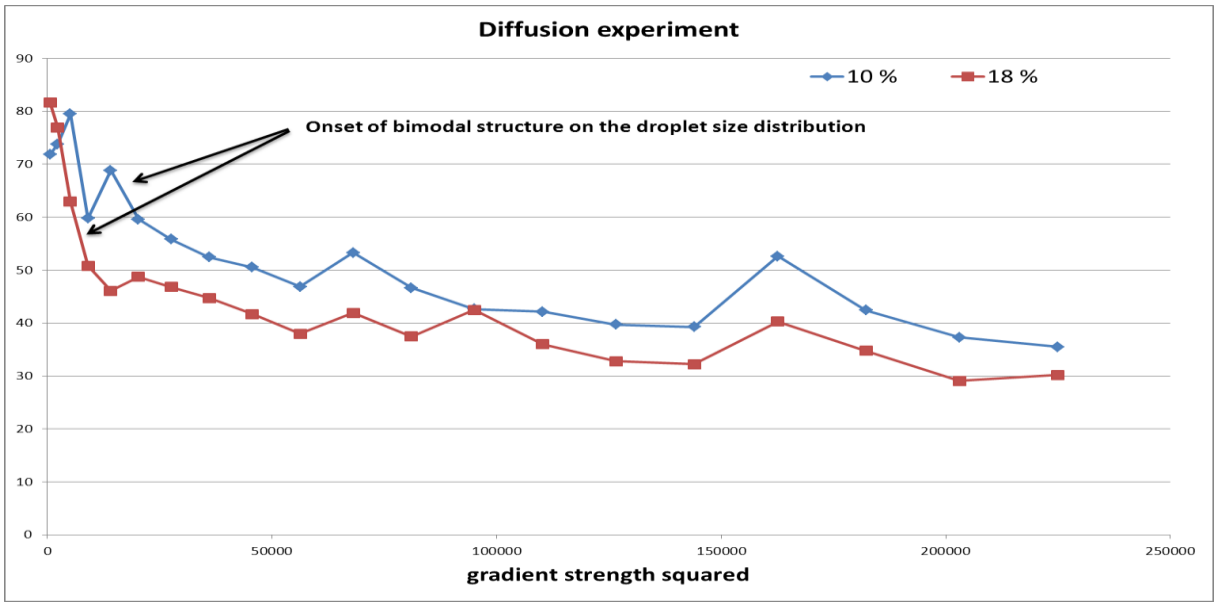

Figure 5.7: An NMR diffusion experiment performed on the systems with water content of 10% and 18%.

In figure 5.7 we see the attenuation of the NMR signal as a function of applied magnetic field gradient strength. The slope of the attenuation is directly related to the diffusivity according to the following equation 5.1.

$$I = I_0 e^{-2(\gamma^2\delta^2 g^2 D_{(\Delta)}(\Delta+\frac{3\tau}{2}-\frac{\delta}{6}))} e^{-2(\frac{\Delta}{T_1}+\frac{4\tau}{T_2})} \quad (5.1)$$

where I_0 is the initial NMR signal intensity, γ is the gyromagnetic ratio, δ is the gradient pulse length, g is the strength of the gradient of the applied pulsed magnetic field, *D(Δ)* is the molecular diffusion coefficient, Δ is the z-storage delay, T_1 is the longitudinal relaxation time, T_2 is the transverse relaxation time and 2τ is the inter echo spacing.
In our experiment all parameters are fixed except *D(Δ)* and the gradient strength. Thus the slope is only dependent on the diffusion coefficient *D(Δ)*.

Even at 10% we may see a small component of higher diffusivity, but it is almost within its noise value. The overall contribution to the droplets within the system thus arises from the population of smaller droplets (~ 10 um (according to figure 5.6))

At 18% the situation is very different, as the population of larger droplets has increased significantly while the population of smaller droplets has remained constant or even been slightly reduced. From the NMR diffusion measurements it is therefore quite clear that the evolution of the two populations is very different. It seems as if the oil is saturated with smaller droplets and the excess forms a population of larger droplets.

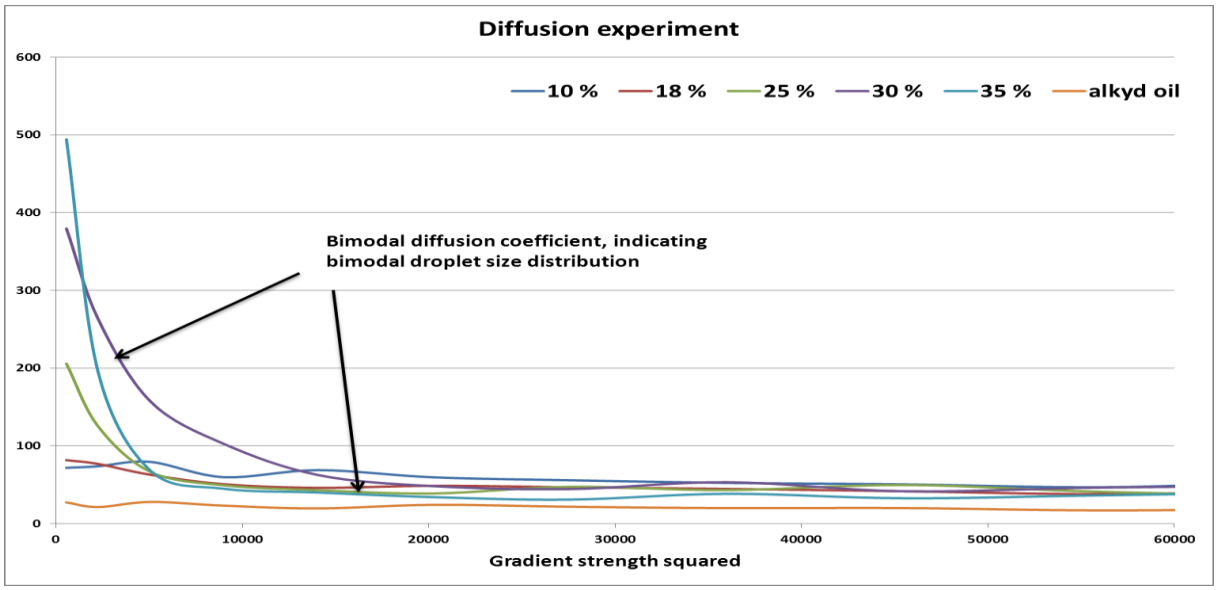

Figure 5.8 An NMR diffusion experiment performed on all the systems investigated.

In figure 5.8 we show the results from all the diffusion experiments + we have done the experiment on pure alkyd oil. This was done to ensure that the population of smaller droplets did not origin from residual oil signal. As seen in figure 5.8 all attenuations are located above the oil signal, which verifies the existence of a population of smaller droplets.

As for the increase from 10% to 18% the excess water was placed in the population of larger droplets while the population of smaller droplets remained constant or got slightly decreased. The fraction of smaller droplets at 35% seems to be the smallest one and is probably not more than ~1% of the total fraction.

What about inversion?

In figure 5.9 we have displayed the initial decay of the natural logarithm of the attenuations shown in figure 5.8. Then the slope is directly proportional to the slop of the attenuations, and we disregard the smallest population which is less than 105 for all systems investigated.

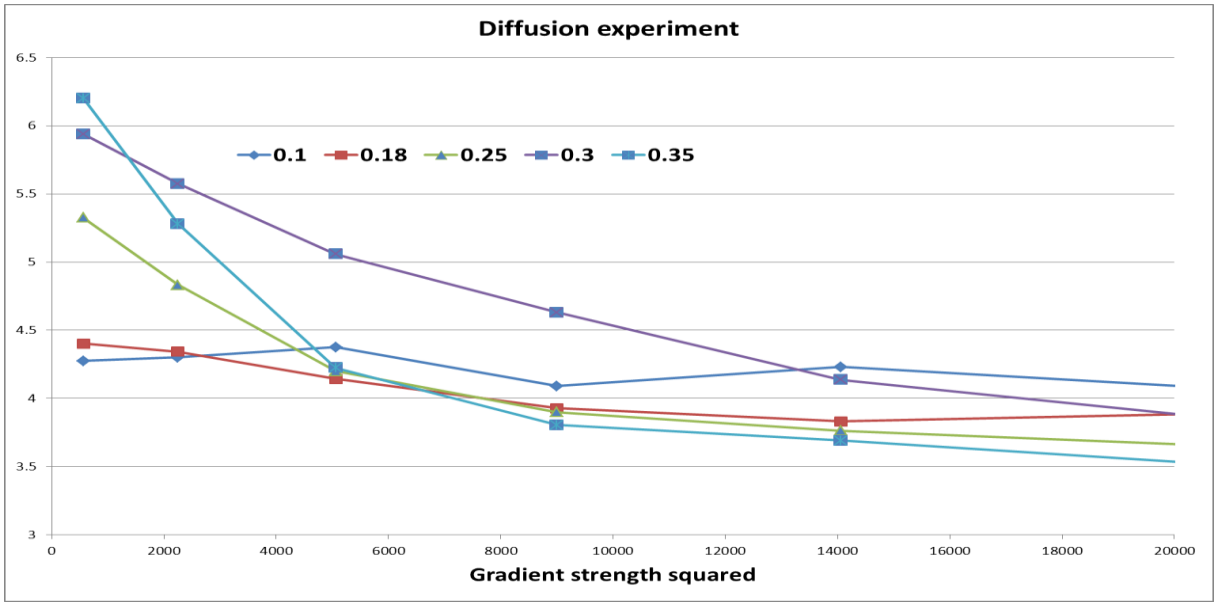

Figure 5.9 An NMR diffusion experiment performed on all the systems investigated.

As the water content increases from 18% to 25% the slope is steeper. This indicates that the droplet sizes are getting bigger in the population of bigger droplets. However, when going from 25% to 30%, we see that the initial slope is not steeper than at 25%. This may suggest that a maximum droplet size has been reached, and that the added water forms bigger droplets around that size or smaller.

At 35% the slope is getting much steeper compared to 30%, and it is likely that this is a manifestation of an inversion having taken place.

Conclusions

- It is likely that inversion has taken place between 30% and 35 %.
- Bot oil and water emulsions are most likely present at 35%.
- A bimodal droplet size distribution is more or less present in all samples. The least in the 10% sample.
- The DSD of the smaller droplets remains approximately constant but is being reduced in fraction as the water content is increased.
- The DSD of the larger droplets increases as the water content is increased up to 25%. Then it remains constant.
- Reducing the measuring temperature for better resolving of the water and oil signal prior to DSD and diffusion measurements is highly recommended for future measurements.

0-1

Appendix C Risk assessment

Participants in the identification process (including their function): Martine Lefsaker (M.Sc) Wilhelm Glomm (supervisor) and Stian Engebretsen (Jotun AS)

Short description of the main activity/main process: Emulsification of Alkyd and testing of the emulsion

Activity/process	Responsible person	Laws, regulations etc.	Existing documentation	Existing safety measures	Comment
Heating of reactants to 60 degrees Reactants: alkyds and surfactants	Martine Lefsaker	AML, Laboratory- and workshop handbook NTNU	Instructions from Jotun AS, Safety data sheets	Safety glasses, Lab coat, gloves	All reactants have critical heating temperature higher than 60 degrees, but below 60 degrees one/more of the surfactants is wax and not compatible for mixing.
Use of neutralizer	Martine Lefsaker	AML, Laboratory- and workshop handbook NTNU	Safety data sheets		
Weighing of reactants directly in the glass reactor	Martine Lefsaker	AML, Laboratory- and workshop handbook NTNU	Instructions from Jotun AS	Safety glasses, Lab coat, gloves	Clean spill immediately with ethanol to avoid sticky surfaces.

Weighing of water and tempering in water bath	Martine Lefsaker	AML, Laboratory- and workshop handbook NTNU	Instructions for use of water heater	Safety glasses, Lab coat, gloves	
Emulsion of Alkyd Continuous stirring and addition of water from burette.	Martine Lefsaker	AML, Laboratory- and workshop handbook NTNU	Instructions from Jotun AS	Safety glasses, Lab coat, gloves and training before use	Equipment set up as close as possible to equipment in Jotun laboratory. Clean spill immediately with ethanol to avoid sticky surfaces.
Sampling Using disposable pipette's and small gas containers	Martine Lefsaker	AML, Laboratory- and workshop handbook NTNU		Safety glasses, Lab coat, gloves	Clean spill immediately with ethanol to avoid sticky surfaces.
Use of Nanosizer for testing of droplet size	Martine Lefsaker	AML Laboratory- and workshop handbook NTNU	Instructions from Jotun, and the Nanosizer procedure	Safety glasses, Lab coat, gloves and training before use	Diluted 1 droplet in 150 ml dest. water
Using of NIR	Martine Lefsaker		Procedure and training	Safety glasses, Lab coat, gloves and	Use original sample vials

				training before use	
Using of Rheometre	Martine Lefsaker		Procedure and training	Safety glasses, Lab coat, gloves and training before use	Clean spill immediately with ethanol to avoid sticky surfaces.
Use of e-critical cell	Martine Lefsaker	AML, Laboratory- and workshop handbook NTNU	Procedure and training	Safety glasses, Lab coat, gloves and training before use	Clean spill immediately with ethanol to avoid sticky surfaces.
Using of NMR	Geir Sørland	AML, Laboratory- and workshop handbook NTNU	Procedure		
Use of alcohol for cleaning	Martine Lefsaker	AML, Laboratory- and workshop handbook NTNU	Data sheet, extremely flammable	Safety glasses, Lab coat, gloves, work in fume hood, minimize spill	
Waste handling	Martine Lefsaker	AML, Laboratory- and workshop handbook NTNU, National Waste handling regulations	Data sheets, alternative surfactants are toxic for water living creatures.	Safety glasses, Lab coat, gloves, minimize spill	Al but alternative surfactants goes in the drain if inverted to water continuous. Emulsions containing alternative surfactants needs to be handled as special waste

Unit: IKP **Date: 17.10.2012**

Line manager:

Participants in the risk assessment (including their function): Martine Lefsaker (M. Sc) and Wilhelm Glomm (supervisor)

Activity from the identification process form	Potential undesirable incident/strain	Likelihood:	Consequence:			Risk value	Comments/status Suggested measures
		Likelihood (1-5)	Human (A-E)	Environment (A-E)	Economy/ material (A-E)		
Heating of reactants to 55 degrees	Burns due to spill of hot chemicals	3	A-B	A	A	A-B3	Status: Using gloves and labcoat and keeping lids on at all times when not in use to minimize likelihood.
Heating of reactants to 55 degrees	Fire hazard due to spill	2	A-B	A-B	A-E	A-B2	Status: Always keep clean, and clean immediately when spilling in order of avoiding sticky residues on surfaces or weight. None of the chemicals are rated extremely flammable.
Use of neutralizer	Spill that might cause skin irritation	2	B	A	A	B2	Status: Using gloves and lab coat and keeping lids on at all times when not in use to minimize likelihood.
Weighing of reactants directly in the glass reactor	Spill	2	A	A	A	A2	Status: Using gloves and lab coat and keeping lids on at all times when not in use to minimize likelihood.

Weighing of water and tempering in water bath	**Electric shock due to bad isolation of wires**	**2**	**B**	**A**	**A**	**B2**	**Status: No wires near the water bath. Pump placed on the edge closest to the contact point.**
Emulsion of alkyd **Continuous stirring and addition of water from dripping funnel.**	**Skin or /and eye reaction** **from the spill or splatter of reaction media**	**3**	**A**	**A**	**A**	**A3**	**Status: Safety glasses mandatory. Use of nitrile gloves . Experiments are performed in in fume hood**
Emulsion of alkyd **Continuous stirring and addition of water from dripping funnel.**	**Crushing of reactor or temperature probe due to unstable stirring.**	**2**	**A**	**A**	**A**	**A2**	**Status: Continuously watching of the stirring speed and viscosity of the emulsion in order to keep stabile stirring.**
Sampling **Using disposable pipettes and small gas containers**	**Risks of cuts due to sampling near rotating devise.**	**2**	**A**	**A**	**A**	**A2**	**Status: Using disposable plastic pipettes that will break rather that crush and cut, try to take samples as fare from the stirrer as possible.**
Using of Rheometre	**Risks of burning the heating device due to fail in cooling**	**2**	**A**	**A**	**C**	**A2**	
Use of e-critical cell	**Risk of shock due to un isolated probes or wires**	**2**	**A**	**A**	**A**	**A2**	**Low and slowly increasing current, Probes kept with in the cell at any operating time. Visual inspection of wires prior to electricity usage.**
Use of alcohol for cleaning	**Spill may be extremely flammable**	**2**	**B**	**B**	**A-E**	**B2**	**Always keep clean and wash when spilling. Use gloves, lab coat and safety glasses.**

Consequence, e.g.:	*Risk value (each one to be estimated separately):*
A. Safe	*Human = Likelihood x Human Consequence*
B. Relatively safe	*Environmental = Likelihood x Environmental consequence*
C. Dangerous	*Financial/material = Likelihood x Consequence for Economy/materiel*
D. Critical	
E. Very critical	

Potential undesirable incident/strain

Identify possible incidents and conditions that may lead to situations that pose a hazard to people, the environment and any materiel/equipment involved.

Criteria for the assessment of likelihood and consequence in relation to fieldwork

Each activity is assessed according to a worst-case scenario. Likelihood and consequence are to be assessed separately for each potential undesirable incident. Before starting on the quantification, the participants should agree what they understand by the assessment criteria:

Likelihood

Minimal 1	Low 2	Medium 3	High 4	Very high 5
Once every 50 years or less	Once every 10 years or less	Once a year or less	Once a month or less	Once a week

Consequence

Grading	Human	Environment	Financial/material
E Very critical	**May produce fatality / ies**	**Very prolonged, non-reversible damage**	**Shutdown of work >1 year.**
D Critical	**Permanent injury, may produce serious health damage/sickness**	**Prolonged damage. Long recovery time.**	**Shutdown of work 0.5-1 year.**
C Dangerous	**Serious personal injury**	**Minor damage. Long recovery time**	**Shutdown of work < 1 month**
B Relatively safe	**Injury that requires medical treatment**	**Minor damage. Short recovery time**	**Shutdown of work < 1 week**
A Safe	**Injury that requires first aid**	**Insignificant damage. Short recovery time**	**Shutdown of work < 1 day**

The unit makes its own decision as to whether opting to fill in or not consequences for economy/materiel, for example if the unit is going to use particularly valuable equipment. It is up to the individual unit to choose the assessment criteria for this column.

Risk = Likelihood x Consequence

Please calculate the risk value for “Human”, “Environment” and, if chosen, “Economy/materiel”, separately.

About the column ”Comments/status, suggested preventative and corrective measures”:

Measures can impact on both likelihood and consequences. Prioritise measures that can prevent the incident from occurring; in other words, likelihood-reducing measures are to be prioritised above greater emergency preparedness, i.e. consequence-reducing measures.

MATRIX FOR RISK ASSESSMENTS AT NTNU

CONSEQUENCE						
	Very critical (E)					
	Critical (D)					
	Danger-ous (C)					
	Relativ. safe(B)		3			
	Safe(A)		7	2		
		Minimal	Low	Medium	High	Very high
		LIKELIHOOD				

Principle over accept criterion. Explanation of colours used in risk matrix.

colour		Description
Red		Unacceptable risk. Action must be carried out to minimize risk.
Yellow		Assessment area. Action must be evaluated.
Green		Acceptable risk. Action might be evaluated from other considerations.

Appendix D Process reports

Process reports for al emulsifications performed during the project.

Table 8: Process report emulsification 9, system 1, anchor impeller, results from earlier study (Lefsaker, 2012)

Test nr:	EML 9	Date: 5,11,12				Av DRS:	188	
						PDI:	0,07	
Comment: System 1, Anchor stirrer								
	T Alkyd	**Water addition**	**Conductivity**	**Stirring**			**e-critical**	**Comments**
[min]	**[C°]**	**[mL]**	**[µS/cm]**	**RPM**	**Z avg**	**PDI**		
0	34,5	0	0	200	1720	0,863	1,94293	water start
2	34,9	40	0	250	420	0,573	1,95505	
4	35	80	0	250	190	0,183	0,02994	
6	35	120	0	300	182	0,141	1,94599	
8	34,9	160	0	300	218	0,239	1,99613	Lots of air
10	34,8	200	0	300	191	0,2	1,81595	--- || ---
11	34,7	220	0,2	300	191	0,14	0,85062	--- || ---
12	34,7	240	0,5	300	195	0,275	0,28196	
13	34,6	260	1,4	350	193	0,173	0,20539	
14	34,6	280	2,7	350	196	0,159	0,14142	
15	34,6	300	4,4	350	188	0,125	0,15328	
16	34,6	320	9,7	400	185	0,091	0,1292	
17	34,4	340	14,5	400	165	0,166	1,02523	
18	34,3	360	0	400	162	0,157	0,80783	
19	34,2	380	0	400	175	0,095	0,22131	
20	34,1	400	0,1	450	163	0,055	0,07866	
21	34,1	420	2	450	162	0,044	0,05079	

[min]	T Alkyd [C°]	Water addition [mL]	Conductivity [µS/cm]	Stirring RPM	Z avg	PDI	e-critical	Comments
22	34,1	440	2,9	450	177	0,082	0,04807	
24	34,2	480	770	550	241	0,557	0,04932	
25	34,2	500	1040	550	625	0,766	0,07235	
26	34,2	520	1060	550			0,04408	
28	34,3	560	1100	600	208	0,041	0,04837	thick
30	34,3	600	1135	500	195	0,025	0,03969	
35	34,4	700	1211	450				
40	34	800	1230	450	188	0,07	0,04409	
45	33,8	900	1245	350				ending water
50	33,6		1240	350			0,04408	

Table 9: Process report emulsification 11, system 1, jetstream mixer,

Test nr:	EML 11	Date:	30,01,2013	Av DRS:	179
				PDI:	0,052
Purpose:	Testing the Jet stream mixer				
	stirring constant 4500 rpm (ca. 1,5)				
	-1 g to much AMP				
Comments:	Difficult to get it Tempered to 35 degrees, Try starting with cooling water at low temp not 35 degrees,				
	Cooling takes a long time Temp water start 25 degrees, end 23 degrees				
	Too slow water addition, especially in the start				

Time [min]	T Alkyd [C°]	Water addition [mL]	Conductivity [µS/cm]	Z avg	PDI	E-critical	NIR	Comments
0	40,5	0	0					water start
4	39,5	50	0	249	**0,307**	1,847977	0,17727	- some water on top
8	39,2	80	0	1010	**0,779**	1,94925	0,12710	
10	39,1	100	0			1,9385467	0,12988	
12	39	120	0	887	**0,72**	1,8913667	0,15289	to slow water addition
14	38,7	150	0			1,9672447	0,14578	
16	38,4	200	0	178	**0,12**	0,3278967	4,14669	
18	37,7	275	0,34			0,1334717	1,65982	
20	37,4	325	0,42	172	**0,221**	0,5372293	0,79233	2 min stop in stirring + due to heating (viscosity)
22	36,8	400	0,21			0,0907241	0,72569	
24	36,5	450	0,39	177	**0,124**	0,0599857	4,30650	
26	35,8	475	195	196	**0,338**	0,1014011	4,53470	

Test nr:	EML 11	Date:	30,01,2013		Av DRS:	179		
					PDI:	0,052		
Time [min]	**T Alkyd [C°]**	**Water addition [mL]**	**Conductivity [µS/cm]**	**Z avg**	**PDI**	**e-crit**	**NIR**	**Comments**
28	35,4	525	260	314	**0,61**	0,0666319	4,75071	very viscous
35	34,6	625	279	193	**0,34**	0,0440284	4,52526	
40	34,2	725	289	187	**0,6**	0,0440326	4,36650	
45	33,3	850	295					milk ich
50	33,3	950	296	183	**0,56**			ending water

Table 10: Process report emulsification 12, system 1, jetstream mixer

Test nr:	EML 12	Date:	01.02.2013		Av DRS:	183		
					PDI:	0,044		
Purpose:	Testing of the Jet stream mixer with faster water addition (ca 40 mL/min) Stirring constant 4500 rpm (ca 1,5) Better cooling with cold water from the start, start the heater at the same time as the water addition Preheat water separately to 35 degrees, heat loss ca. 5 degrees pr. 15 min. Water start at 35 degrees							
Time [min]	**T Alkyd [C°]**	**Water addition [mL]**	**Conductivity [µS/cm]**	**Z avg**	**PDI**	**e-critical µS/cm**	**NIR optical density**	**Comments**
0	36	0	0,4					water start
1	36,2	40	0,5					water on top
2	36,4	80	0,4			1,882764	0,16479	- not soluble for Z avg
3	36,4	100	0,4					water on top
4	37	120	0,4			1,8560113	0,17112	- bad correlation, and no good results
5	37	160	0,4					lots of water on top

Time [min]	T Alkyd [C°]	Water addition [mL]	Conductivity [µS/cm]	Z avg	PDI	e-critical µS/cm	NIR optical density	Comments
7	37,3							water added at 33 degrees
8	37,3	250	0,5	182	0,172	0,3294167	3,96823	stirs in water at better rate
9	37,2	300	5,2					
10	37	340	1,5	186	0,162	0,5613333	0,42856	
11	37,1	380	0,6					less water on top, thickens the stirrer slakes due to resistance,
12	37,2	400	1	172	0,044	0,0959528	0,3535	turned it back up to 4500 rpm
13	37,2	440	753					
14	37,2	480	1020	237	0,398	0,0854475	4,61347	
15	37,2	520	1180					
16	37,1	560	1200	325	0,468	0,0626769	4,90004	still water on top, water added at 30 degrees
17	36,9	580	1250					very viscous
18	36,8	640	1285	187	0,066	0,0439975	5,04732	
19	36,5	680	1330					
20	36,2	720	1350	186	0,058	0,04401	4,80101	
21	36	780	1360					milky
22	36,7	820	1370	185	0,036	0,0480676	5,04674	
23	35,7	860	1370					
24	34,8	900	1370	181	0,045	0,0440082	4,80253	stopping water addition
25	34,8							
26	34,8			183	0,044			Ending emulsion

Table 11: Process report emulsification 13, system 1, jetstream mixer

Test nr:	EML 13	Date:	06.02.2013	Av DRS:	177
				PDI:	0,062

Purpose: Testing of the Jet stream mixer with moderate water addition (ca 30 mL/min)
Stirring constant 4500 rpm (ca 1,5)
Better cooling with cold water from the start, start the heater at the same time as the water addition
Preheat water separately to 35 degrees, heat loss ca 5 derees pr 15min.
Water start at 35 degrees
testing visk as well

Time [min]	T Alkyd [C°]	Water temp [C°]	Water addition [mL]	Conductivity [µS/cm]	Z avg	PDI	e-critical µS/cm	NIR optical density	Viscosity	Comments
0	36		0	0						lots of water on top,
2	35,8	32,5	50	0	NAN	NAN				difficult to stir
4	35,7	32	120	0	NAN	NAN	1,9666747	0,16968	2,58	pull stirrer a bit up
6	35,6	32	160	0	NAN	NAN	1,93342	0,17607	2,77	still lots of water on top, bad stirring
7	35,6	31,4	200	0						
8	35,1	31,1	240	0,3	179	0,169	0,288077	4,14424	3,29	bad stirring rpm =4500
9	35	30,9	270	5,7						lift stirrer some more
10	34,8	30,7	300	12,4	173	0,174	0,343848	0,74177	5,95	-lots of water dragged in suddenly
11	34,7	30,5	340	0,1						still water on top, getting viscous
13	33,7	30	410	10						first stop 30 sek. Next stop 2 min, stopping water and time.
14	33,3	29,8	440	45	195	0,129	0,0654065	4,39562	3,93	rpm =1170 2 min of stop
15	33,2	29,7	470	989						- went 10 micro Siemens up during 2 min of stop.
16	33	32	500	1089	219	0,53	0,0734137	4,78738	7,04	mega viscous
18	32,9	31,6	580	1190	183	0,066	0,0533595	4,4376	11	

Time [min]	T Alkyd [C°]	Water temp [C°]	Water addition [mL]	Conductivity [µS/cm]	Z avg	PDI	e-critical µS/cm	NIR optical density	Viscosity	Comments
20	33,2	31,5	640	1309	180	0,05	0,0480869	4,48771	4,35	
22	33,5	31,4	700	1335	178	0,052	0,0399248	4,34901	3,37	
25	34,6	31,1	800	1351	175	0,049	0,039923	4,37987	1,63	
30	35,3	31,1	1000	1350	177	0,045	0,0399258	4,51252	0,607	

Table 12: Process report emulsification 14, system 1, jetstream mixer

Test nr:	EML 14	Date:	08.02.2013	Av DRS:	178
				PDI:	0,063

Purpose: Testing of the Jet stream mixer with moderate water addition (ca 30 mL/min) take 2
Stirring constant 4500 rpm (ca 1,5)
Better cooling with cold water from the start, start the heater at the same time as the water addition
Preheat water separately to 35 degrees, heat loss ca 5 degrees pr 15 min. Refill hot water (heat something in the tub)
Water start at 35 degrees
testing viscosity as well

Time [min]	T Alkyd [C°]	Water temp [C°]	Water addition [mL]	Conductivity [µS/cm]	Z avg	PDI	e-critical µS/cm	NIR optical density	Viscosity	Comments
0	36,4	36,2	0	0						
2	36,3	35,6	50	0,1						lots of water on top, bad stirring
5	36,3	34,3	120	0			1,34941135	0,21053	2,79	
8	36	33,3	0,057	0	772	0,63	2,00025334	0,28418	3,59	
9	35,8	33,1	225	0						lift stirrer more

Time [min]	T Alkyd [C°]	Water temp [C°]	Water addition [mL]	Conductivity [µS/cm]	Z avg	PDI	e-critical µS/cm	NIR optical density	Viscosity	Comments
10	35,6	32,8	250	0	178	0,079	0,16196647	4,20895	2,63	- Water contamination of sample, from top water
11	35,5	32,7	275	0,1						still water on top, getting viscous
12	34,9	32,3	300	0,1	180	0,128	0,59868735	0,34518	7,3	-lots of water dragged in suddenly
13	35,1	32	325	0,1						
14	35,3	31,7	350	0	189	0,234	0,31737533	1,33723	8,46	not so much water on top
15	35,6	31,5	375	0,2						
16	35,7	31,3	400	2,6	165	0,051	0,07341293	2,45927	1,69	mega viscous
17	35,9	31	420	60,5						
18	35,9	33	440	727	183	0,307	0,06253713	5,06838	4,83	high viscosity
19	36	32,5	460	1090						
20	36,1	32	480	1138	230	0,187	0,0672816	4,55436	9,14	
21	36,3	31,9		1210						
22	36,5	31,9	540	1248	183	0,059	0,0480819	4,76145	12,4	
23	36,7	31,8		1277						
24	36,9	31,7	600	1299	181	0,034		4,52684	7,41	
25	36,9	31,7		1297						
26	37,4	31,5	640	1329	181	0,066	0,0440142	4,52573	5,12	water back on top
28	37,5	31,5		1345						
30	37,5	31,5	750	1357	179	0,046	0,047754	4,54867	2,61	
36	37,1	30,7		1369						milky
38	37	30	920	1369						stopping water
40	37	29,5		1369	178	0,063		4,36822	0,72	ending emulsion

Table 13: Process report emulsification 15, system 1, jetstream mixer

Test nr:	EML 15	Date:	13.02.2013	Av DRS:	183	216	1 mai (2 mnd +)
				PDI:	0,086	0,019	

Purpose: Testing of the Jet stream mixer with moderate water addition (ca 20 mL/min)
Stirring constant 4500 rpm (ca 1,5)
Better cooling with cold water from the start, but motor failed at 37,5 degrees. Difficult to stir at 35 degrees.
Preheat water separately to 40 degrees, heat loss ca 5 degrees pr 15 min. Refill hot water (heat something in the tub)
Water start at 40 degrees , testing of viscosity

Time [min]	T Alkyd [C°]	Water temp [C°]	Water addition [mL]	Conductivity [µS/cm]	Z avg	PDI	e-critical µS/cm	NIR optical density	Viscosity	Comments
0	37,5	40	0	0						Motor fail before water start
2	37,9	39,5	40	0						Stirs better than EML 13, 14
5	39,8	39	100	0			1,89329067	0,18084	2,89	less water on top
8	41,1	38,8	140	0			1,90992867	0,19078	3,29	
10	41,6	38,6	180	0	175	0,1	1,976634	0,3642	4,51	
12	41,9	38,4	220	0,6	199	0,292	0,257984	4,17391	3,16	conductivity rise
14	42	38,1	260	5	190	0,147	0,15347133	4,35871	2,47	
16	41,9	37,9	280	30,7	171	0,074	0,13210533	1,435	2,24	top conductivity 44
18	41,9	37,7	320	0,4	165	0,164	0,561184	0,2914	7	conductivity 0
20	42,3	30	360	0,4	173	0,066	0,181468	1,32722	2,7	
22	42,2	37,2	400	3,2	178	0,087	0,05876687	3,25556	3,17	
24	41,6	36,6	450	921	355	0,492	0,0521368	4,58154	6,2	Thickens
26	41,3	35,9	500	1209	217	0,057	0,0460472	4,59281	12,9	
28	40,8	36	550	1283			0,0440073	4,54819	8,63	
30	40,7	35,7	600	1300	190	0,059	0,0460447	4,24678	6,02	
35	39,7	35,3	720	1343	188	0,06	0,035867	4,42754	2,41	
40	38,4	35	850	1359	183	0,086	0,0440076	4,40041	1,15	milky

Table 14: Process report emulsification 16, system 1, jetstream mixer

Test nr:	EML 16	Date:	18.02.2013	Av DRS:	182	237	1. May (2 mnd. +)
				PDI:	0,037	0,036	
Purpose:	Testing of the Jet stream mixer with moderate water addition (ca 20 mL/min) Stirring constant 4500 rpm (ca 1,5) Better cooling with cold water from the start, alkyd cooled only to 37 degrees. Water start at 35 degrees testing visk as well						

Time [min]	T Alkyd [C°]	Water temp [C°]	Water addition [mL]	Conductivity [µS/cm]	Z avg	PDI	e-critical µS/cm	NIR optical density	Viscosity	Comments
0	37,8	35,1	0	0						
2	37,5	35	40	0						
5	37,3	34,4	100	0			1,88664467	0,20489	3,08	+ 5 ml warm water
8	37,2	35,5	160	0			1,96658533	0,20108	3,56	
10	37,4	35,3	200	0,1			1,59620936	0,20489	4,62	stirs ok, not so much water on top
12	37,7	35,2	240	1,2	180	0,165	0,1600748	4,32673	2,55	
13	37,7	35,1	260	2,3						
14	37,9	35,1	280	8,2			0,111888	0,94674	2,46	thick , conductivity top
16	38,4	34,4	320	0,5	178	0,208	0,398604	0,80706	5,36	
17	39	35,8	340	0,8						
18	39,1	35,6	360	0,8			0,10019573	0,91499	1,93	Stop in stirring due to overheating of motor (30 sek, no stop in water addition or clock)
19	38,8	35,5	380	128						
20	38,6	35,4	400	257	167	0,056	0,05860467	3,15236	2,52	
21	38,6	35,3	420	821						

Time [min]	T Alkyd [C°]	Water temp [C°]	Water addition [mL]	Conductivity [µS/cm]	Z avg	PDI	e-critical µS/cm	NIR optical density	Viscosity	Comments
22	38,4	35	440	1009			0,04670453	4,59483	5,06	some water on top
24	38,4	34,7	480	1185	186	0,706	0,04670533	4,77555	5,29	extremely thick
26	38,4	35,7	520	1233			0,041954	4,60604	10,8	
28	38,4	35,7	560	1273			0,041953	4,53151		
30	37,9	35,2	700	1307	193	0,052	0,041952	4,43227	7,03	still thick
35	37,1	34,9	800	1347						
40	36,8	33	900	1373	182	0,037	0,039906	4,45755	1,55	stop water addition
45				1373						end emulsion

Table 15: Process report emulsification 17, NMR testing of system 1, jetstream mixer

Test nr:	EML 17	Date:	20.02.2013	Av DRS:	179,4
				PDI:	0,058

Purpose: Testing of the Jet stream mixer with moderate water addition (ca 20 mL/min)
NMR testing
Stirring constant 4500 rpm (ca 1,5)
Better cooling with cold water from the start, alkyd cooled only to 40 degrees.
Preheat water separately to 40 degrees, heat loss ca 5 degrees pr 15 min. Refill hot water
Water start at 40 degrees
- Logging failure, only sparse written data on temperatures and conductivity
T Alkyd between 39-42 C° and water between 39 – 42 C°

Time [min]	T Alkyd [C°]	Water temp [C°]	Water addition [mL]	Conductivity [µS/cm]	Z avg	PDI	e-critical µS/cm	NIR optical density	Viscosity	Comments NMR
0	40,7	39,9	0	0						Water start
2			25	0						
5			50	0			1,91312867	0,17679	2,64	
										-NMR 1: 160 mL (ca 10%) water on top
8			110	0			1,90653867	0,20651	3,4	Possible a bit earlier
10			175				1,99003267	0,21611	4,53	stirs ok
12			200	4	288	0,428	0,50006867	4,13113	3,27	- local conductivity maximum
14			240	7	189	0,201	0,246548	4,25551	2,6	
16			260		186	0,179	0,1320856	1,69560	2,19	-NMR 2: 280 mL (ca 18%)
18			310		240	0,457	0,31479667	0,44613	6,85	
20			360	0,7	175	0,059	0,09595053	0,59228	1,55	
22			425	8	232	0,355	0,04671467	4,34283	5,41	-NMR 3: 400 mL (ca 25%)
24			475	450	412	0,454	0,0480646	4,49354	8,87	
26			550	1120	192	0,049	0,048066	4,47323	13,1	-NMR 4: 500 mL (ca 30%)
28			620	1210						
30			660		183	0,068	0,048061	4,40764	5,05	-NMR 5: 700 mL (ca 38%)
35			820		186	0,058				
40			900	1325	179,4	0,058	0,0440008	4,53512	1,1	- stop water, stop stirring after 42 min

Table 16: Process report emulsification 18, system 1, reference anchor impeller

Test nr:	EML 18		Date:	01.03.2013	Av DRS:	183	194	01.05.2013 (2 mnd)	
					PDI:	0,054	0,061	considered stabile	
Purpose:	Testing of the Anker mixer with moderate water addition (ca 20 mL/min) Reference for anchor stirrer made emulsions								
Time	**T Alkyd**	**Water temp**	**Water addition**	**Conductivity**	**Z avg**	**PDI**	**NIR optical density**	**Viscosity**	**stirring**	**Comments**
[min]	**[C°]**	**[C°]**	**[mL]**	**[µS/cm]**						**NMR**
0	34,3	37,3	0	0					200	Water start
2	35,1	37,1	60	0						
5	36,5	37	100	0			0,19546	3,24	250	
8	36,8	36,6	160	0			0,21971	4,15		
10	36,9	36,5	200	0,4			4,17201	3,39		
11			220	7,7					300	
12	36,9	36,2	240	21,5			3,76283	2,37		
13			260	23,5	188	0,085				no problems during the emulsification
14	36,9	36,6	280	0,7	186	0,287	0,54468	9,04	350	
16	36,9	35,8	320	0	184	0,178	1,02643	9,07		
18	37,1	35,5	360	3,2	170	0,043	2,23389	1,7	400	
19			380	200						
20	37	35,1	400	1007	180	0,079	4,05915	3,9		
22	37	35,9	440	1107	237	0,393	4,5497	5,02		
24	37,1	35,8	480	1171	221	0,084	4,23093	13,1	500	
26	37	35,6	520	1243	186	0,052	4,36961	10,3	600	
28	37,1	35,4	580	1299	189	0,073	4,22266	6,1		
30	37,2	35,4	640	1320	187	0,062	4,17334	5,26	700	
35	37	34,6	750	1354	181	0,058		0,85	500	

Time [min]	T Alkyd [C°]	Water temp [C°]	Water addition [mL]	Conductivity [µS/cm]	Z avg	PDI	NIR optical density	Viscosity	stirring	Comments NMR
40	36,2	34	900	1353	183	0,054			300	- stop water, stop stirring after 42 min

Table 17: Process report emulsification 19, system 3, anchor impeller

Test nr:	EML 19	Date:	06.03.2013	Av DRS:	4096
				PDI:	-
Purpose:	Testing of the Anker mixer with moderate water addition (ca 20 mL/min)				
	NON inversion, system 3				

Time [min]	T Alkyd [C°]	Water temp [C°]	Water addition [mL]	Conductivity [µS/cm]	Z avg	PDI	NIR optical density	Viscosity	stirring	Comments NMR
0	35,9	34,1	0	0					200	Water start
2	35,6	34,3	40	0						
5	34,9	35	80	0			0,22593	2,88		get withe early
8	34,7	35,5	150	0			1,10106	4,04		
10	34,6	35,9	200	0			0,70748	5,4		
11	34,5	35,9	240	0,1				6,01		
12	36,7	36,2	280	0			0,49646	5,04		
14	36	36,3	340	0			2,8858	2,25		will not thicken
16	35,5	36,5	360	0,1			2,40431	1,52		
18	35,2	36,5	380	0,1			4,19812	3,3		
20	35,1	36,5	400	0			4,10737	3,88	300	
22	34,7	36,7	450	0,1			4,30985	5,82		

Time [min]	T Alkyd [C°]	Water temp [C°]	Water addition [mL]	Conductivity [µS/cm]	Z avg	PDI	NIR optical density	Viscosity	stirring	Comments NMR
24	34,5	36,7	480	0,1			4,05573	6,7		little bit thicker and whiter
26	34,7	36,7	520	0,1			4,01057	6,15	400	
28	34,7	36,6	600	0,1			3,98269	6,91		
30	36,8	36,4	620	0,1			4,16807	8,15	350	plastic
35	37,3	36,5	750	0,1				8,63	500	
40	36,7	36,6	900	0,1			4,5878	2,62		- not soluble for measuring z avg and PDI
45	36,7	35,5	1000	0,1					300	- stop water, stop stirring after 47 min
47	30	30	1000	0,7						

Table 18: Process report emulsification 20, system 2, anchor impeller

Test nr:	EML 20	Date:	11.03.2013	Av DRS:	216
				PDI:	0,014
Purpose:	Testing of the Anker mixer with moderate water addition (ca 20 mL/min) NON stabile, system 2				

Time [min]	T Alkyd [C°]	Water temp [C°]	Water addition [mL]	Conductivity [µS/cm]	Z avg	PDI	NIR optical density	Viscosity	stirring	Comments NMR
0	35,3	35,9	0	0					200	Water start
2	35,4	35,3	60	0						
5	35	34,2	100	0			0,17152	2,716		
8	34,9	34,3	150	0			0,20007	3,247		
10	34,7	33,9	200	0			0,22106	3,94	300	

Time [min]	T Alkyd [C°]	Water temp [C°]	Water addition [mL]	Conductivity [µS/cm]	Z avg	PDI	NIR optical density	Viscosity	stirring	Comments NMR
12	34,6	33,5	240	0,1			0,38123	4,163		
14	34,7	35,3	280	1	189	0,25	4,36474	3,792	350	thickens and gets white
16	34,9	35,1	340	32,8	199	0,266	4,7561	2,481	400	
17	35,3	36,5	380	57,8						
18	35,4	36,5	380	47,8	190	0,119	4,69791	2,018		problems with stirrer and conductivity meter
20	35,5	35,4	400	70,9	191	0,119	4,4691	1,954		
22	35,7	35,2	440	80,7	185	0,073	4,5063	1,91		
24	35,9	35,2	480	272	179	0,07	4,59727	2,912	500	
26	36,1	35	540	1243	196	0,277	4,989	3,717		
28	36,2	34,5	580	1363	220	0,54	4,67281	3,768		did never turn really thick
30	36,3	35	600	1404	244	0,67	5,01924	3,572	350	
35	36,5	33,9	680	1448			4,80781		300	
40	36,4	33,2	800	1483	217	0,04	4,8439	1,684		
45	36,4	32,6	900	1498					300	- stop water, stop stirring after 47 min

Table 19: Process report emulsification 21, system 4, anchor impeller

Test nr:	EML 21	Date:	13.03.2013	Av DRS:	297				
				PDI:	0,178				
Purpose:	Testing of the Anker mixer with moderate water addition (ca 20 mL/min) NO neutralizer, system 4								
Time	**T Alkyd**	**Water temp**	**Water addition**	**Conductivity**	**Z avg**	**PDI**	**NIR optical density**	**Viscosity**	**stirring**	**Comments**
[min]	**[C°]**	**[C°]**	**[mL]**	**[µS/cm]**						
0	**34,2**	**35,6**	**0**	**0**					**200**	
2	33,3	35,6	40	0					250	early white
5	33,2	35,4	80	3,5				1,881		water on top
8	33,8	35,3	160	283				25,45	300	Thick and ductile porridge/pudding slips during stirring , try to add a lot of water
9	34	35,2	200	100						water and emulsion not miscible
10	34,4	35	300	352	297	0,178		10,51		
12	34,6	32,5	400	472	296	0,169		12,52	500	
14	35,5	32,2	500	472	302	0,153		6,986	850	
16	36,2	32	550	518	316	0,251		3,354	1000	better consistence, smoothly
18	36,4	31,8	600	489	297	0,138		2,216	800	
20	36,4	31,1	700	461	297	0,128		1,543	700	
22	36	31	900	498	303	0,164		1,194	600	very creamy and full of air bubbles.
					296	0,124				Not enough sample volume possible to test NIR

Table 20: Process report emulsification 22, system 4, anchor impeller

Test nr:	EML 22	Date:	14.03.2013	Av DRS:	256	259	1 mai (1,5 mnd)
				PDI:	0,167	0,173	
Purpose:	Testing of the Anker mixer with moderate water addition (ca 20 mL/min) NO neutralizer, system 4						

Time [min]	T Alkyd [Cº]	Water temp [Cº]	Water addition [mL]	Conductivity [µS/cm]	Z avg	PDI	NIR optical density	Viscosity	stirring	Comments
0	**39,8**	**37,8**	**0**	**0**					**200**	
2	38,1	37,3	30	0,1				2,09		easily white
4	38,2	36,9	70	38,9				2,07	250	large water droplets
6	37,8	36,6	120	305				2,93		some water on top
8	37,7	36,3	160	159				3,5	300	ductile
10	37,6	35,9	200	345				38,3	400	extremely thick and bulky, impossible to take out a sample
12	37,9	35,7	240	432				41,4		pudding like
14	38,2	35,5	280	471				40,7		
16	38,6	35,4	320	480	259	0,124		8,3	300	pudding with watery sauce, slips at to high speed
18	38,5	36,2	360	522	266	0,15		13,2	500	transforms to more smooth cream
20	38,9	35,8	400	527	264	0,145		14,2	700	
22	39,4	35,5	440	527	264	0,153		10,7		
24	39,6	35,3	480	528	263	0,149		6,51		
26	39,7	35	520		270	0,132		4,53		conductivity fail
28	39	34,5	560		266	0,154		2,87	500	
30	38,4	34,3	600		256	0,167		1,53	300	
40	38,3	33,6	900							Smooth, but not milky. To much air. Not enough sample volume possible to test NIR

Table 21: Process report emulsification 23, system 7, anchor impeller

Test nr:	EML 23	Date:	15.03.2013	Av DRS:	227				
				PDI:	0,095				
Purpose:	Testing of the Anker mixer with moderate water addition (ca 20 mL/min) Alternative alkyd, system 7								
Time	**T Alkyd**	**Water temp**	**Water addition**	**Conductivity**	**Z avg**	**PDI**	**NIR optical density**	**Viscosity**	**stirring**	**Comments**
[min]	**[Cº]**	**[Cº]**	**[mL]**	**[µS/cm]**						**NMR**
0	52	49	50	0					200	Water start
2	51,9	48,7	80	0				6,82		
5	51,7	47,9	120	0				7,4		
8	51,3	46,8	180	20				7,88	300	
10	50,4	45,9	220	35				5,32	350	thick and white
12	49,9	45	260	130				4,86		ductile
14	49,8	44,6	300	540				6,95	400	water on top, bulky
16	49,9	44	340	575				10,9	450	difficult to get good stirring, conductivity meter in the way
18	50,2	47,1	380	620	236	0,106		21,8	500	difficult to take samples
20	50,8	46,3	420	680	236	0,085		35,1	600	
22	51,2	45,4	460	702	230	0,094		36,2		bulky and foam and water on top
24	51,3	43,1	500	714	233	0,08		32	700	
26	52	42	540	733	236	0,115		26,2		lots of water along the edge
28	51,2	41,9	580	747	234	0,125		18,1		smoother
30	50,9	42,4	630	758	233	0,106		11,6		
35		41,9	750	730					500	milky
40	50,2	41,2	900	732	227	0,095		2,36	400	ending emulsification

Table 22: Process report emulsification 24, system 5, anchor impeller

Test nr:	EML 24	Date:	18.03.2013	Av DRS:	129/1292			
				PDI:	1			
Purpose:	Testing of the Anker mixer with moderate water addition (ca 20 mL/min)							
	Testing of system 5, Standard system without non-ionic surfactant							

Time [min]	T Alkyd [C°]	Water temp [C°]	Water addition [mL]	Conductivity [µS/cm]	Z avg	PDI	NIR optical density	Viscosity	stirring	Comments
0	36,8	34	0	0					200	lots of air in the start
2	36,8	33,8	40	0			2,20678	2,13		almost foaming on top
5	36,4	35	100	0			4,59718	2,43		yellow and white
8	36,6	34,5	160	0,1			4,54199	2,77		less air but still thin
10	36,8	34,4	200	0					250	
12	37,1	38,1	240	0			4,89616	3,02		thinner and more yellow
14	37,4	37,3	280	0,1						
16	37,5	37,1	340	0			4,78651	3,37		
18	37,7	36,7	380	0						still thin
20	37,8	36,5	400	0,1			4,60897	3,15	300	
22	37,9	36,2	440	0						
24	38,1	41,5	480	0			4,6361	3,17		
26	38,3	40,8	520	0						
28	38,5	40,3	580	0,1			5,05206	2,58	350	
30	38,6	40,1	620	0,1						
32	38,8	39,7	660	0,1			4,59517		400	
35	38,8	39,6	700	0,1						
40	39	38,8	900	0,1					450	two tops on the nanosizer
45	39,2	38,5	1100	0,1	129/1292	1				

Table 23: Process report emulsification 25, system 7, anchor impeller

Test nr:	EML 25	Date:	19.03.2013	Av DRS:	226	235	1 . Mai (1 mnd +)
				PDI:	0,089	0,106	
Purpose:	Testing of the Anker mixer with moderate water addition (ca 20 mL/min)						
	Alternative alkyd, system 7 at higher temperature						

Time [min]	T Alkyd [C°]	Water temp [C°]	Water addition [mL]	Conductivity [µS/cm]	Z avg	PDI	NIR optical density	Viscosity	stirring	Comments
0	59,4	67,2	0	0					200	white stripes, good mixing
2	59,9	67,3	40	0			0.14923	6,77		
5	60,4	64,5	100	0			0.16033	7,9	250	6 =17, 7=90
8	59,8	62,1	160	40			3.58603	8,53	300	
10	59,6	60,5	200	105			0.22490	5,33	400	thickens
12	59,2	61,4	240	450			0.58580	5,13	450	
14	63,2	60,1	280	620			4.56071	8,12		ductile and thick
16	59,2	59	320	665			4.91213	38,4	550	separates, bulky and dificult to sample
18	59,8	57,4	360	772			4.79521	41,2	650	difficult to sample but smoother
20	61,1	62,1	420	790	228	0,132	4.87610	34,1	700	
22	62,1	58,9	480	807				20	600	smoother
24	62,2	57,7	500	815	234	0,108	4.65570	15,2		
26	62,5	56,3	540	830	230	0,112		12,2	550	
28	62,4	55,5	580	827	221	0,12	4.72719	9,98	450	
30	62,2	54,7	600	831	226	0,147		7,94	400	
35	61,2	53,7	740	845						
40	60,4	51,5	900	848	232	0,105	4.97490	2,12	350	
45	59,7	50	1000	832					300	stopping emulsion

Table 24: Process report emulsification 26, system 1, anchor impeller

Test nr:	EML 26	Date:	05.04.2013	Av DRS:	174
				PDI:	0,048

Purpose: Testing of the Anker mixer with moderate water addition (ca 20 mL/min)
A rapid water addition (approx. 40-60 mL/min) after addition of 440 mL and ensured inversion by conductivity.
Test the significance of the viscosity top at approximately 500 mL

Time [min]	T Alkyd [C°]	Water temp [C°]	Water addition [mL]	Conductivity [µS/cm]	Z avg	PDI	NIR optical density	Viscosity	stirring	Comments NMR
0	36,1	39,3	0	0					200	Water start
2	36,1	38,6	40	0						
5	36	38,7	100	0			0,16414	2,95		
8	35,8	38,4	160	0			0,22469	4,03	250	
10	35,7	38,1	200	0,1			3,96335	3,62	350	wihtiening
11			220	2,2						
12	35,5	37,7	240	10,1			4,31608	2,7		
13			250	35,4						no problems during the emulsification
14	35,3	37,8	270	16,9			1,69692	2,61		
15			280	0,2						
16	35,2	37,3	300	0			0,47171	7,65		
18	35,2	37,1	350	0			0,88862	2,16	400	thickening
20	35,2	36,7	400	185	181	0,211	0,80011	2,64	550	
22	35,4	36,5	440	1030	182	0,186	4,67361	5,32	600	more rapid water addition
24	35,5	43,7	550	1156	178	0,035	4,75523	8,94	700	
26	36	37,7	650	1296	171	0,063	4,91583	2,87		thicker
27	36,1	43,5	700	1320					600	
28	36,2	43,3	800	1316	167	0,048	4,79518	1,44		

Time [min]	T Alkyd [C°]	Water temp [C°]	Water addition [mL]	Conductivity [µS/cm]	Z avg	PDI	NIR optical density	Viscosity	stirring	Comments NMR
30	36,2	42,3	900	1313	172	0,061	5,09618	0,875	500	- stop water, stop stirring after 32 min

Table 25: Process report emulsification 27, system 1, anchor impeller

Test nr:	EML 27	Date:	08.04.2013	Av DRS:	193				
				PDI:	0,043				
Purpose:	Testing of the Anker mixer with moderate water addition (ca 20 mL/min)								
	Slow water addition (10 mL/min) between 200 mL and 500 mL (testing of creamy condition								
Time [min]	**T Alkyd [C°]**	**Water temp [C°]**	**Water addition [mL]**	**Conductivity [µS/cm]**	**Z avg**	**PDI**		**Viscosity**	**stirring**	**Comments**
0	36,9	38,3	0	0					200	start emulsion
2	36,4	37,9	40	0						
5	36,3	37,5	100	0			0,16085	2,98		
8	36,1	37,2	160	0			0,21837	4,12	250	
10	35,7	36,6	200	0			4,13935	3,9	300	lower water addition to 10 ml/min
12,5	35,4	36,2	225	1,5			4,47884	3,05		
15	35,2	35,8	250	4,9			4,43493	2,8	350	
17,5	35	35,9	275	11,9			4,00242	2,82	400	
20	34,9	37,7	300	0,1			0,4136	8,83		
22	35,2	37,3	330	0			1,06026	9,56	500	
24	36	37	350	0			1,53866	11		stirs in to much air
26	37	36,5	370	0			1,94276	1,95		
28	38,8	35,9	390	160			3,27959	1,9	600	thickening

Time [min]	T Alkyd [C°]	Water temp [C°]	Water addition [mL]	Conductivity [µS/cm]	Z avg	PDI		Viscosity	stirring	Comments
30	39,2	35,5	410	570			4,61005	3,28		ductile
32	40,1	35,1	430	710			4,5915	5,18		
34	40,4	35	450	980	171	0,09		7,88		
36	40,5	34,5	460	990			4,70334	2,68		
38	40,4	34,1	480	1030	218	0,226		7,4		thickening
40	40,2	34	500	1070	212	0,125	5,03793	8,03		increase water addition to 20 ml/min
42	39,9	35,8	540	1100	192	0,068		14,8	500	
45	39,7	35,4	600	1140	180	0,065	4,82468	9,98		
50	38,9	35	700	1220	187	0,083	4,76004	2,98		
60	38	34,8	900	1250	193	0,043	4,91943		400	finishing emulsion

Table 26: Process report emulsification 28, system 1, anchor impeller

Test nr:	EML 28	Date:	10,04,2013	Av DRS:	183
				PDI:	0,049

Purpose: Testing of the Anker mixer with moderate water addition (ca 20 mL/min)
Water break after 300 mL (approx. 15 min) Normal stirring but break in emulsion time and water addition for 30 min,
Test of process failure

Time [min]	T Alkyd [C°]	Water temp [C°]	Water addition [mL]	Conductivity [µS/cm]	Z avg	PDI	NIR optical density	Viscosity	stirring	Comments NMR
0	36,5	42,3	0	0					200	Water start
2	35,7	41,3	40	0						
5	35,9	41	100	0			0,14907	2,93		
8	35,9	40,4	160	0			0,21799	3,83	250	

Time [min]	T Alkyd [C°]	Water temp [C°]	Water addition [mL]	Conductivity [µS/cm]	Z avg	PDI	NIR optical density	Viscosity	stirring	Comments NMR
10	35,8	39,9	200	0,2			4,08705	3,64	300	wihtiening
12	35,7	39,7	240	6,9			4,29089	2,59	350	
14	35,5	39,3	280	16,2			1,40175	2,58		
15 f	35,5	39,3	300	11			1,54103	3,25	350	cut the water for 30 min, keep the stirring
15 e	352	39,6	300	0			0,27468	7,72	350	reduces to 0 cond after 2 min f stirring
16	35,1	39,6	320	0			0,24626	8,57		
18	35,1	39,3	330	0			0,26952	8,52		
20	35,1	39,1	380	0			2,73888	1,83	450	
22	35,3	39	440	26,4	161	0,048	4,55591	4,48	500	thickening
24	35,4	38,8	470	1047			4,6126	7,28		
26	35,7	38,5	520	1077	202	0,072	4,7827	11	600	more rapid water addition
28	35,9	38,3	560	1127			4,5036	11,3		
30	36,1	37,8	600	1206	182	0,085	5,02697	4,89		thicker
35	36,1	35,3	700	1226	185	0,071				
40	35,6	34,7	800	1300	185	0,056	4,93342	2,29		
50	35,2	34,6	1000	1313	183	0,049			500	- stop water, stop stirring after 32 min

Table 27: Process report emulsification 29, system 1, anchor impeller

Test nr:	EML 29	Date:	12,04,2013	Av DRS:	193
				PDI:	0,162

Purpose: Testing of the Anker mixer with moderate water addition (ca 20 mL/min)
Water spill (200 mL) after 300 mL (approx. 15 min) increase stirring but normal water addition
Test of process failure

Time [min]	T Alkyd [C°]	Water temp [C°]	Water addition [mL]	Conductivity [µS/cm]	Z avg	PDI	NIR optical density	Viscosity	stirring	Comments NMR
0	37,7	39,6	0	0					200	Water start
2	36,3	39,3	40	0,1						
5	36,5	39,1	100	0			0,26748	3,1		
8	36,2	38,7	160	0			0,2048	4,15	250	
10	35,9	38,3	200	0,1			4,14699	4,09		
12	35,8	38,1	250	14,3			4,1566	2,61	300	
13			265	20,3				2,76		
14	35,5	37,4	280	15,6	197	0,227	1,94347	9,94	350	- slip in 200 mL real fast
16	34,7	35,7	500	830	242	0,221	4,90897	10,3	500	thickening
18	35,6	37,4	540	877	200	0,141	4,66753	14		thick
20	35,9	38,8	600	1108	191	0,161	4,78347	10,1		
22	36	38,5	640	1147			4,94047	6,92		still thick
24	35,9	38,3	680	1177	190	0,152	4,85831	4,73		
26	35,9	38,2	720	1194			5,0456	1,99	600	more rapid water addition
28	35,8	38,1	800	1213	194	0,173	4,71052			
30	35,5	37,9	850	1225	194	0,153	4,94893			
35	35,3	37,7	1000	1224	193	0,162			500	- stop water, stop stirring after 32 min

Table 28: Process report emulsification 30, system 1, anchor impeller

Test nr:	EML 30	Date:	15.04.2013	Av DRS:	188
				PDI:	0,169

Purpose: Testing of the Anker mixer with moderate water addition (ca 20 mL/min)
Stirrer fail after 300 mL (approx. 15 min) Normal water addition for 10 min (200 mL) but a break in water as well for 30 min with water on top.
Test of process failure

Time [min]	T Alkyd [C°]	Water temp [C°]	Water addition [mL]	Conductivity [µS/cm]	Z avg	PDI	NIR optical density	Viscosity	stirring	Comments
0	36,5	40	0	0					200	start
2	36,2	39,9	40	0						
5	36,4	39,4	100	0			0,17853	3,04		
8	36,1	38,9	160	0			0,38401	3,94	250	
10	35,8	38,5	200	0,1			4,0389	3,72	300	thickening
12	35,7	38,3	250	12			4,4416	2,6	350	whitening
13	35,6	37,9	270	18						
14	35,5	37,8	280	10,3			1,60499	4,77	400	
15 f	35,3	37,3	300	0			0,30943	8,41		stop stirring, let water run for 10 min
15 e	33,7		500	0,1						start up after 30 minute of rest with water on top
16	33,8	31,3	500	677	391	0,31	4,84753	9,92	400	difficult to start stirring and to pull in all the water
18	34,3	36,6	520	978	240	0,105	4,5863	14	500	Thickening quickly- but ok stirring
20	34,9	36,1	560	1050	202	0,117	4,91465	13,2		Some water at the edge, otherwise no problem
22	35,1	35,9	600	1111	201	0,131	5,0018	9,46	600	
24	35,3	35,7	640	1156			4,46035	7,05		
27	35,3	35,5	700	1176	193	0,123	5,23411	3,77		

Time [min]	T Alkyd [C°]	Water temp [C°]	Water addition [mL]	Conductivity [µS/cm]	Z avg	PDI	NIR optical density	Viscosity	stirring	Comments
30	35,3	35,3	800	1208	188	0,147		1,59	500	
35	35	31,6	900	1213	188	0,169	4,9227		400	ending

Table 29: Process report emulsification 31, system 1, anchor impeller

Test nr:	EML 31	Date:	09,05,2013	Av DRS:	182,5
				PDI:	0,052

Purpose: Testing of the Anker mixer with moderate water addition (ca 20 mL/min)
Stirrer fail after 200 mL (approx. 10 min) Normal water addition for 7 min (150 mL) but a break in water as well for 30 min with water on top,
Test of process failure

Time [min]	T Alkyd [C°]	Water temp [C°]	Water addition [mL]	Conductivity [µS/cm]	Z avg	PDI	NIR optical density	Viscosity	stirring	Comments
0	37,1	39,7	0	0					200	start
2	36,6	39	40	0						
5	36,6	38,7	100	0			0,19470	3,13		
8	36,2	38,3	160	0			0,24040	4,4	250	
10	35,9	38	200	0,5			4,00566	3,53	300	stopp stirring and water
11	34	38,9	350	2			2,58772	1,48		start stirring afetr 30 min
12	34,5	38,7	370	92,3			1,65907	2,33	350	start water
14	34	38,5	400	989			5,03376	6,38	450	Still thick and uneven
16	34,8	38,4	460	1069			4,76802	10,7		
18	34,9	38,3	500	1098	186	0,056	5,02016	14,8	500	thick but stirrs ok
20	35,3	38,1	540	1120	187	0,066	4,83784	14,9		

Time [min]	T Alkyd [C°]	Water temp [C°]	Water addition [mL]	Conductivity [µS/cm]	Z avg	PDI	NIR optical density	Viscosity	stirring	Comments
22	35,5	37,9	600	1159				7,47		
25	35,6	37,7	700	1234	181,5	0,07	4,93146	3,41		Thinner
30	35,4	37	800	1247	186,7	0,042	4,71221	1,24		
35	35,1	35,1	900	1247	182,8	0,052			400	milky

Table 30: Process report emulsification 32, system 6, anchor impeller

	EML 32	Date:	10,05,2013	Av DRS:	-
				PDI:	-
Purpose:	Test of alternative surfactant take one, Failure, most likely due to old neutralizer Testing of the Anker mixer with moderate water addition (ca 20 ml/min) Did not invert and did not solve in water for droplet size testing, Possible solution, old neutralizer?				

Time [min]	T Alkyd [C°]	Water temp [C°]	Water addition [mL]	Conductivity [µS/cm]	Z avg	PDI	NIR optical density	Viscosity	stirring	Comments
0	47,6	46,6	0	0					200	start
2	47,6	46,2	40	0,7						whitening
5	47,5	45,6	100	0			4,00566	2,716		
8	46,6	45	160	0						coarse but thin
10	46,1	44,6	200	0			5,03376	3,247		
12	45,3	44,3	240	0					250	
14	45,1	45,5	280	0			4,76802	2,481	300	
16	45,1	45,4	320	0						more even but still thin

Time [min]	T Alkyd [C°]	Water temp [C°]	Water addition [mL]	Conductivity [µS/cm]	Z avg	PDI	NIR optical density	Viscosity	stirring	Comments
18	45	45,1	360	0						
20	45	45,5	400	0			4,83784	2,018		
22	45,1	44,9	440	0						
24	45,2	45,5	480	0					400	
26	45,4	44,7	520	0			4,93146	1,954		smotth but thin
28	45,5	44,3	600	0						
30	45,6	45,9	700	0						
35	45,6	44,7	800	0						
40	45,6	44,1	900	0						

Table 31: Process report emulsification 33, system 6, anchor impeller

Test nr:	EML 33	Date:	12,05,2013	Av DRS:	239
				PDI:	0,128
Purpose:	Test of alternative surfactant take two, Testing of the Anker mixer with moderate water addition (ca 20 ml/min) Inverted but got too thick for samples big enough for NIR measurements				

Time [min]	T Alkyd [C°]	Water temp [C°]	Water addition [mL]	Conductivity [µS/cm]	Z avg	PDI	NIR optical density	Viscosity	stirring	Comments
0	47,8	50,8	0	0					200	Foam on the top
2	47,3	50,2	40	0			2,31988		250	Water pockets
5	47,6	49,5	100	25			4,80841	3,67	300	inhomogeneous
6	47,3	49,3	120	27					350	

Time [min]	T Alkyd [C°]	Water temp [C°]	Water addition [mL]	Conductivity [µS/cm]	Z avg	PDI	NIR optical density	Viscosity	stirring	Comments
8	46,7	48,9	150	31					400	thick and ductile
10	44,9	48,1	180	282			4,73517	4,38	300	thick stops , difficult to sample
12	43,1	47,7	200	398				69,7	250	separate, impossible to get full sample
14	42,1	46,8	250	394					200	stops x 2, do not stir in water
16	42,7	46,5	300	386				63,2	350	makes a ball around stirrer, sticky on the wall
18	43	45,9	350	387					600	almost solid after sampling
20	44,9	43,5	400	387				108	400	stops, slips and spins - rise the stirrer one cm
22	44,9	43,3	500	393	233	0,096	4,62182	9,54	450	inverts in the middle, sticky edges, problems including lumps in the stirring
24	46,1	42,5	550	656				12,2	600	smooth in the middle
28	45,6	42,5	600	790				6,57	500	
30	45,6	41,7	700	820	243	0,12	4,90731		450	
35	45,1	39,8	900	850	239	0,128	4,91893	1,15	300	stops, due to full reactor

Appendix E Summation plots and measurement data of the emulsion process

The data from conductivity measurements, Figure 36 and Figure 37, e-critical measurement, Figure 38, NIR baseline measurements, Figure 39, and viscosity measurements, Figure 40, in order to back up the reproducibility of the trends for system 1. The systems or process conditions that differ from system 1 is not reported here since the results deviate from the main trend of system 1. The reproducibility of the droplet size distribution is shown in Figure 41.

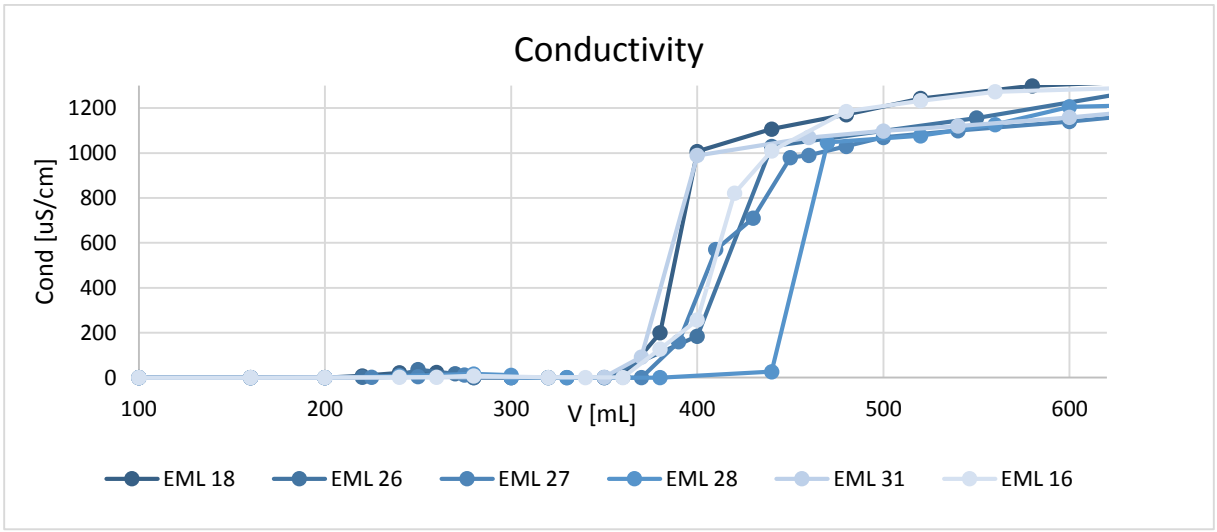

Figure 36: Reproducibility of the conductivity measurements for system 1. EML 16, EML 18, EML 26, EML 27 and EML 31

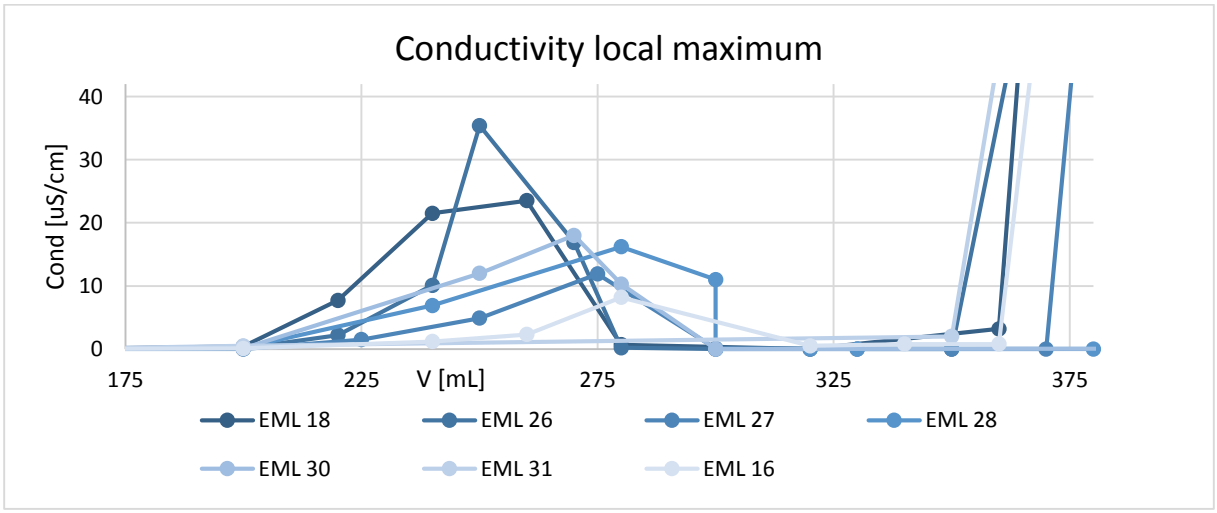

Figure 37: Reproducibility of the conductivity measurements, trend of local maximum around 250 mL for system 1. EML 16, EML 18, EML 26, EML 27, EML 28, EML 30 and EML 31

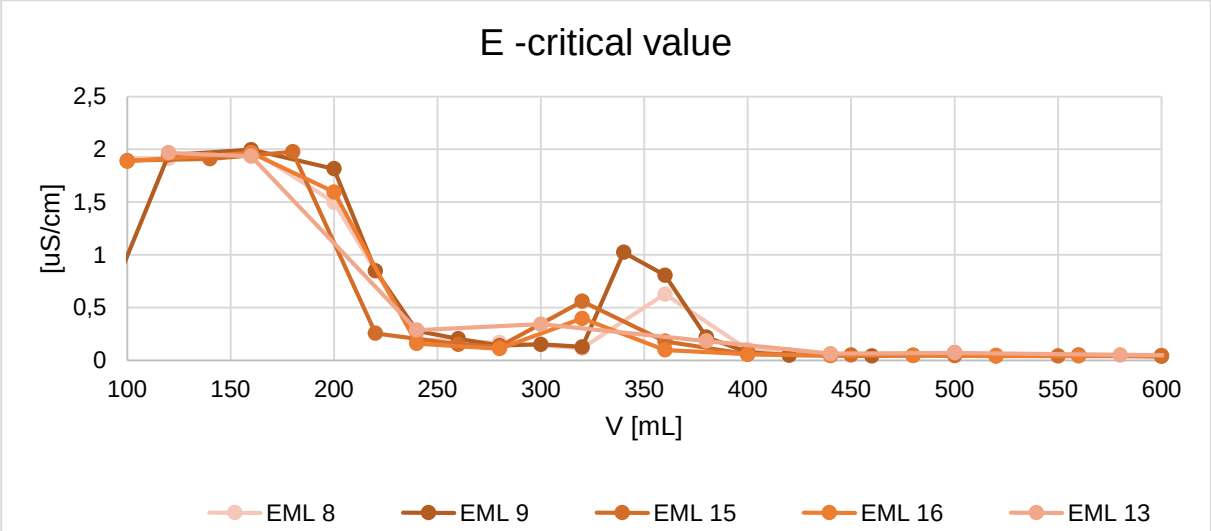

Figure 38: Reproducibility E-critical values for the early emulsifications of system 1. EML 8, EML 9, EMl 13, EML 15 and EML 16

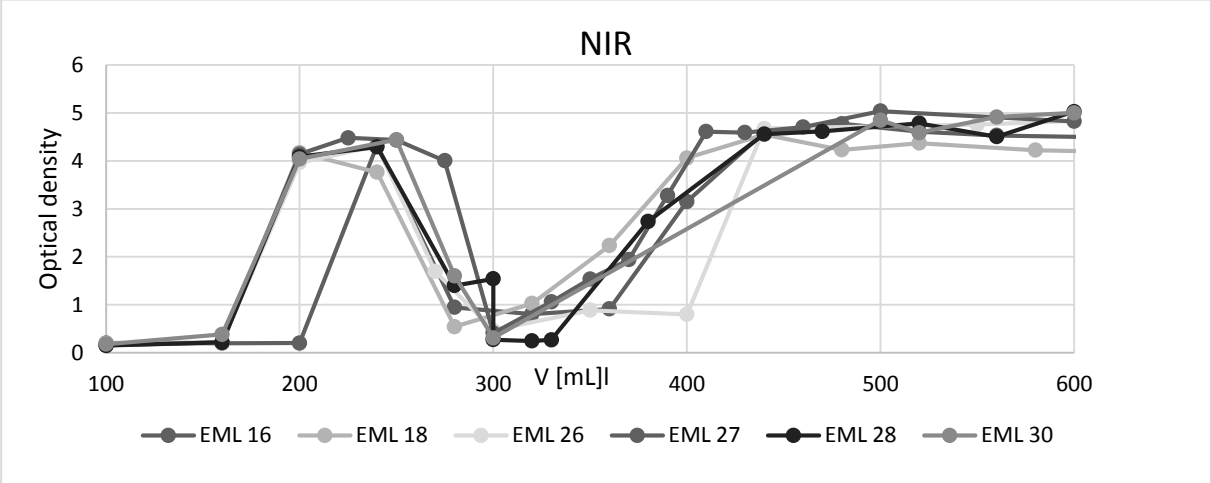

Figure 39: Reproducibility of the NIR measurements for system 1. EML 16, EML 18, EML 26, EML 27, EML 28 and EML 30.

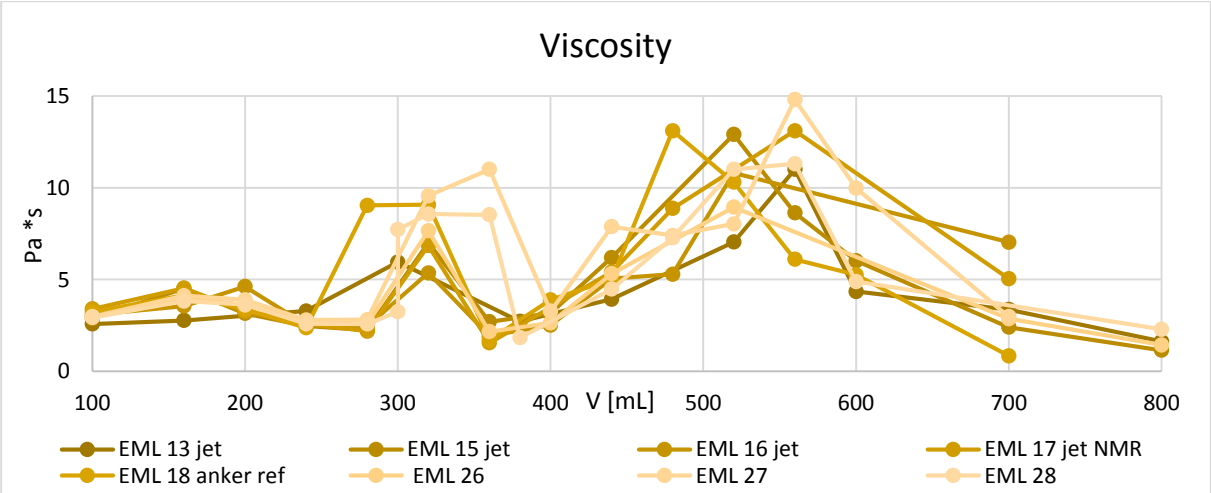

Figure 40: Reproducibility of viscosity for system 1. EML 13, EML 15, EML 16, EML 17, EML 18, EML 26, EML 27 and EML 28.

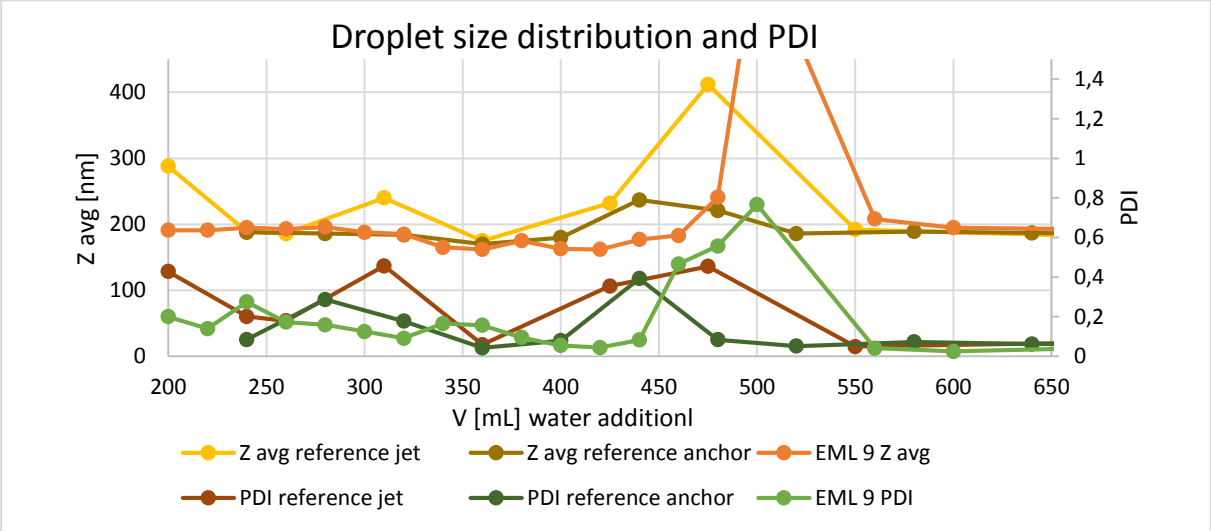

Figure 41: Reproducibility of droplet size distribution. EML 9, EML 17 and EML 18

Appendix F NIR Spectre

The NIR spectra from the respective emulsion, EML 9, and from the pure components making up the emulsification is plotted in Figure 42, Figure 43, Figure 44.

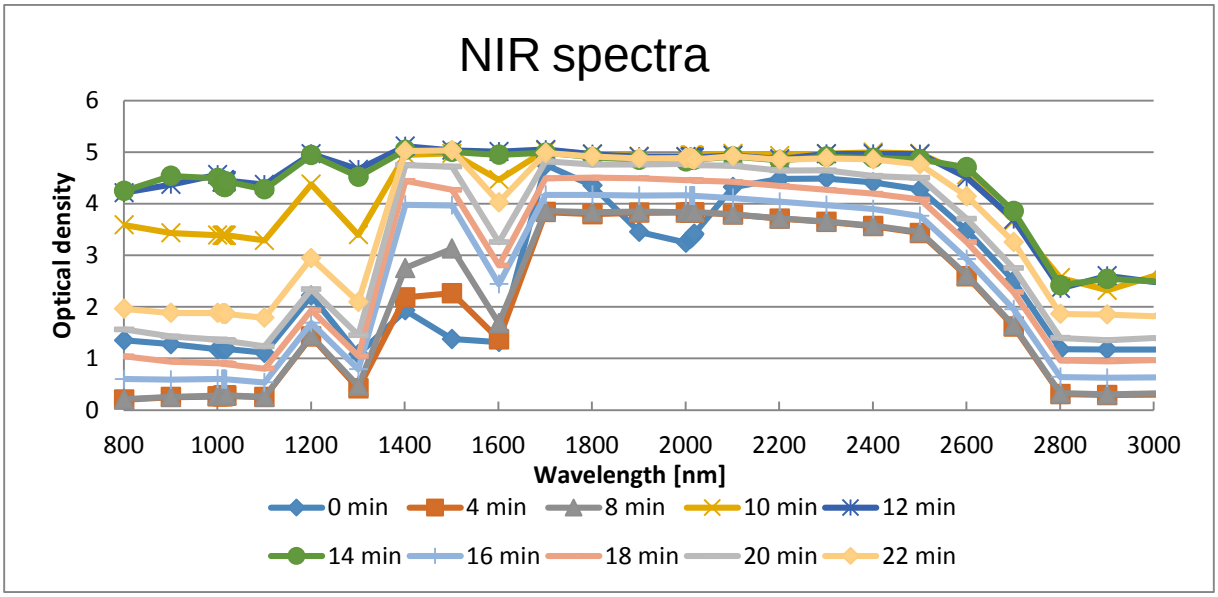

Figure 42: NIR spectra for EML 9

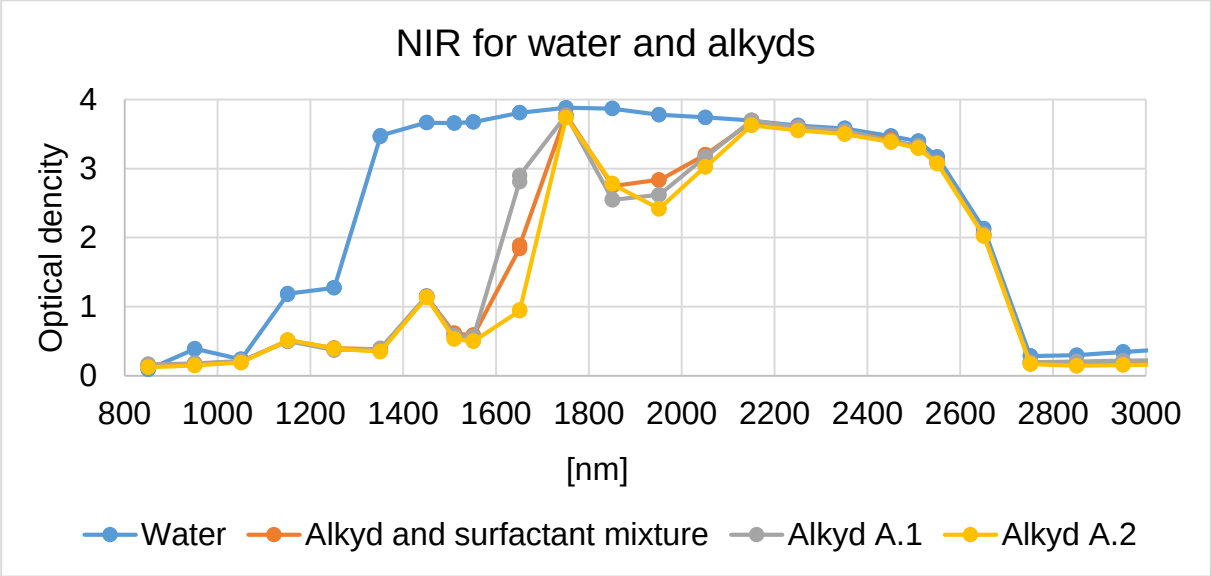

Figure 43: NIR spectra for the alkyd components of system 1 compared to water

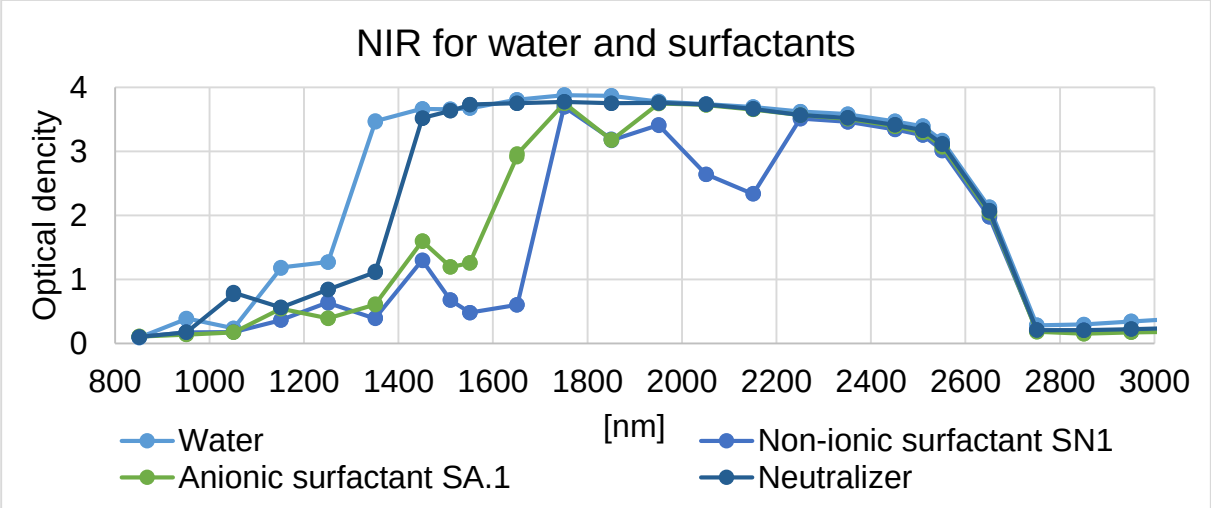

Figure 44: NIR spectra for the surfactants and neutralizer of system 1 compared to water.

Appendix G Viscosity, Stress vs. Strain

A picture of the stress development as a function of strain, constant strain rate, is shown in Figure 45. Different shear thinning and thickening tendencies can be seen and would be interesting to further investigate.

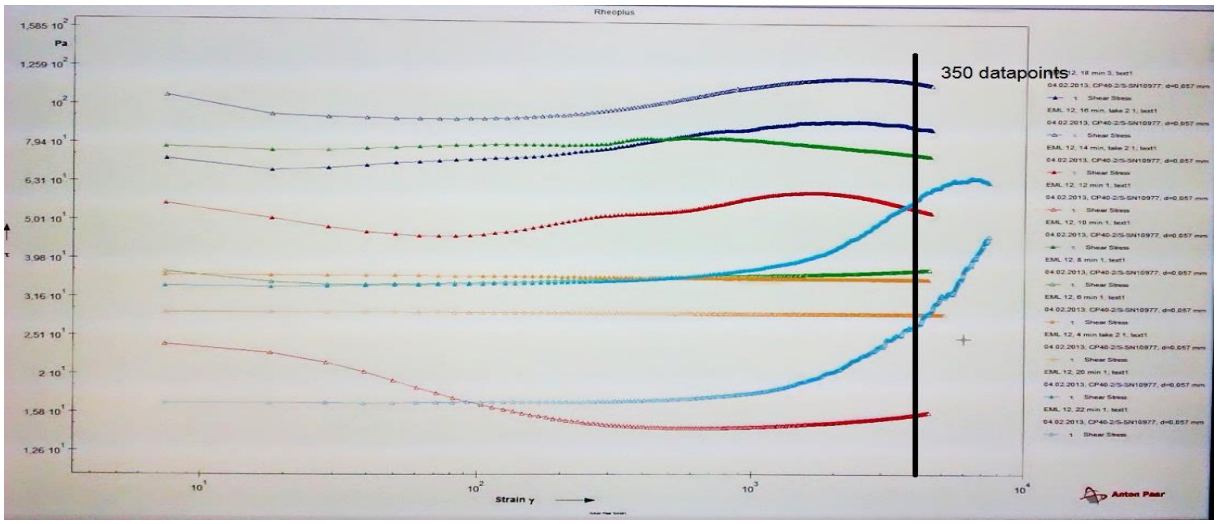

Figure 45: Stress vs. strain development curves for emulsification EML 12. Constant strain rate